

ABSTRACT

Title of Document:

DEVELOPMENT OF MAGNETIC
NANOPARTICLE-BASED ENRICHMENT
TECHNIQUES AND MASS
SPECTROMETRY METHODS FOR
QUANTIFICATION OF THE CLINICAL
BIOMARKER CARDIAC TROPONIN I

Nicole A. Schneck, Doctor of Philosophy, 2016

Directed By:

Professor Sang Bok Lee
Department of Chemistry and Biochemistry

Human cardiac troponin I (cTnI) in serum is a well-known clinical biomarker for cardiac tissue damage and is used for diagnosing myocardial infarction.

Unfortunately, commercial cTnI immunoassays from different manufacturers can produce significantly different measurement results for the same sample. In order to improve the comparability of these measurements, clinical cTnI immunoassays need to be standardized. Ultimately, the goal of this work was to develop an isotope dilution-liquid chromatography-mass spectrometry (ID-LC-MS/MS) reference measurement procedure that could be used to assign concentration values to cTnI reference materials. However, given that most serum protein biomarkers are low abundant, enrichment was mandatory to successfully quantify cTnI at clinically significant concentrations ($\approx 1\text{-}10\text{ ng/mL}$). As such, the specific aim of this work was to develop enrichment techniques and an ID-LC-MS/MS method to quantify cTnI in patient serum samples.

In order to achieved the required LC-MS/MS sensitivity, novel enrichment strategies were investigated to selectively isolate cTnI from serum and plasma. Silica

coated magnetic nanoparticles were synthesized and conjugated with antibodies to act as immunoaffinity carriers. Magnetic nanoparticles were selected due to their variable surface modifications, high binding capacity, and the fact that they can be easily isolated using a magnet. After optimizing the enrichment and digestion procedures, isotopically labeled cTnI proteins were used as an internal standard for ID-LC-MS/MS analysis of cTnI to compensate for variations in the sample preparation. Finally, the developed LC-MS/MS-based assay was applied to measure cTnI concentrations in patient plasma samples. Effective enrichment methods proved to be crucial for achieving quantification of cTnI by ID-LC-MS/MS. To this end, a complementary ID-LC-MS/MS method was also developed to evaluate different antibody immobilization strategies and magnetic particle types as part of the method optimization. Overall, this work demonstrates significant improvements in magnetic particle enrichment techniques and LC-MS/MS detection for the analysis of cTnI in patient samples.

DEVELOPMENT OF MAGNETIC NANOPARTICLE-BASED ENRICHMENT
TECHNIQUES AND MASS SPECTROMETRY METHODS FOR
QUANTIFICATION OF THE CLINICAL BIOMARKER CARDIAC TROPONIN I

By

Nicole A. Schneck

Dissertation submitted to the Faculty of the Graduate School of the
University of Maryland, College Park, in partial fulfillment
of the requirements for the degree of
Doctor of Philosophy
2016

Advisory Committee:
Professor Sang Bok Lee, Chair
Professor Sheryl Ehrman
Doctor Mark Lowenthal
Professor Zhihong Nie
Professor Paul Paukstelis

© Copyright by
Nicole A. Schneck
2016

Preface

Great things are done by a series of small things brought together.

--Vincent Van Gogh

Dedication

To my family, your love and encouragement will always mean the world to me.

Acknowledgements

I would like to first thank my advisor, Dr. Sang Bok Lee for his guidance over the years. I truly appreciated his enthusiasm and shrewdness. With his support, I was able to form a dissertation project that featured two of my scientific interests, bioanalytical and nanomaterials chemistry, as well as, help me start a collaboration with the National Institute of Standards and Technology (NIST). During my graduate studies, Dr. Lee also allowed me to accept a summer internship at a pharmaceutical company and was very supportive of letting me expand my research experiences and professional network. I am so grateful to have been able to take advantage of these excellent opportunities with the support of my advisor. I would also like to extend a special thank you to my UMD committee members, Dr. Zhihong Nie, Dr. Paul Paukstelis and Dr. Sheryl Ehrman, for their support and valuable time.

I would like to thank Dr. Karen Phinney for all of her guidance helping me find a project that fits the research goals and interests of both her and Dr. Lee's group. I am so grateful that I had the opportunity to obtain my Ph.D while working with some of the finest scientists at NIST under a student appointment. In particular, I am indebted to Dr. Mark Lowenthal for all of his advice during my Ph.D studies. Dr. Lowenthal took me under his wing and taught me how to stand as an independent researcher. Thank you for sharing your vast knowledge and experiences, and providing me the groundwork of my research project. I greatly appreciate everything that you have taught me and have shared with me, as a mentor and as a friend.

I have gained so many colleagues and friends while working at UMD and NIST. A huge thank you goes out to my labmates from both institutions, both past and present. I have thoroughly enjoyed all of the time we spent together, whether it be inside or outside the lab. I personally would like to thank Lauren Graham, Jaehee Song, and Lacey Brent for helping me maintain my sanity and giving me a few laughs throughout this long process. I could not have asked for a better set of friends to help me balance my Ph.D. work and social life. I want to also thank Dr. Sz-Chian Liou and Dr. Wen-An Chiou for their assistance in characterizing my nanomaterials. Similarly, I'd like to thank Dr. Eric Kilpatrick from NIST and Dr. Andrew Hoofnagle from the University of Washington for collaborating with me and providing me valuable patient plasma samples for my final experiments. In addition, a heartfelt thank you goes out to Dr. Lou Ann Tom from Susquehanna University and Dr. Paula Lei, whom I first met at Sanofi Pasteur, for being my role models and guiding me into a Ph.D. level scientific career path.

Above all, I would like to express my deepest appreciation for my family. I am sincerely thankful for your love, genuine support, and confidence in me. To my parents, thank you for raising me to understand the importance of education, teamwork and communication as it has helped me in everyday life. To my sister, thank you for always cheering me on in any endeavor. Lastly, I would like to thank Drew Champney for being by my side, always believing in me and reassuring me even when I had my doubts.

Table of Contents

Chapter 1: Introduction to the development of enrichment and measurement techniques for low abundant protein biomarkers.....	1
1.1. Protein biomarkers of myocardial infarction.....	2
1.1.1. Cardiac troponin.....	3
1.1.2. ELISA as the diagnostic tool for cardiac troponin I (cTnI)	5
1.1.3. The need for standardization of cTnI assays.....	7
1.2. Targeted mass spectrometry (LC-MS/MS)	9
1.2.1. Protein and peptide identification by LC-MS/MS and bioinformatics tools	11
1.3. Isotope dilution for LC-MS/MS-based quantification	14
1.4. Limitations for LC-MS/MS detection of cTnI in serum	16
1.5. Affinity purification strategies	17
1.5.1. Immunodepletion enrichment strategy	18
1.5.2. Immunoaffinity enrichment techniques	19
1.5.2.1. cTnI protein enrichment.....	20
1.5.2.2. cTnI peptide enrichment	20
1.5.3. Magnetic particle-based separation.....	22
1.6. Proposed strategies to enrich cTnI for targeted LC-MS/MS analysis.....	24
Chapter 2: Synthesis of silica coated magnetic nanoparticles	25
2.1. Introduction	25
2.2. Experimental method	28
2.2.1. Preparation of magnetic iron oxide nanoparticles	28
2.2.2. Silica coating of magnetic iron oxide nanoparticles	29
2.2.3. Characterization of silica coated magnetic nanoparticles	29
2.3. Results and discussion.....	29
2.3.1. Influence of water concentration on nanoparticle size and morphology ..	29
2.3.2. Coating magnetic nanoparticles with silica	31
2.4. Conclusion.....	33
Chapter 3: Quantification of anti-cTnI antibody bound to magnetic particles by LC-MS/MS.....	35
3.1. Introduction	35
3.2. Materials and methods.....	38
3.2.1. Materials	38
3.2.2. Conjugation of antibody to various functionalized magnetic particles	39
3.2.2.1. Surface modification of the silica coated magnetic nanoparticles..	39
3.2.2.2. Antibody coupling to the amine-modified magnetic particle	39
3.2.2.3. Antibody coupling to epoxy-modified magnetic particles.....	39
3.2.3. Calibrant preparation	40
3.2.4. Sample processing for ID-LC-MS/MS analysis	40
3.2.5. ID-LC-MS/MS analysis	41

3.2.6. LC-MS/MS antibody sequence analysis for peptide selection	42
3.3. Results and discussion	43
3.3.1. ID-LC-MS/MS method development	43
3.3.2. Antibody quantitation on magnetic particles	46
3.3.3. Optimization of antibody-magnetic particle conjugates	50
3.3.4. Advantages of the developed ID-LC-MS/MS method	51
3.4. Conclusion	53
Chapter 4: Quantification of cTnI in human plasma by protein immunoaffinity capture and LC-MS/MS	
4.1. Introduction	55
4.2. Experimental design	57
4.2.1. Materials	57
4.2.2. Immobilization of anti-cTnI monoclonal antibody onto magnetic nanoparticles	58
4.2.3. Calibrant and sample preparation for recoveries studies	59
4.2.4. Calibrant and sample preparation for patient plasma sample analysis using an isotopically labeled protein internal standard	60
4.2.5. Trypsin digestion	61
4.2.6. LC-MS/MS analysis	62
4.3. Results and discussion	63
4.3.1. Development of the LC-MS/MS-based assay	63
4.3.2. Recovery efficiency of the magnetic particle-based protein immunoaffinity enrichment	70
4.3.3. cTnI quantification in patient plasma samples	79
4.4. Conclusion	87
Chapter 5: cTnI analysis by peptide immunoaffinity enrichment and LC-MS/MS analysis	
5.1. Introduction	89
5.2. Experimental design	91
5.2.1. Materials	91
5.2.2. Immobilization of anti-peptide polyclonal antibodies onto magnetic nanoparticles	92
5.2.3. Calibrant and sample preparation for recovery studies	92
5.2.4. LC-MS/MS analysis	94
5.3. Results and discussion	95
5.3.1. Polyclonal anti-peptide antibodies	95
5.3.2. Magnetic particle-based peptide immunoaffinity recovery	95
5.3.3. Potential considerations for improvement of cTnI recovery via peptide immunoaffinity enrichment in further studies	99
5.4. Conclusion	101
Chapter 6: Summary and outlook	
6.1. Summary	103
6.2. Outlook and future work	106

Appendix A: Human subject determination forms from the University of Maryland, College Park, and the National Institute of Standards and Technology (NIST)	108
Appendix B: Estimation of recovery efficiency of peptide immunoaffinity enrichment using Protein A/G beads	110
References	113

List of Tables

Table 3.1 Optimized fragmentation parameters for MRM analysis of antibody peptides. The fragmentor voltage was set at 380 V. Labeled residues (indicated with an asterisk) contained ^{13}C and ^{15}N isotopes. The cysteine amino acid (AA) residues in the unlabeled and labeled TDSFSCNVR peptides were alkylated by the manufacturer, which increased the mass by 57 daltons.	46
Table 4.1 Optimized MS parameters and two peptides (unlabeled and labeled) with two transitions each were selected to represent cTnI and a single peptide (unlabeled and labeled) with two transitions was used to represent the capture antibody (IgG _{2b}).	67
Table 4.2 Intra- and interday repeatability statistics for cTnI in diluted goat serum..	74
Table 4.3 MRM transitions of NITEIADLTQK* and TLLLQIAK* from the isotopically labeled cTnI protein internal standard. Asterisk indicates the isotopically labeled amino acid.	77
Table 4.4 cTnI levels in five replicate sample preparations from a pooled myocardial infarction patient plasma sample lot.	82
Table 4.5 Updated MRM transitions of cTnI surrogate peptides used for quantification, and MRM transitions for the antibody peptide (for identification and relative quantification).	84
Table 4.6 cTnI levels in five individual myocardial infarction patient plasma samples.	87
Table 5.1 Optimized MS parameters and monitored transitions for cTnI identification and quantification. Two transitions (unlabeled and labeled) were monitored for each peptide.....	94

List of Figures

Figure 1.1 Schematic representation of cardiac troponins released from a myocardial cell as complexes or free protein after myocardial infarction. Adapted with permission [22].	4
Figure 1.2 Suggested reference measurement system for cTnI standardization. Reproduced with permission [40].	7
Figure 1.3 Overview of targeted LC-MS/MS analysis using MRM. A tryptic peptide (TLLQIAK) uniquely representing cTnI is selected in the first quadrupole (Q1), fragmented in the collision cell (Q2), and the fragment (product) ions (LLQIAK and LQIAK) from the third quadrupole (Q3) are selected for detection. Precursor-product transition ions can be monitored over time for peptide quantification and identification.	11
Figure 1.4 Overview of designing a LC-MRM-MS/MS experiment using cTnI as a model protein of interest. Protein sequence, peptide masses and fragmentation patterns can be determined using literature, predictive tools, or data from previous experiments. Crystal structure of cardiac troponin from RSCB protein data bank [68].	14
Figure 1.5 Basic workflow of ID-LC-MS/MS using a full length isotopically labeled protein. The recombinant full-length protein containing stable-isotope labels can be spiked in as internal standards. Labeled to unlabeled peak area can be compared for precise relative quantification of the endogenous protein.	16
Figure 1.6 Immunoaffinity with magnetic particles can be performed by targeting protein or peptides for enrichment; followed by preparation for LC-MS/MS-based analysis. Workflow A entails capturing target proteins from biofluids by using anti-protein antibody. Workflow B entails capturing target peptides from a tryptic digestion of biofluids. Adapted with permission [9].	23
Figure 2.1 TEM images of the silica coated magnetic nanoparticles prepared with the same molar ratios of FeCl ₃ : sodium acetate (0.025 M: 0.13 M) and varying concentrations of water (a) 1.3 M, (b) 2.0 M, (c) 2.6 M, and (d) 3.2 M.	31
Figure 2.2 TEM images of (a) bare nanoparticles and (b)-(d) nanoparticles whose surfaces have been coated with as silica shell of various thicknesses. The thickness of the shell was adjusted by changing the concentration of TEOS to magnetic nanoparticles (b) 1.2, (c) 1.9, and (d) 3.8.	32
Figure 2.3 (a) TEM images of silica coated magnetic nanoparticles, and (b) the histogram of particle size distribution.	33

Figure 3.1 Schematic depicting the functionalization of silica coated magnetic particles with common coupling agents, (a.) APTES or (b.) GPTMS, to covalently attach antibody by either a glutaraldehyde-activated or epoxide coupling reaction. NaCNBH ₃ = sodium cyanoborohydride.	36
Figure 3.2 Schematic illustration of the ID-LC-MS/MS-based workflow to directly measure antibody bound to magnetic particles (MP).	43
Figure 3.3 (a) Total ion chromatogram (TIC) of a tryptic digest of anti-cTnI antibody. Analysis of the digest was performed by LC-MS/MS (ion trap) and searched against a mammalian protein database using Sequest HT (Proteome Discover). (b) Two tryptic antibody peptides were selected based on signal intensity in the extracted ion chromatograms (subset) within the TIC trace. (c) MS/MS spectra of DLPSPIER and TDSFSC[+57]NVR (d) Amino acid sequence of the antibody constant region. The two target peptides used for antibody quantification are indicated in red font. The sequence was obtained from the National Center for Biotechnology Information protein database.	45
Figure 3.4 Representative extracted ion chromatogram for quantification of immobilized antibody using the glutaraldehyde coupling protocol with amine functionalized magnetic nanoparticles. Two transitions for the unlabeled and labeled targeted antibody peptide (TDSFSC[+57]NVR and DLPSPIER) were monitored, along with two transitions of the unlabeled TDSFSCNVR to monitor alkylation efficiency. Asterisk indicates the isotopically labeled amino acid.	47
Figure 3.5 Calibration curves for each magnetic particle support are provided for monitored anti-cTnI antibody peptide transitions as a plot of unlabeled : labeled integrated peak area ratios versus unlabeled : labeled measured mass ratios. A regression equation of the best-fit line is provided for each plot along with a R ² estimate of the correlation for fit to the line. The error bars represent standard deviation of the mean peak areas from duplicate injections.	48
Figure 3.6 Bar graph summarizes the amount of immobilized anti-cTnI antibody per mg of nanoparticles and microparticles. Quantification was based on monitoring two transitions for two antibody peptides. The standard deviation error bars represent duplicate injections of all of the monitored transitions from triplicate sample preparations.	49
Figure 3.7 Glutaraldehyde-activated magnetic nanoparticles (0.25 mg) were incubated with an increasing amount of anti-cTnI antibody. Antibody binding capacity was determined using a ID-LC-MRM-MS/MS method specific for anti-cTnI antibody. The standard deviation error bars represent duplicate injections of all of the monitored transitions from each sample.	51

Figure 3.8 Representative total ion chromatograms of five cTnI samples enriched using magnetic nanoparticles conjugated with anti-cTnI antibody. MRM transitions for two cTnI peptides and one anti-cTnI antibody peptides are monitored. LC-MRM-MS/MS detection can be used to monitor antibody differences found between sample replicates, which may affect capture recoveries. A higher (relative) concentration of antibody (DLPSPIER) peptide was calculated in Sample 1 compared to the other samples, which resulted in a slightly higher cTnI recovery..... 53

Figure 4.1 (a) Total ion chromatogram (TIC) of a tryptic digest of human cardiac troponin complex from SRM 2921. (b) Representative extracted ion chromatogram of tryptic cTnI peptide, TLLLQIAK. (c) and MS/MS spectra of TLLLQIAK..... 64

Figure 4.2 Amino acid sequence of human cTnI. Peptides in blue were identified from a digest of SRM 2921 (human cardiac troponin complex) during sequence coverage analysis by LC-MS/MS (ion trap). Tryptic peptides underlined were selected for subsequent MRM screening and assay development. 65

Figure 4.3 Extracted ion chromatogram of tryptic cTnI peptides screened for MRM analysis and assay development. Two transitions per cTnI peptide were analyzed. The blue highlighted tryptic peptides NITEIADLTQK and TLLLQIAK produced the highest signal response in electrospray LC-MS/MS (triple quadrupole). These peptides are referred to as “surrogate peptides,” and were used to build a MRM-based assay for cTnI. Isotopically labeled versions of these peptides were synthesized to act as internal standards for LC-MS/MS quantification. 66

Figure 4.4 Effect of digestion condition on peptide formation yield. Bar graphs represent the peak area ratio of the unlabeled peptide to the spiked-in labeled peptide. Reduction and alkylation conditions were varied: 10 mM DTT, 10 mM IAM (blue line), 5 mM DTT, 15 mM IAM (red line), and 0.5 mM DTT, 2 mM IAM, 1.5 mM DTT (green line). For each of the reduction and alkylation conditions, the trypsin-to-protein ratios were varied (1) 1:2.5, (2) 1:5, (3) 1:10, (4) 1:20, (5) 1:50. Data and error bars represent the mean and standard deviation for two transitions per peptide and duplicate sample preparations..... 68

Figure 4.5 Representative MRM chromatograms of cTnI (from SRM 2921 digest), monitoring two transitions of the unlabeled cTnI peptides (NITEIADLTQK and TLLLQIAK) at the (a) absolute limits of detection at 163 pg and (b) absolute limits of quantification at 325 pg cTnI. S/N ratios are shown for each transition. 69

Figure 4.6 Percent recovery of cTnI was tested using different volumes of antibody-nanoparticle conjugates during immunoaffinity enrichment. Quantification was determined by analyzing two transitions for two cTnI peptides. The standard deviation error bars represent all of the monitored transitions from duplicate sample preparations..... 70

Figure 4.7 Percent recovery of cTnI (at the protein level) from diluted goat serum following a range of incubation time periods. Quantification was determined by analyzing two transitions for each cTnI peptides; followed by averaging the four transitions (total) for overall cTnI recovery. For the positive control samples, the standard deviation error bars represent all of the monitored transitions from triplicate sample preparations. For the negative control samples, the standard deviation error bars represent all of the monitored transitions from a single sample preparation. 72

Figure 4.8 Percent recovery of cTnI (at the peptide level) from diluted goat serum following a range of incubation time periods. Quantification was determined by analyzing two transitions for each cTnI peptide. The standard deviation error bars represent the monitored transitions per peptide from triplicate sample preparations. 73

Figure 4.9 Percent recovery of cTnI (at the protein level) from normal plasma at three different amounts. Quantification was determined by analyzing two transitions of two cTnI peptides. The standard deviation error bars represent all of the monitored transitions from triplicate sample preparations. 75

Figure 4.10 Extracted ion chromatograms of TLLLQIAK* and NITEIADLTQK* from a digest of isotopically labeled cTnI protein internal standard. Asterisk indicates the isotopically labeled amino acid. MS/MS spectra of both cTnI peptides are also shown. 76

Figure 4.11 Representative MRM chromatograms of digested isotopically labeled cTnI protein internal standard to determine isotope incorporation level. Unlabeled and labeled MRM transitions for NITEIADLTQK and TLLLQIAK were monitored. Zoomed insets of the unlabeled peptides are shown. 78

Figure 4.12 MRM chromatogram of cTnI enriched from a pooled cTnI-positive patient plasma sample. 80

Figure 4.13 Calibration curves are provided for monitored cTnI peptide transitions as a plot of unlabeled : labeled integrated peak area ratios versus unlabeled : labeled measured mass ratios. A regression equation of the best-fit line is provided for each plot along with a R^2 estimate of the correlation for fit to the line. 81

Figure 4.14 MRM chromatogram of cTnI recovered from normal plasma samples (spiked with SRM 2921). Two transitions from each (unlabeled and labeled) cTnI peptide, AYATEPHAK, NIDALSGMEGR, NITEIADLTQK and TLLLQIAK were monitored. Two transitions for (unlabeled and labeled) DLPSPIER, representative of the antibody, were also monitored. 83

Figure 4.15 Representative MRM chromatogram of cTnI enriched from an individual cTnI-positive patient plasma sample. 85

Figure 4.16 Calibration curves are provided for monitored cTnI peptide transitions as a plot of unlabeled : labeled integrated peak area ratios versus unlabeled : labeled measured mass ratios. A regression equation of the best-fit line is provided for each plot along with a R^2 estimate of the correlation for fit to the line.....	86
Figure 5.1 MRM chromatogram of cTnI enriched from buffer using magnetic nanoparticle-based peptide immunoaffinity capture.....	96
Figure 5.2 Calibration curves are provided for monitored cTnI peptide transitions as a plot of unlabeled : labeled integrated peak area ratios versus unlabeled : labeled measured mass ratios. A regression equation of the best-fit line is provided for each plot along with a R^2 estimate of the correlation for fit to the line.....	97
Figure 5.3 Percent recovery of cTnI (at the peptide level) spiked into buffer at three different amounts. Quantification was determined by analyzing two transitions for two cTnI peptides. The standard deviation error bars represent the monitored transitions per peptide from duplicate sample preparations.	98
Figure 5.4 Representative MRM chromatograms of spiked cTnI enriched from (a) buffer and (b) normal plasma using magnetic nanoparticle-based peptide immunoaffinity capture and LC-MS/MS analysis.....	99
Figure B-1 Representative MRM chromatograms of cTnI after (a) trypsin digestion only and (b) after digestion, peptide immunoaffinity enrichment, and peptide elution. Zoomed inset shows unlabeled peptides of TLLLQIAK, which cannot be clearly seen in chromatogram b.	112

List of Abbreviations

MS, MS/MS	Mass spectrometry, tandem mass spectrometry, mass spectrometer
cTnI	Cardiac troponin I
cTnT	Cardiac troponin T
cTnC	Cardiac troponin C
ELISA	Enzyme-linked immunosorbent assay
LC	Liquid chromatography
Q, QQQ	Quadrupole, triple quadrupole
MRM	Multiple reaction monitoring
SRM	Standard reference material
m/z	Mass-to-charge ratio
CID	Collision induced dissociation
ID	Isotope dilution
SISCAPA	Stable isotope standards (for use with) capture by anti-peptide antibodies
TEM	Transmission electron microscope
TEOS	Tetraethylorthosilicate
APTES	3-aminopropyltriethoxysilane
GPTMS	Glycidyloxypropyltrimethoxysilane
ACN	Acetonitrile
H ₂ O	Water
S/N	Signal-to-noise ratio
DTT	Dithiothreitol
IAM	Iodoacetamide
PBS	Phosphate buffer solution
% CV	Percent coefficient of variation
KLH	Keyhole limpet hemocyanin
NIST	National Institute of Standards and Technology

Chapter 1: Introduction to the development of enrichment and measurement techniques for low abundant protein biomarkers

This chapter has been reproduced in part with permission from: Schneck, N. A., Lowenthal, M., Phinney, K. & Lee, S. B. Current trends in magnetic particle enrichment for mass spectrometry-based analysis of cardiovascular protein biomarkers. *Nanomedicine* **10**, 433-446, doi:10.2217/nnm.14.188 (2015).

There are an estimated 1.5 million cases of myocardial infarction, commonly known as a heart attack, that need medical evaluation every year in the United States alone.¹ The term myocardial infarction is used within the clinical setting when there is evidence of cardiac muscle (myocardial) cell death caused by prolonged ischemia.^{2,3} Myocardial infarction is commonly diagnosed by detecting specific protein biomarkers, such as the cardiac troponins, that are released into the bloodstream as a result of cardiac cell death or damage. One subunit of the cardiac troponin complex, cardiac troponin I (cTnI), is a protein that normally functions within myocardial cells and is known to be elevated in blood following myocardial injury.⁴ Due to its high myocardial tissue specificity, cTnI is an important biomarker for the diagnosis of myocardial infarction. Measurement of cTnI in human plasma or serum by immunoassays (e.g. enzyme-linked immunosorbent assay, ELISA) is already a useful clinical tool for detecting heart damage; however, cTnI immunoassays need to be harmonized and/or standardized, as well as improved with respect to the specificity and accuracy of the analytical measurements. Measurement discrepancies between different commercial cTnI assays have been previously demonstrated in a number of reports and are thought to be caused by differences in assay platforms, calibration or interferences.⁵⁻⁷

While immunoassays have shown great utility in clinical medicine laboratories, there has been interest in implementing liquid chromatography (LC) coupled with mass spectrometry (MS, LC-MS, LC-MS/MS)-based detection methods to complement immunoassay results. LC-MS/MS assays are attractive due to their ability to directly measure the clinical biomarker with improved specificity. However, the inherently lower sensitivity of LC-MS/MS techniques relative to immunoassays is insufficient for low abundant protein biomarker quantification. As a result, enrichment strategies are needed to measure low clinical concentrations of cTnI released into the bloodstream after myocardial injury. One common approach towards enriching these low abundant biomarkers is through the use of magnetic particle-based immunoaffinity enrichment approaches. The advantages of magnetic nanoparticle-based enrichment make it an ideal method to lower limits of detection of current LC-MS/MS instruments for analysis of cTnI. This thesis focuses on investigating magnetic-based separation techniques to enrich cTnI for LC-MS/MS analysis. With myocardial infarction as a leading cause of death in the developed world¹, our broad goal is to help improve current clinical cTnI biomarker measurements for better patient management and clinical decision-making.

1.1. Protein biomarkers of myocardial infarction

Cardiac biomarkers play an essential role in the diagnosis, clinical decision-making and management of patients with myocardial injury.^{1,8,9} Since the 1970s, proteins such as myoglobin, creatine kinase, and the MB isoenzyme of creatine kinase (CK-MB) were utilized clinically as cardiac markers for detecting myocardial cell damage; however these markers lacked sufficient sensitivity and specificity to the

heart.^{1,10} In the 1990s, cTnI received international endorsement as the preferred biomarker for myocardial infarction due to its high specificity for the heart, and has become a critical component in the diagnosis of myocardial infarction.^{10,11}

1.1.1. Cardiac troponin

Troponin I is a component of the three-subunit troponin complex (sometimes designated individually as TnI, TnT and TnC) and plays a key role in the regulation of skeletal and cardiac muscle contraction. The troponin complex is located on the thin filament of the muscle cell along with other structural proteins like tropomyosin and actin.^{1,12,13} Each troponin subunit has skeletal and cardiac isoforms expressed in muscle tissue cells.^{1,14} Troponin T and troponin I have skeletal and cardiac isoforms that differ in amino acid sequence, which allows antibodies to differentiate between the different isoforms.¹⁰ Additionally, the cardiac-specific troponin I (referred earlier as cTnI) isoform, with a molecular mass of 24 kda, differs from its skeletal muscle form by an additional 31 amino acid fragment at the N-terminus, and the cardiac troponin T (cTnT) isoform differs from its skeletal isoforms by 6-11 amino acid residues.¹⁵ Conversely, the skeletal and cardiac isoforms of troponin C have the same amino acid sequence.¹⁰ Therefore, troponin C is not cardiac-specific and is not used as a biomarker for myocardial infarction. Because cTnT and cTnI are expressed exclusively in heart tissue, these proteins have been the preferred biomarkers for diagnosing myocardial infarction.^{1,10} However, while both proteins have been used as diagnostics markers, cTnI is the gold standard among clinicians because cTnT is thought to be transiently expressed in some forms of diseased skeletal muscle tissue, such as in the case of renal disease.¹⁶⁻¹⁸

After myocardial cell damage, the troponin complex is gradually released into the bloodstream and degrades into the troponin I-troponin C binary complex and free troponin T, as shown in Figure 1.1.^{5,19-22} In addition, a small amount of soluble unbound troponin I and troponin T exists in the cytoplasm and is rapidly released after myocardial damage.^{5,15,23} It is thought that the binary troponin I-troponin C complex is the predominant form in circulation.²¹

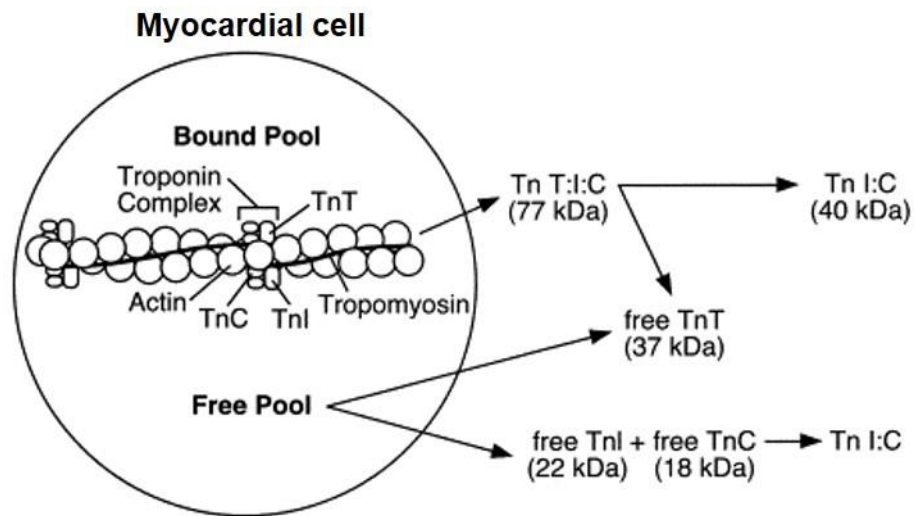


Figure 1.1 Schematic representation of cardiac troponins released from a myocardial cell as complexes or free protein after myocardial infarction. Adapted with permission [22].

Once in the bloodstream, the various troponin forms undergo substantial modifications. The cTnI complex is susceptible to proteolysis, oxidation, reduction and phosphorylation.^{6,24} The N- and C-terminal regions of cTnI are also known to undergo proteolytic degradation. However, the central region of cTnI, located between residues 30 and 110, has a higher resistance to proteolysis and is very stable. The central region of cTnI is thought to be protected from proteolytic degradation because this region contains the inhibitory peptide that tightly interacts with cardiac

troponin C (cTnC).²⁴ Due to this reason, most immunological techniques target the central region of cTnI.^{7,25}

The measurement of cTnI in blood is particularly efficient for late diagnosis of myocardial infarction.¹⁰ Elevated levels of cTnI can be found in the bloodstream for up to seven days after myocardial infarction.¹⁰ cTnI levels usually peak around 0.001 to 100 ng/mL depending on the severity of the myocardial infarction, with highest concentrations being observed 18-24 hours after the onset of the infarction.^{15,26} Since the concentration of cTnI is still relatively low even at peak hours, highly sensitive detection methods are needed for clinical measurement.^{23,26}

1.1.2. ELISA as the diagnostic tool for cardiac troponin I (cTnI)

Even though cardiac troponin was discovered in the 1970's, the first cTnI immunoassay was not described until the late 1980's by Cummins et al.^{18,27}

Immunoassays have been heavily relied on for protein quantification within the clinical laboratories primarily because of their high sensitivity, high throughput and low per-sample cost.²⁸ Two-site “sandwich” immunoassays, (e.g., ELISAs) are commonly used to measure protein biomarkers for diagnostic purposes. ELISAs entail the use of a capture antibody to bind to the protein of interest and a secondary, fluorescently-labeled antibody that is used to detect and measure the amount of protein bound to the capture antibody.⁵ Currently, there is a wide variety of capture antibodies specific to several different regions, referred to as epitopes, of the cTnI molecule.^{7,29} The protein concentration can be determined from a calibration curve, which plots the analytical signal from the labeled antibody versus the concentration of calibrators.⁵

The first commercialized cTnI assay was introduced in 1996 using the Stratus I analyzer (Dade Behring).²⁷ Since then, the cTnI immunoassays have improved considerably regarding assay sensitivity and precision. Current generations of commercially available assays can reliably measure cTnI at the lower end of the reference range (~ 1-10 pg/mL) while meeting precision guidelines (< 10 % variation).^{27,30,31}

Currently, there are more than 20 immunometric cTnI commercial assays on the market and most of these assays are constructed very differently, leading to performance variations.⁷ Commercial cTnI assays vary from each other by the types of antibodies used, specificity to different epitopes of the complexed, free and modified cTnI, calibrators used, and detection techniques (spectrophotometric, fluorescent, chemiluminescent or electrochemical).^{7,18} As a consequence, cTnI measurements from different assays on identical samples can vary 10 to 100-fold.^{7,32,33} These assays also suffer from various non-specific interferences such as the possibility of anti-cTnI autoantibodies, heterophilic antibodies, anticoagulants and other endogenous proteins that may be present in plasma or serum.^{7,18} These non-specific interferences can lead to false positives and false negatives.¹⁸ Circulating autoantibodies in patient samples have been known to confound immunoassays and give false-negative results.³⁴⁻³⁷ For example, anti-cTnI antibodies used for commercial assays typically target the stable mid-fragment region (amino acid residues 30-110) of cTnI; although, autoantibodies have been observed to block capture antibodies from binding to amino acid residues 41-91.^{35,36} With so many assay-related issues, clinical interpretation of the biomarker results may be clouded.

For instance, discrepancies between cTnI results obtained using different assays can cause problems when a clinician is comparing test results from different laboratories, or when laboratories attempt to change assay platforms.^{26,33}

1.1.3. The need for standardization of cTnI assays

Standardization of cTnI measurement is needed to achieve comparable results between assays and to define common decision limits for cTnI biomarker interpretation. Standardization of quantitative measurements in laboratory medicine often involves the application of a reference measurement system.^{7,38,39} The critical components of the system include the use of primary and secondary reference materials and a higher-ordered reference measurement procedure, as shown in Figure 1.2.⁴⁰ The primary reference measurement procedure, which is calibrated using the

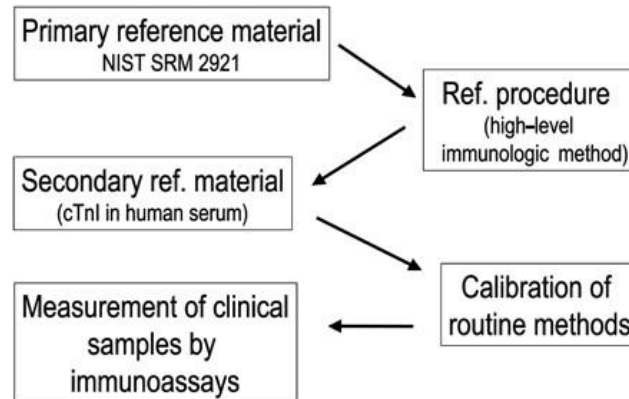


Figure 1.2 Suggested reference measurement system for cTnI standardization. Reproduced with permission [40].

primary buffered-based material, is used to assign a certified value to the secondary matrix-based reference material.^{6,7,38,41-43} Manufacturers can use their own testing procedures with the certified (secondary) matrix-matched material to assign values to commercial calibrators.^{7,38} Furthermore, the clinical laboratories can use the validated

calibrators with their routine procedures to measure cTnI values in patient serum samples, which would be traceable to the same reference procedure and materials.⁷ The establishment of a reference measurement system for cTnI would ensure calibration traceability of cTnI measurements and sample comparability.⁴²

However, neither a primary reference measurement procedure nor a secondary serum-based certified reference material for cTnI has been developed. The cTnI Standardization Committee of the American Association for Clinical Chemistry collaborated with the National Institute of Standards and Technology (NIST) to develop a primary standard reference material (SRM) 2921, consisting of the ternary complex of cardiac troponin (cTnC-cTnI-cTnT) extracted and purified from human heart tissue under non-denaturing conditions.^{7,33,41,44} The certified concentration of cTnI in SRM 2921 was determined by reverse phase LC and amino acid analysis.³³ An attempt to use SRM 2921 as a common calibrator in commercial assays was tested to determine if only a primary reference material was sufficient enough to improve harmonization, but the material demonstrated commutability in only 50 % of commercial cTnI assays.^{7,41,45,46} SRM 2921 was made in an attempt to mimic cTnI found in patient serum samples; however, a buffered solution of the cardiac troponin complex purified from human heart tissue proved to be very different from cardiac troponin found in serum.⁴⁶ Removing the matrix background when purifying cardiac troponin for SRM 2921 was also determined to cause structural changes to cTnI, which potentially affected immunological behavior and further raised commutability issues.^{6,26} Consequently, a complete reference measurement system, including a secondary reference material with a composition and matrix similar to that in clinical

samples, was needed to calibrate commercial assays.³⁸ In order to certify cTnI values in the secondary reference materials, a well-characterized and defined reference measurement procedure would be needed.

An immunochemical procedure using monoclonal antibodies was developed as a candidate to support higher metrological order measurements for cTnI.^{40,42} This ELISA-based method displayed suitable linearity, good sensitivity and appeared to show no bias when tested on samples with heterogeneous cTnI forms.⁴² However, an ELISA-based procedure was thought to be too dependent on the assay platform because it uses an indirect measurement approach.³⁸ ELISA assays coupled with fluorescence-based detection measure indirect, nonspecific signals and cannot discriminate interferences or protein variants from the target protein.⁹ Alternatively, a non-immunochemical technique, such as targeted LC-MS/MS, can directly measure cTnI based on molecular mass and fragmentation patterns with a higher level of structural specificity.

1.2. Targeted mass spectrometry (LC-MS/MS)

The establishment of reference measurement methods for clinical protein biomarkers is usually performed by targeted LC-MS/MS and isotope dilution (ID) approaches. There are a variety of LC-MS/MS platforms, but for targeted protein quantification the most common is a LC coupled with triple quadrupole MS using the multiple reaction monitoring (MRM) technique.⁴⁷ LC-MS/MS analysis is based on protein/peptide mass-to-charge (m/z) ratios and fragment ions, which enable unambiguous identification.⁴⁸ Almost all LC-MRM-MS/MS-based protein quantification work is performed at the peptide level because peptides are more

amendable for the mass spectrometer, which is typically referred to as the bottom-up approach. In bottom-up analysis, proteins are digested (e.g. with trypsin) into peptides. The resulting peptide mixture can be fractionated using LC and ionized out of solution by electrospray ionization for MS detection.^{49,50} All LC-MS/MS-based experiments discussed in this dissertation will involve sample preparation for bottom-up analysis.

MRM is a powerful method that exploits the unique capabilities of the triple quadrupole MS instrument and provides superior sensitivity and specificity compared to other MS platforms. In the MRM method, a particular ion of the targeted (precursor) peptide is selected in the first quadrupole and fragmented by collision induced dissociation (CID) in the second quadrupole to yield one or several specific peptide fragment (product) ions, which are then filtered and measured in the third quadrupole.^{51,52} Several such precursor-product ion pairs, termed MRM transitions, can be sequentially and repeatedly monitored during the chromatographic elution of the peptide, yielding chromatographic peaks for each transition. Therefore, concurrent quantitation can be achieved by integrating the peak intensities of the fragment ions for each of the targeted peptides.⁵¹ Figure 1.3 demonstrates the detection of a representative cTnI peptide using a LC-MS/MS (triple quadrupole) instrument in MRM mode. During MRM analysis, the MS focuses exclusively on the targeted precursor-product ion pairs and filters out any co-eluting background ions.^{53,54} Therefore, the two levels of mass selection enables high selectivity, and the targeted MRM mode translates into higher sensitivity compared to other MS platforms.⁵³ The superior sensitivity, selectivity, and reproducibility of the triple quadrupole MS

instrument with MRM technology makes it capable of detecting low abundant protein extracts from complex mixtures.^{43,53,54}

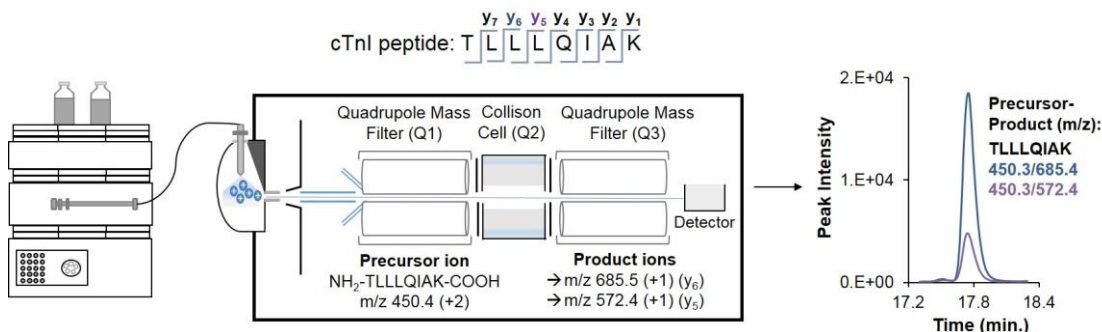


Figure 1.3 Overview of targeted LC-MS/MS analysis using MRM. A tryptic peptide (TLLLQIAK) uniquely representing cTnI is selected in the first quadrupole (Q1), fragmented in the collision cell (Q2), and the fragment (product) ions (LLQIAK and LQIAK) from the third quadrupole (Q3) are selected for detection. Precursor-product transition ions can be monitored over time for peptide quantification and identification.

The LC-MS/MS detection of a targeted peptide using MRM scanning relies on the correct m/z and peptide sequence.^{47,51} Peptides are selected to act as surrogates/signatures for the protein of interest, which is usually based on information obtained from previous LC-MS/MS experiments, scientific literature, and predictive software tools.⁵¹ Accordingly, section 1.2.1 will briefly introduce the use of another LC-MS/MS instrument, a high-resolution hybrid ion-trap-Orbitrap MS/MS, to identify amino acid sequences of proteins. In addition, a software program, Skyline⁵⁵, that uses algorithms to generate MRM data for MRM assay development will also be introduced.

1.2.1. Protein and peptide identification by LC-MS/MS and bioinformatics tools

For MRM analysis, unique peptides from the protein of interest must first be chosen to act as surrogate peptides for quantification. “Trapping” MS/MS instruments, such as the hybrid ion-trap-Orbitrap MS/MS⁵⁶ are commonly used in a

non-targeted approach to identify the best “proteotypic” peptide targets for subsequent MRM analysis.⁵⁷⁻⁵⁹ In a typical experimental workflow, a protein sample is digested with a proteolytic enzyme (e.g. trypsin) and analyzed by the linear ion trap-Orbitrap MS/MS using data dependent analysis. Unlike MRM analysis, data-dependent methods involve analyzing all of the peptide ions introduced into the LC-MS/MS at a given time and then selecting the most abundant peptide (precursor) ions for fragmentation via CID.⁶⁰ The resulting fragment (product) ions are then detected in an MS/MS spectrum containing m/z values of the fragment ions generated from the CID of an isolated peptide ion.^{57,60,61} Over the entire course of the LC-MS/MS analysis, a large dataset of MS/MS spectra can be acquired to identify the protein components in a sample.⁴⁹ Data interpretation by *de novo* approaches is technically challenging and tedious work. Software for interpreting mass spectra (e.g. Sequest⁶²) can be used to search each MS/MS spectrum against a protein sequence database to identify the amino acid sequences of the peptides found in the sample. The analysis software first identifies the individual peptide from a MS/MS spectra and then a set of peptide sequences can be used to infer which proteins may be present in the sample.^{60,61,63} Identifying representative peptides and fragmentation patterns for the targeted protein can be used to derive MRM transitions based on the precursor and product ions.

Another way to select peptides representative of a protein of interest and corresponding MRM transitions is to use predictive tools, such as Skyline.⁵⁵ Skyline, which is a freely available program, predicts MRM transitions based on theoretical digestion and fragmentation rules, and protein sequence databases. By inputting a file

of the protein sequence, the program automatically generates a list of proteolytic peptides (based on an enzyme chosen) and lists the predicted MRM transitions for each peptide.^{55,64,65}

In this dissertation, both computational and experimental workflows were used to select tryptic peptides and corresponding transitions for MRM analysis. When selecting optimal surrogate peptides to represent the targeted protein, some criteria should be considered. For instance, a selected tryptic peptide should be specific to the corresponding protein, contain no post-translational modifications, and have good LC-MS/MS signal response.^{47,51} In addition, peptides should have an average length of ~10 amino acids. Longer peptides may possess unfavorable LC properties and be difficult to synthesize, whereas very short peptides have limited fragmentation ions and are often not unique enough for a single protein within a complex mixture.⁶⁶ Multiple representative peptides per protein (2-4 peptides with multiple transitions per each peptide) are needed for confident MRM analysis to infer the presence of the protein and determine protein abundance.^{51,53,67} Figure 1.4 depicts an overview of designing a bottom-up-LC-MRM-MS/MS based experiment for peptide quantification.⁶⁸

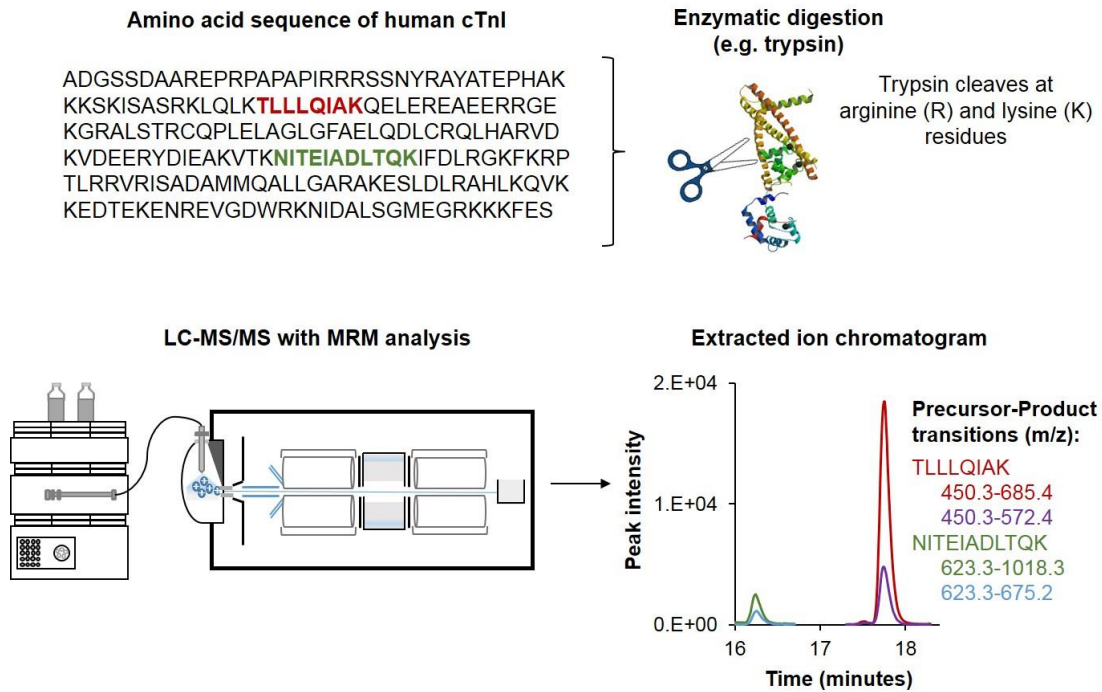


Figure 1.4 Overview of designing a LC-MRM-MS/MS experiment using cTnI as a model protein of interest. Protein sequence, peptide masses and fragmentation patterns can be determined using literature, predictive tools, or data from previous experiments. Crystal structure of cardiac troponin from RSCB protein data bank [68].

1.3. Isotope dilution for LC-MS/MS-based quantification

LC-MS/MS-based assays (using MRM) in combination with stable-isotope labeled internal standards have been extensively used for protein biomarker quantification and standardization purposes.⁶⁹ Specifically, ID-LC-MS/MS is a quantitative technique used in reference measurement procedures for many clinically relevant proteins.⁷⁰ Measurements based on ID-LC-MS/MS are more accurate and precise because the method requires the use of an isotopically labeled internal standard analogous to the target protein/peptide to account for biases associated with sample processing and instrument variability.^{9,70}

The most commonly used ID-based approach relies on spiking the sample with isotopically labeled reference peptides at known concentrations and comparing signal intensities of native and reference peptides in order to quantify the corresponding targeted endogenous protein.^{47,51} The reference peptides are typically synthesized with an incorporated stable isotope label of ^{13}C and/or ^{15}N on one or more selected amino acids in the peptide sequence. They have the same physiochemical properties as the targeted endogenous peptide, including the chromatographic co-elution, ionization efficiency, and fragmentation patterns.^{47,67} Unlike immunoanalyzer systems, LC-MS/MS can unambiguously distinguish the (light) native peptide from the (heavy) isotopically labeled reference peptide because of the defined mass difference. The quantification of the endogenous protein is based on the peak area or intensity ratio of the native peptide to the labeled reference peptide.⁴⁷ However, synthetic reference peptides cannot be used to account for biases in protein digestion. Accuracy of this approach can be negatively affected if the target protein undergoes an incomplete digestion or is partially lost during sample preparation.^{51,71}

To further improve the accuracy of protein quantification, a full-length isotope labeled protein, analogous to the target protein, can be spiked into the samples at the beginning of the analytical workflow to act as an internal standard. As shown in Figure 1.5, the isotopically labeled protein allows for all sample preparation steps to be accounted for and decreases any technical variability.⁵³ This approach assumes that the native and standard proteins have the same extent of post-translational modifications, protein-protein interactions and proteolytic cleavage efficiency.^{51,72}

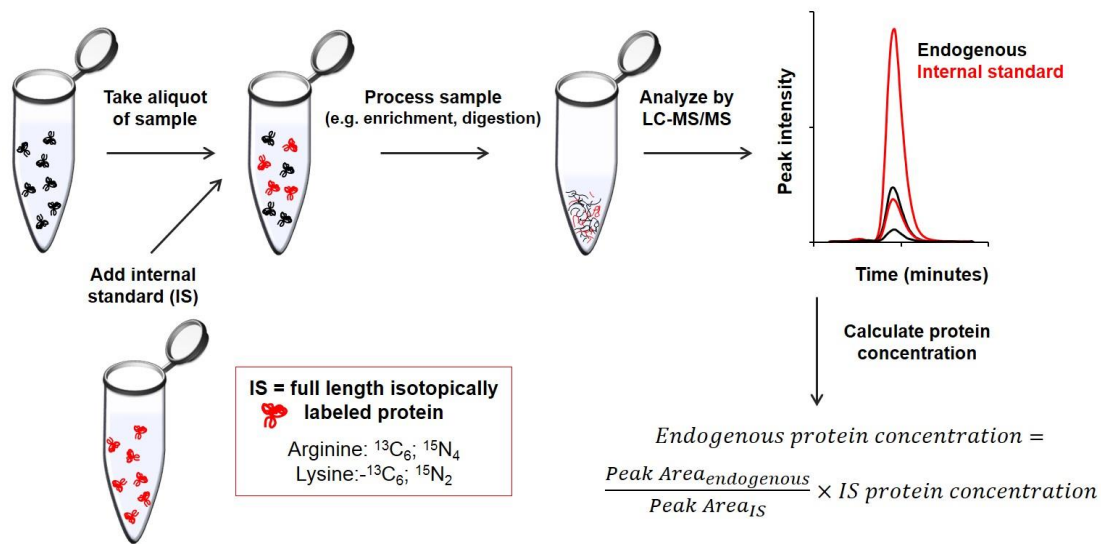


Figure 1.5 Basic workflow of ID-LC-MS/MS using a full length isotopically labeled protein. The recombinant full-length protein containing stable-isotope labels can be spiked in as internal standards. Labeled to unlabeled peak area can be compared for precise relative quantification of the endogenous protein.

Unfortunately for many clinically relevant proteins, synthesizing an isotopically labeled standard protein that has the same post-translational modifications and protein-protein interactions as the target protein is quite challenging.⁷⁰

Although ID-LC-MS/MS is the preferred approach to use for a reference measurement procedure, current LC-MS/MS-based assays lack the measurement sensitivity needed to directly detect low abundant cTnI in human sera/plasma.³⁸ Therefore, an enrichment step prior to LC-MS/MS analysis is needed to reduce the complexity, dynamic range and intrinsic interferences found in biological samples.

1.4. Limitations for LC-MS/MS detection of cTnI in serum

The human plasma proteome is complex and many factors are responsible for the difficulty in detecting low abundant proteins in clinical samples by LC-MS/MS. One major hurdle is the vast number of proteins and protein modifications that exist

in blood.⁴⁹ Another impediment to LC-MS/MS detection is the wide dynamic range of protein concentrations in blood. Protein concentrations in biological samples span greater than 10 orders of magnitude, ranging from mg/mL to pg/mL levels whereas current LC-MS/MS (triple quadrupole) only span 4-5 orders of magnitude.^{4,9} At the high abundance end, serum albumin (normal concentration 35-50 mg/mL) and immunoglobulins account for nearly 55 % and 17 %, respectively, of the blood plasma proteome by mass.^{4,73} Furthermore, 99 % of the total human plasma proteome is dominated by the 22 most abundant proteins including albumin and immunoglobulins. The remaining 1 % consists of low abundant proteins, such as tissue leakage proteins (e.g. the cardiac troponins) or other modified and degraded products.^{4,9,49,72,74} The high abundant proteins can dominate LC-MS/MS detection and may suppress or even prevent the detection of proteins at lower concentration levels.⁷⁴

1.5. Affinity purification strategies

Currently, LC-MS/MS (triple quadrupole) can detect proteins down to the 0.1-1 µg/mL range.^{28,75} However, most clinically relevant biomarkers are present in the mid pg/mL to low ng/mL range in serum or plasma and are below the lower limits of detection.⁵² Although LC-MS/MS technology continues to improve, front-end sample processing strategies are needed to enhance the overall sensitivity of LC-MS/MS-based assays and enable the detection of low abundant proteins. Different sample processing strategies utilizing affinity purification are discussed.

1.5.1. Immunodepletion enrichment strategy

Given the extremely wide dynamic range of protein concentrations in biological samples, immunoaffinity depletion of the top high abundant proteins (e.g. serum albumin and immunoglobulins) has become a popular strategy to decrease sample complexity.⁷⁶ Columns or cartridges containing immobilized antibodies are used to remove up to 58 high abundant proteins from plasma.^{77,78} By removing 90-95 % of the total protein mass, low abundant proteins are enriched.⁷⁶ For instance, combining immunodepletion along with strong cation exchange chromatography has been used to reduce the complexity of plasma samples prior to LC-MS/MS detection and has successfully lowered limits of quantification to the ng/mL range to measure clinically relevant biomarkers including some cardiovascular-related proteins.^{9,69,79-81}

While immunodepletion columns can deplete the most abundant interfering proteins efficiently, there are some caveats that must be considered. Proteins of interest can unintentionally bind to either the immunodepletion devices or to the depleted proteins (e.g. albumin or other abundant proteins) and negatively impact protein enrichment.^{69,82,83} In fact, cTnI has been shown to interact with abundant proteins retained on immunodepletion devices, resulting in low protein recovery.^{81,84} The low capacity of most immunodepletion devices is another potential limitation. Furthermore, using many antibodies to remove many high abundant proteins increases in cost.^{9,28,69,78,85} A better strategy includes enriching the low abundant protein or peptide target while simultaneously simplifying the sample matrix.⁶⁹

1.5.2. Immunoaffinity enrichment techniques

Selective enrichment of target proteins or surrogate peptides by immunoaffinity approaches is one of the most effective methods for the sensitive detection of low abundant proteins in complex samples. Immunoaffinity purification relies on the use of an antibody to capture and recover the analytes (protein or peptides) of interest from biological samples.^{86,87} A major advantage of this technique is the highly selective interaction between the antibody and antigen.⁸⁶ Antibodies consist of two identical heavy chains (F_c region) and two identical light chains (F_{ab} region) that are linked together by disulfide bonds. The F_c region is highly conserved within each antibody subclass, whereas the F_{ab} region is highly variable between different antibodies. This variability in the F_{ab} regions allows the antibodies to bind to a wide range of antigens.²⁹ The concept of immunoaffinity-based LC-MS/MS assays is similar to that of ELISAs because both rely on the use of antibodies to capture the target protein, but the LC-MS/MS acts analogously to the secondary, detection antibodies used within ELISAs.⁷⁶

The success of immunoaffinity capture depends heavily on which antibodies are used in the assay.⁸⁸ Not all antibodies have the same affinity or specificity for the protein/peptide of interest.⁸⁷ Antibodies can be produced in either monoclonal or polyclonal systems.⁸⁹ Monoclonal antibodies have higher specificity and recognize only one epitope on the antigen whereas polyclonal antibodies can detect multiple epitopes on the antigen. Due to the higher binding strength, monoclonal antibodies typically have higher affinity for their antigen than analogous polyclonal antibodies.^{29,89} Antigen-antibody binding is a result of a variety of noncovalent

interactions, which can result in association equilibrium (K_a) constants usually ranging from 10^5 - 10^{12} . Lowenthal et al.⁹⁰ determined the optimal capture antibody for cTnI (SRM 2921) by developing a quantitative LC-MS/MS method to evaluate the relative binding affinities of six pre-screened candidate monoclonal anti-cTnI antibodies. Clone 19C7 (HyTest, Finland) was selected as the capture antibody for future immunoaffinity development work due to its high binding affinity ($K_a = 10^7$) for intact cTnI. As such, this clone was used for protein immunoaffinity enrichment in this dissertation.

1.5.2.1. cTnI protein enrichment

Enrichment of cTnI can be performed at either the protein or peptide level. Anti-protein monoclonal antibodies, such as clone 19C7, can be used to capture intact cTnI in human plasma. Anti-cTnI antibody can be coupled to a solid support (e.g. magnetic particles) and incubated within a human plasma sample to capture cTnI. The captured proteins can be then released from the antibody and solid support by elution (e.g. change in pH) or denaturation (*in situ* with the magnetic particles during trypsin digestion).⁹¹ cTnI and any other associated proteins captured in the enrichment process can be analyzed by LC-MS/MS.⁶⁷ Monoclonal antibodies specific for human cTnI are readily available by several manufacturers due to the ongoing efforts to improve cTnI immunoassays.

1.5.2.2. cTnI peptide enrichment

As mentioned earlier, cTnI immunoassays have been confounded by a variety of interferences, including antireagent antibodies and endogenous autoantibodies. In contrast to the protein-based immunoaffinity strategy, the peptide enrichment-based approach avoids these types of interferences because the endogenous proteins are

destroyed by the tryptic digestion.^{28,89} Since protein measurements are usually performed at the peptide level, anti-peptide antibodies can be used as an alternative enrichment strategy to capture peptides of cTnI for protein quantification.⁷⁶ In 2004, Anderson et al.⁹² introduced this concept by using immobilized anti-peptide polyclonal rabbit antibodies to enrich four blood plasma proteins and their corresponding isotope-labeled peptide standards for ID-LC-MS/MS analysis.⁷⁶ In this initial demonstration, human plasma was digested, filtered, desalted and loaded onto a nanoliter-sized affinity column immobilized with anti-peptide antibodies. After loading/washing, the peptides were eluted and concentrated on a C₁₈-trap column for LC-MS/MS analysis.^{92,93} Anderson et al.⁹² reported an average 120-fold enrichment of the target peptides relative to nontargeted peptides for each protein. This peptide enrichment strategy coupled with the ID-LC-MS/MS approach is also known as “stable isotope standards (for use with) capture by anti-peptide antibodies” (SISCAPA).^{92,93}

Typically, polyclonal anti-peptide antibodies are custom produced for peptide enrichment instead of using monoclonal anti-peptide antibodies. Monoclonal antibody production for several surrogate peptides from the target protein is usually too expensive in terms of labor.⁸⁹ Polyclonal antibodies can be produced against a given target by attaching a peptide as a hapten to a carrier protein and injecting the conjugate into a laboratory animal (e.g. rabbit).^{29,89} A carrier protein, such as keyhole limpet hemocyanin (KLH), is needed because peptides are generally too small to be presented as antigens in mammals, and the carrier protein also serves as an adjuvant to help activate the immune system.⁸⁹ Contrary to monoclonal antibodies, polyclonal

antibodies can bind with various strengths and to a variety of epitopes on the antigen peptide.²⁹ However, some polyclonal antibodies may not have an affinity strong enough to enrich its target peptide. Additionally, the antibody production yield may be too small for method development and application purposes.⁸⁹

1.5.3. Magnetic particle-based separation

For the SISCAPA approach, Anderson's group initially implemented the nanoliter-capacity columns immobilized with anti-peptide antibodies to enrich low abundant plasma peptides, but later switched to magnetic particles as an alternative antibody solid support.⁹² Anderson et al.⁹⁴ noted several disadvantages with using affinity columns, which included sample-to-sample carry-over after column regeneration, concerns with binding kinetics and limited multiplexing for high throughput validation studies.⁹

Magnetic iron oxide particles coupled with antibodies have been demonstrated to effectively isolate and purify low abundant proteins from biological fluids. Magnetic particles are particularly effective solid supports for purification procedures because of their magnetic properties, high binding surface area-to-volume ratios and flexibility to handle large sample volumes.^{9,95,96} As depicted in Figure 1.6, magnetic separation of proteins or peptides typically involves mixing the magnetic particles

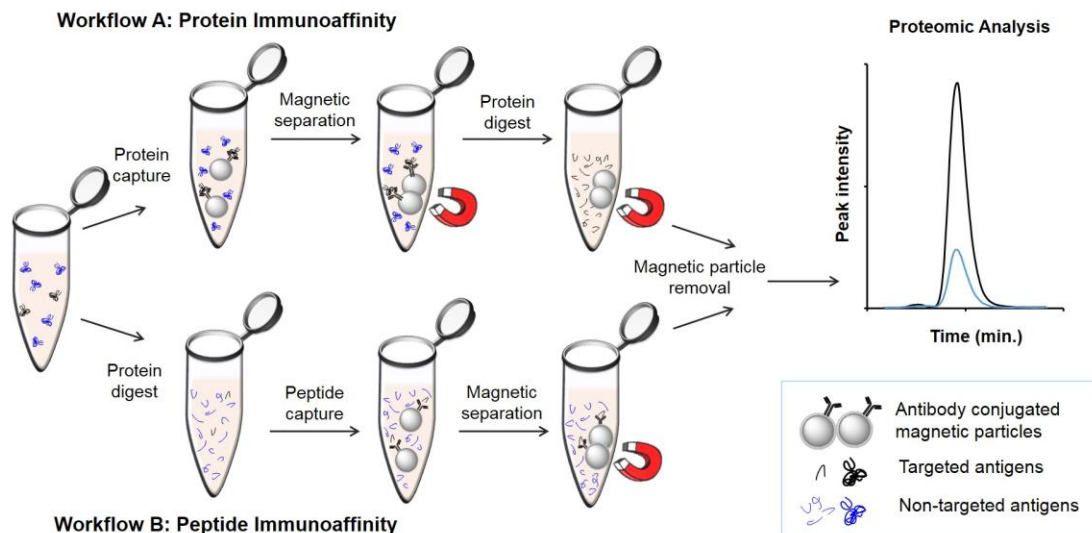


Figure 1.6 Immunoaffinity with magnetic particles can be performed by targeting protein or peptides for enrichment; followed by preparation for LC-MS/MS-based analysis. Workflow A entails capturing target proteins from biofluids by using anti-protein antibody. Workflow B entails capturing target peptides from a tryptic digestion of biofluids. Adapted with permission [9].

conjugated with antibodies within the biological sample. During incubation, the magnetic particles immobilized with antibodies can selectively capture antigens and be isolated from the rest of the sample using a magnetic separator, thereby enriching the target antigen for subsequent LC-MS/MS detection.⁹ The whole separation procedure can be performed in the same tube with few handling steps, allowing multiple samples to be processed in parallel.

Magnetic particles can be engineered with small diameters (1 nm -5 μ m), resulting in high surface area per unit volume. Additionally, the particle surface can easily be functionalized to ensure good stability and dispersion in solutions and allow for facile antibody immobilization.⁹⁵ Magnetic particle-based separation techniques have many advantages over the standard, non-magnetic separation procedures. The most obvious advantage of magnetic particles is their ease of manipulation and ability to be magnetized with inexpensive magnets.⁹⁷ Most magnetic particles behave with

paramagnetic characteristics and respond to an external magnetic field, but do not interact with each other in the absence of an external magnetic field.^{9,97,98}

Furthermore, magnetic particles enable fast kinetic processes in solution compared with bulk solid supports. Magnetic iron oxide particles conjugated with antibodies provide a simple, but effective way to enrich antigens from complex serum samples.⁹⁹

1.6. Proposed strategies to enrich cTnI for targeted LC-MS/MS analysis

In this work, an immunoaffinity strategy using magnetic nanoparticles is investigated to enrich cTnI from biological samples for LC-MS/MS-based analysis. In Chapter 2, we describe the methods used to prepare silica coated magnetic nanoparticles. In Chapter 3, we investigate antibody-magnetic particle conjugates for protein enrichment and develop a complementary LC-MS/MS-based method to evaluate different conjugations and magnetic particle supports. In Chapter 4, a protein-based immunoaffinity enrichment strategy combined with an ID-LC-MS/MS method is developed to capture and quantify cTnI from patient plasma samples. Chapter 5 presents preliminary work involving cTnI enrichment at the peptide level and discusses relevant challenges. This dissertation work is a part of a larger effort to use LC-MS/MS and magnetic particle-based immunoaffinity techniques to create a reference measurement procedure and a serum-based reference material for cTnI with the ultimate goal to improve clinical biomarker measurements.

Chapter 2: Synthesis of silica coated magnetic nanoparticles

This chapter has been reproduced in part with permission from: Schneck, N.A.; Phinney, K.W.; Lee, S.B.; and Lowenthal, M.S. Quantification of antibody coupled to magnetic particles by targeted mass spectrometry. *Anal. Bioanal. Chem.* doi:10.1007/s00216-016-9948-3 (2016).

2.1. Introduction

The increased use of magnetic-based separations in clinical diagnostics and other research applications has led to an array of commercially available and synthesized particles with different sizes and functionality types. For instance, micron-sized particles (i.e. microbeads) have been extensively used as immunomagnetic carriers for capturing protein biomarkers from biological samples because commercially available microbeads offer little size variability ($< \pm 5\%$) and are pre-coupled with surface functionalities for simple antibody immobilization.^{9,99} However, using magnetic particles smaller than 1 micron (μm) may achieve higher capture efficiency, especially for low abundant protein biomarkers, due to their relatively higher surface area-to-volume ratio.^{9,100} Currently, nanoparticles below 200 nanometer (nm) are commercially available, but are not monodisperse.

Several chemical methods have now been developed to synthesize magnetic iron oxide nanoparticles of various sizes (1 nm- 1 μm) on a small batch scale for a wide range of applications. In-solution chemical methods for preparing magnetic nanoparticles include co-precipitation, thermal decomposition, and hydrothermal, and polyol processes.^{101,102} The polyol-mediated synthesis is advantageous because this approach is capable of producing hydrophilic iron oxide nanoparticles with high yields, high magnetization and controllable sizes.^{103,104}

In the polyol process, iron oxide nanoparticles are synthesized by modified reduction reactions between a metal salt (e.g. $\text{FeCl}_3 \cdot 6\text{H}_2\text{O}$) and a polyol (e.g. ethylene glycol) at refluxing temperatures. In a typical method, $\text{FeCl}_3 \cdot 6\text{H}_2\text{O}$ is used as the iron precursor and ethylene glycol acts as both a polyol and a strong reducing agent in the presence of sodium acetate and water.^{103,105} Sodium acetate plays an important role in the formation of spherical particles acting as a hydrolysis agent, an alkali and an electrostatic stabilizing agent to prevent particle aggregation.¹⁰⁶

Several groups have studied the formation mechanism of magnetic particles using $\text{FeCl}_3 \cdot 6\text{H}_2\text{O}$ as the iron source and ethylene glycol for the polyol process.^{103,107,108} Iron oxide particles are formed by a two-stage nucleation and growth process in the polyol method. In the nucleation stage, ethylene glycol reduces a portion of Fe^{3+} ions to a lower valence state (Fe^{2+}) at high temperatures. Meanwhile, the hydrolysis of sodium acetate provides an alkaline environment and forces hydrolysis of the metal ions to form $\text{Fe}(\text{OH})_3$ and $\text{Fe}(\text{OH})_2$.^{106,107} Subsequently, the metal hydrates undergo dehydration (condensation) and transform into Fe_3O_4 nanocrystals. Compared to other polyols, ethylene glycol has a lower reductive potential, which slows the formation and growth rate of the iron oxide nanoparticles.¹⁰³ During the formation process, the nanocrystals have enough time to rotate with neighboring nanocrystals to obtain a stable surface energy.^{103,106} Therefore, after nucleation is achieved, the primary magnetite nanocrystals tend to aggregate into larger secondary nanoparticles via oriented attachment. In the second growth stage, the iron oxide nanoparticle clusters can then grow based on Ostwald ripening.^{103,106,110} The advantage of the polyol approach is the ability to prepare

hydrophilic nanoparticles of different sizes by either changing the polyol, concentrations of the starting materials or reflux time.

Maximum coverage of antibodies is often observed for magnetic particles with diameter sizes around 50 nm, which is approximately five times the diameter of an antibody.²⁹ The size range of the magnetic particles should also account for the binding of immobilized antibody to a medium-sized target, such as cTnI (cTnI: 24 kDa, cTnI-cTnC binary complex: 42 kDa, ternary complex: 77 kDa). Furthermore, the magnetic property of iron oxide nanoparticles is strongly dependent on size.¹¹¹ Too small of a particle size may lower or cease magnetic response, making the magnetic particle-based capture inefficient.¹⁰⁰ Therefore, a compromise between particle diameter/surface area and sufficient magnetic properties is necessary to achieve nanoparticles with sizes similar to protein molecules (i.e. ≈ 75 nm in diameter), as well as, high enough magnetic susceptibility for fast and complete separations.¹¹²

In addition to high magnetic properties, magnetic carriers for immunoaffinity enrichment must have good biocompatibility and interactive functions at the surface. For that reason, the surfaces of the nanoparticles are typically modified with a polymer or silica. The nonmagnetic outer shell also helps stabilize colloidal dispersion and provides facile attachment of surface functional groups needed for different bioconjugation methods.^{9,99,100,113} A popular approach to coat magnetic particles with silica involves the Stöber sol-gel process, which is based on hydrolysis and the polycondensation of an alkoxysilane (e.g. tetraethylorthosilicate, TEOS).¹¹⁴⁻
¹¹⁶ As will be discussed in Chapter 3, the silica shell also provides reactive hydroxyl

surfaces, or silanol groups, that can allow for facile functionalization with silane coupling agents.¹¹⁵ It has been reported that the efficiency of silane bonding increases when the nanoparticles are coated with a layer of silica.¹¹⁷ Silane coupling agents with various functional groups can be utilized to immobilize antibody to the magnetic nanoparticles for immunoaffinity enrichment.¹¹³ Therefore, the final step in the synthesis of magnetic nanoparticles will involve a silica coating process.

In this chapter, we demonstrate the preparation of silica coated paramagnetic iron oxide nanoparticles using a facile and economic synthesis strategy. We focus on controlling the size of the magnetic nanoparticles by changing the water concentration in the initial reaction conditions. Finally, the nanoparticles are coated with a thin silica shell to allow easy surface modification.¹¹² This work resulted in an important method for obtaining hydrophilic, biocompatible iron oxide nanoparticles for effective magnetic bioseparations.

2.2. Experimental method

2.2.1. Preparation of magnetic iron oxide nanoparticles

In a typical synthesis, iron (III) chloride hexahydrate, $\text{FeCl}_3 \cdot 6\text{H}_2\text{O}$ (0.25 g, 0.025 M), sodium acetate (0.44 g, 0.125 M) and water (1.5 g, 2 M) were dissolved in 40 mL ethylene glycol and refluxed for 7 hrs. The nanoparticles were magnetically separated from solution and thoroughly rinsed with water and ethanol. The nanoparticles were dried at 100 °C for 2 hours. Overall, 70 milligrams (mg) of magnetic nanoparticles were obtained after drying.

2.2.2. Silica coating of magnetic iron oxide nanoparticles

The silica coating procedure was described previously.¹¹⁸ Bare magnetic nanoparticles (30 mg) were dispersed in water (30 mL, pH 4) and ultrasonicated for 10 minutes. The water was decanted and a mixture (60 mL) of ethanol/water/ammonium hydroxide (70 % / 17 % / 13 % volume fractions, v/v/v) was added to the nanoparticles; followed by the addition of 40 μ L of TEOS. The magnetic nanoparticles were sonicated in the resultant mixture for 30 minutes, and washed with ethanol and water. The silica magnetic nanoparticles were dried and stored at 4 °C.

2.2.3. Characterization of silica coated magnetic nanoparticles

The size and morphology of the bare and silica coated magnetic nanoparticles were investigated with a field emission gun transmission electron microscope (TEM; JEOL JEM 2100F) operated at 200 kV. Before drying, the silica coated magnetic nanoparticles were reconstituted in 30 mL water (final concentration: 1 mg/mL) and a 500 μ L aliquot was added to 20 mL water. The solution was ultrasonicated for 10 minutes. The nanoparticles were then dispersed in 50:50 ethanol/water mixture and a drop of sample solution was placed on a formvar/carbon-coated copper TEM grid. ImageJ software was used to analyze the size of the nanoparticles.

2.3. Results and discussion

2.3.1. Influence of water concentration on nanoparticle size and morphology

Several previous studies have investigated the polyol-mediated mechanism of iron oxide particles using ethylene glycol as the common reaction medium.^{103,107,108}

Various factors in the initial reaction conditions are known to influence the size and morphology of the particles. For instance, synthesis parameters, such as the concentration of reagents and reflux time, affect the size and shape of the particles. Furthermore, a higher concentration of sodium acetate and water can decrease the particle size.^{107,108} By increasing the overall hydroxyl concentration, the hydrolysis rate of FeCl_3 can be accelerated to generate a larger number of smaller particles.^{107,110} Based on those observations, various concentrations of water ranging from 2.0 M to 3.2 M were added to the polyol medium to investigate the effect of hydrolysis and the size of the nanoparticles. While keeping other reaction conditions constant, the size of the iron oxide particles significantly decreased as the water concentration increased from 2.0 M to 3.2 M, which is shown in Figure 2.1. The sizes of the bare iron oxide nanoparticles ranged from 25 nm to 120 nm. However, as seen in Figure 2.1. (c) and (d), a higher water concentration resulted in irregular shaped and more aggregated nanoparticles, with a wider particle size distribution. The irregular shape and wide size distribution may be caused by hydrolysis/condensation occurring too fast for the nanocrystals to uniformly orient into the nanoparticle clusters.¹¹⁹ These results demonstrate that water can be used as an additive to decrease the size of iron oxide nanoparticles grown by the polyol method.

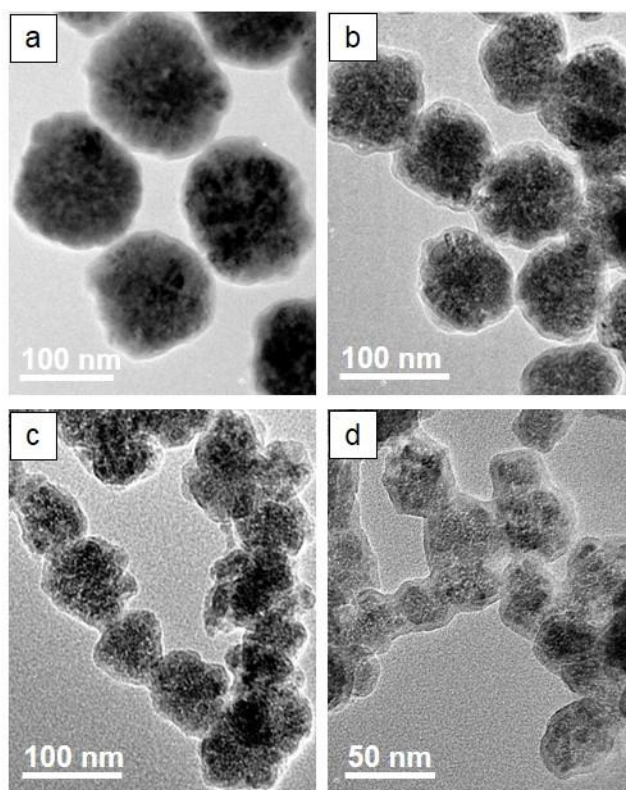


Figure 2.1 TEM images of the silica coated magnetic nanoparticles prepared with the same molar ratios of FeCl_3 : sodium acetate (0.025 M: 0.13 M) and varying concentrations of water (a) 1.3 M, (b) 2.0 M, (c) 2.6 M, and (d) 3.2 M.

2.3.2. Coating magnetic nanoparticles with silica

The magnetic nanoparticles were coated with a thin silica layer using a previously described protocol.¹¹⁸ Adding a silica layer improves the stability of the nanoparticles in solution and provides reactive silanol groups for covalent bonding of various functionalization molecules. A very thin silica layer was sought since the nonmagnetic silica layer lowers the magnetic property and surface area-to-volume ratio of the magnetic nanoparticle. The thickness of the silica shell was controlled by changing the concentration ratio of TEOS to magnetic nanoparticles. Sonication was used to minimize aggregation between nanoparticles prior to and during the coating

process to avoid trapping multiple nanoparticles in a single silica shell. As the concentration ratio of TEOS to iron oxide nanoparticles decreased from 3.8 to 1.2, the thickness of the silica shell decreased from ≈ 30 nm to ≈ 5 nm. Figure 2.2 (b)-(d) shows the TEM images of magnetic nanoparticles whose surfaces have been coated with silica using different ratios of TEOS to a bulk amount of nanoparticles. It was

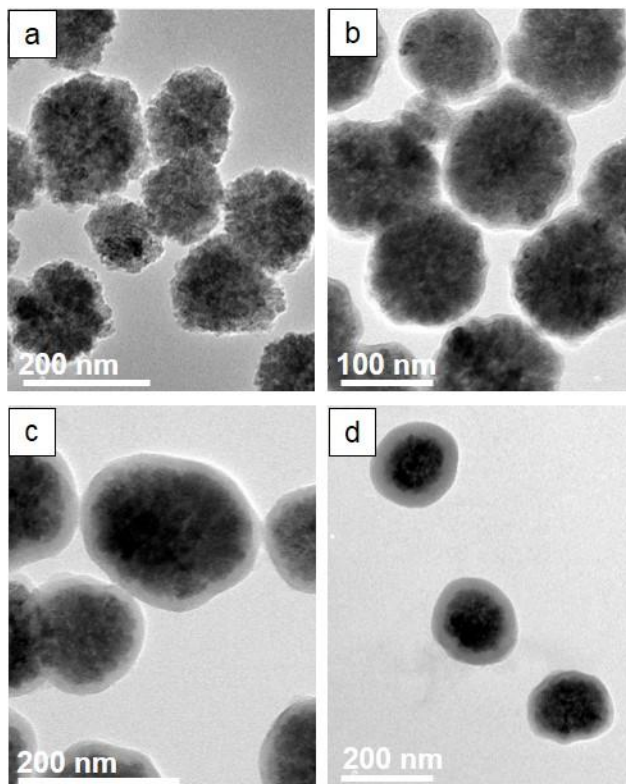


Figure 2.2 TEM images of (a) bare nanoparticles and (b)-(d) nanoparticles whose surfaces have been coated with as silica shell of various thicknesses. The thickness of the shell was adjusted by changing the concentration of TEOS to magnetic nanoparticles (b) 1.2, (c) 1.9, and (d) 3.8.

most convenient and reproducible to adjust the shell thickness by changing the ratio of TEOS to nanoparticles, but other parameters, such as growth time, could have been changed to control the thickness of the silica shell. The nanoparticles coated with a ≈ 5 nm silica shell, as shown in Figure 2.1. (b), were prepared for future immunoaffinity enrichment experiments.

Overall, the ultimate synthesis method produced silica coated magnetic nanoparticles with an average diameter of $\approx 85 \pm 10$ nm. Figure 2.3 shows the histogram of the particle size distribution with the corresponding TEM image. Additionally, the nanoparticles were stable and dispersible in aqueous buffered solution when rotary mixed and easily manipulated when an external magnet was applied.

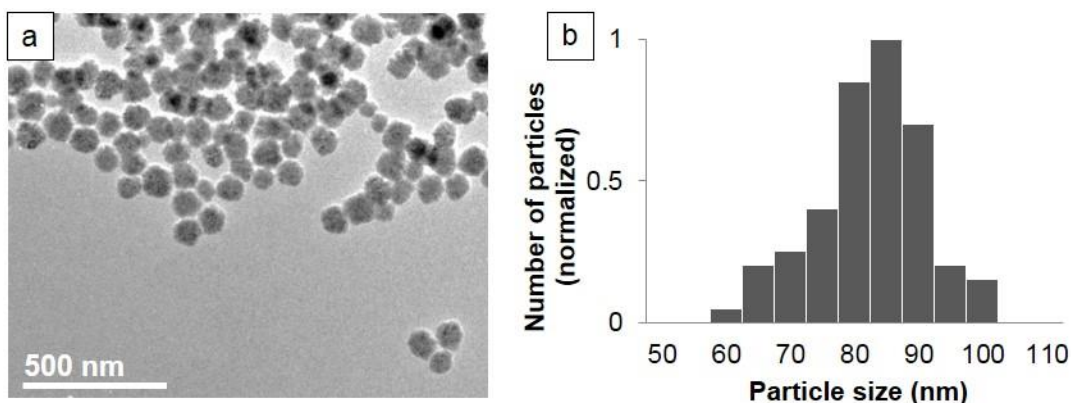


Figure 2.3 (a) TEM images of silica coated magnetic nanoparticles, and (b) the histogram of particle size distribution.

2.4. Conclusion

Magnetic nanoparticles were prepared by a facile, one-pot inexpensive polyol process with tunable diameters ranging from 25 nm to 120 nm. The average size of the magnetic nanoparticles could be decreased by increasing the concentration of

water added to the synthesis. The bare magnetic nanoparticles were coated with silica to improve the surface reactivity of the nanoparticles for further antibody functionalization. The thickness of the silica surface layer was controlled by varying the concentration ratio of TEOS to magnetic nanoparticles. Silica coated magnetic nanoparticles with an average size of 85 nm exhibited a narrow size distribution, paramagnetism and good dispersion in water, which are all important attributes for protein enrichment applications.

Chapter 3: Quantification of anti-cTnI antibody bound to magnetic particles by LC-MS/MS

This chapter has been reproduced in part with permission from: Schneck, N.A.; Phinney, K.W.; Lee, S.B.; and Lowenthal, M.S. Quantification of antibody coupled to magnetic particles by targeted mass spectrometry. *Anal. Bioanal. Chem.* doi:10.1007/s00216-016-9948-3 (2016).

3.1. Introduction

For antibody immobilization, silica coated magnetic nanoparticles need to be functionalized with reactive surface groups that can covalently bind to the target antibody. The most commonly employed method for surface modification of silica coated magnetic nanoparticles is silanization of a functional moiety, which involves reacting an organosilane coupling reagent with the silica surface to produce a covalent bond.^{116,117,120-122} Magnetic particles can be modified with a variety of surface functionalities (e.g. terminal amine, aldehyde, epoxy groups) using organosilane reagents.^{97,99} For example, an aminosilane, such as 3-aminopropyltriethoxysilane (APTES), can be coupled to the surface of the nanoparticle and the terminal amino group can be further reacted with glutaraldehyde to act as a crosslinker. Antibodies can then be immobilized irreversibly onto the glutaraldehyde-activated particles via an amide bond between the amino groups of the antibody and the aldehyde of the crosslinker.²⁹ Epoxysilane modification of the magnetic nanoparticles via glycidyloxypropyltrimethoxysilane (GPTMS) is another preferred method to covalently immobilize antibodies in a convenient, one-step reaction.^{122,123} Figure 3.1 shows a schematic of functionalizing amine and epoxy groups onto silica coated magnetic nanoparticles for subsequent antibody conjugation.

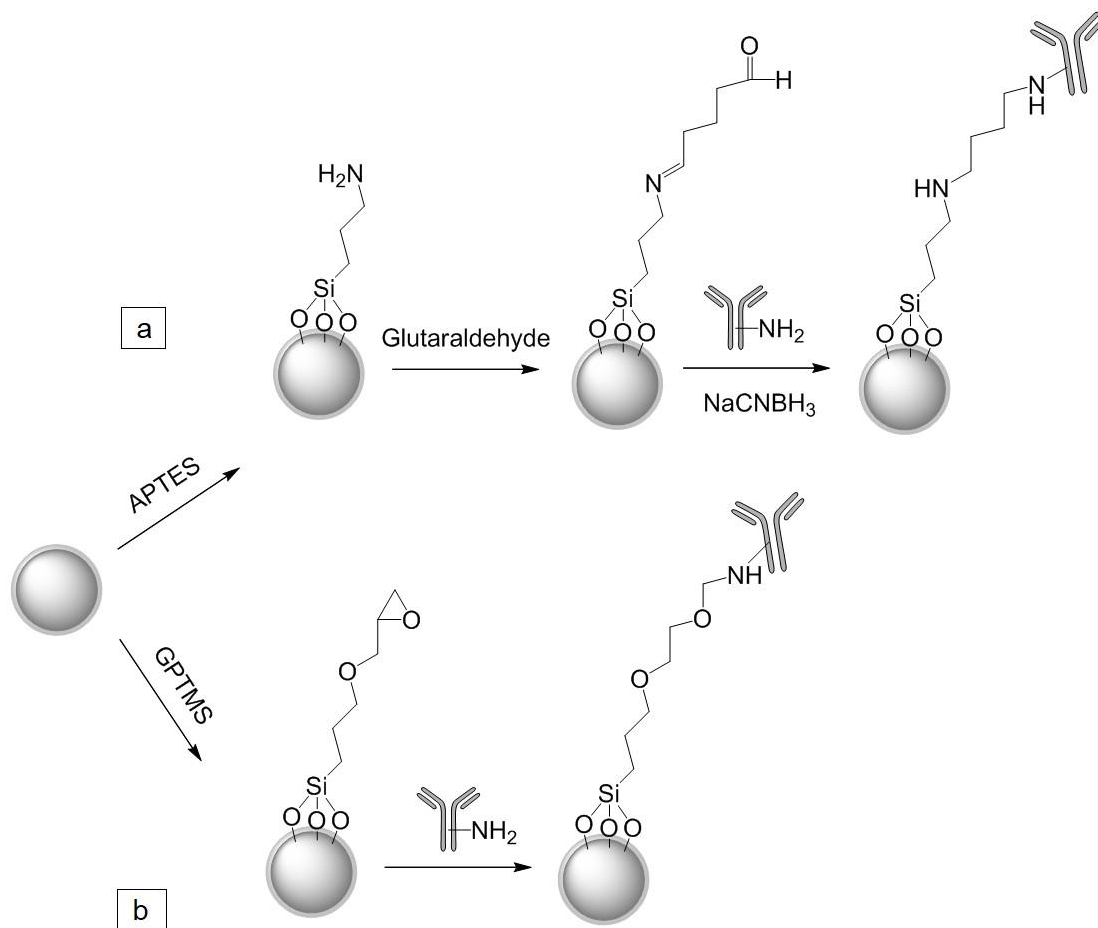


Figure 3.1 Schematic depicting the functionalization of silica coated magnetic particles with common coupling agents, (a.) APTES or (b.) GPTMS, to covalently attach antibody by either a glutaraldehyde-activated or epoxide coupling reaction. NaCNBH_3 = sodium cyanoborohydride.

The numerous routes to antibody immobilization makes reliable prediction of antibody loading capacities difficult. Many factors, such as the physiochemical properties of the antibody and magnetic particles, the antibody immobilization method and surface functionality of the magnetic particles, can certainly influence the performance of the enrichment. Moreover, adequate amounts of antibody conjugated to the surface of magnetic particles is a key factor for efficient protein capture. To quantitatively control for variabilities in particle type, surface modification and

antibody immobilization strategy, it is important to develop general analytical methods to accurately quantify the amount of bound antibody.

Protein assays, such as bicinchonic acid assay and UV-visible spectrophotometry have been used frequently for quantifying antibody immobilized to magnetic particles.¹²⁴⁻¹²⁷ However, these methods require that the magnetic particles first be removed from the sample because the magnetic particles and excess surface ligands can interfere with the analysis and cause inaccurate readings.¹²⁴ Therefore, the amount of immobilized antibody is inferred by measuring the amount of unbound antibody in the supernatant washes.^{124,126} Other semi-quantitative approaches include western immunoblotting and polyacrylamide gel electrophoresis, which rely on external calibrants for quantification.¹²⁷ However, incorporating an internal standard control is preferred because it can decrease measurement variability and improve precision both within and between measurement assays. The ID-LC-MS/MS methodology utilizing MRM can be employed to quantify specific tryptic peptides derived from the protein and is not subject to biases, such as, differences in molar absorptivity or protein size. As described in Chapter 1.3, the peptides can be quantitated against a spiked internal standard (i.e. synthetic, stable-isotope labeled peptides) to determine protein concentrations. A sensitive ID-LC-MS/MS method that can accurately measure antibody loading and is less subject to interference can greatly improve the evaluation of various antibody-magnetic particle conjugates.

Here we present the development of a quantitative ID-LC-MS/MS method to directly measure the amount of antibody immobilized onto magnetic particles, which is independent of magnetic particle type or immobilization strategy. Synthesized

magnetic nanoparticles, described in Chapter 2, are activated with glutaraldehyde or epoxy surface groups to conjugate anti-cTnI antibody. In order to compare antibody coupling efficiency, commercial microparticles pre-functionalized with either amine or epoxy groups are also used to conjugate anti-cTnI antibody using the same binding chemistries. As predicted, the results demonstrate that nanoparticles more efficiently bind antibody when compared to microparticles due to the larger surface area per unit mass of the nanoparticles. Furthermore, this ID-LC-MS/MS method is applied to evaluate the anti-cTnI antibody-magnetic particle coupling process as part of method optimization to ultimately improve cTnI enrichment and subsequent LC-MS/MS detection.

3.2. Materials and methods

3.2.1. Materials

Monoclonal mouse anti-cTnI antibody 19C7 was purchased from HyTest Ltd. (Turku, Finland). The synthetic isotopically labeled peptides, DLPSPIER and TDSFSCNVR, were purchased from AnaSpec, Inc. (San Jose, USA). Dynabeads® M-270 Amine and Dynabeads® M-270 Epoxy were purchased from Life Technologies (New York, USA). The silane reagents, APTES and GPTMS, were purchased from Gelest, Inc. (Pennsylvania, USA). Rapigest™ SF was purchased from Waters Corporation (Massachusetts, USA) and sequencing grade modified trypsin was purchased from Promega Corporation (Wisconsin, USA). High purity LC-MS grade water (H₂O)/formic acid and acetonitrile (ACN) /formic acid were purchased from Honeywell-Burdick and Jackson (Michigan, USA). All other chemicals were purchased from Sigma-Aldrich (Missouri, USA).

3.2.2. Conjugation of antibody to various functionalized magnetic particles

3.2.2.1. Surface modification of the silica coated magnetic nanoparticles

Silica coated magnetic nanoparticles (1 mg) were treated with 10 % APTES in ethanol/water (95 % / 5 % v/v) solution and allowed to react for 30 minutes with end-over-end rotation. The amine functionalized nanoparticles were washed with ethanol and water. The same procedure was also carried out using GPTMS to prepare epoxy functionalized nanoparticles. Calculations to determine the theoretical maximum number of silane groups per bulk amount of particles were performed, which corresponded to the number of functional groups available for antibody binding.¹²⁸

3.2.2.2. Antibody coupling to the amine-modified magnetic particle

Amine functionalized nanoparticles and microparticles (1 mg nanoparticles and 33 μ L of 30 mg/mL Dynabeads M-270 Amine; 2.8 μ m bead size) were treated with 2 % (v/v) glutaraldehyde in phosphate buffer solution (PBS, pH 7.4). The magnetic particles were rotary mixed for 2 hours and washed three times with PBS. The particles were redispersed in PBS and anti-cTnI antibody. The magnetic particles were gently vortexed and sodium cyanoborohydride (final: 50 mmol/L) was added. The magnetic particles were mixed using a rotary mixer for approximately 24 hours. After immobilization, the antibody-magnetic particle conjugates were washed several times with PBS and once with ammonium bicarbonate to remove any unreacted antibodies.

3.2.2.3. Antibody coupling to epoxy-modified magnetic particles

Epoxy functionalized nanoparticles and microparticles (1 mg nanoparticles and 1 mg freeze-dried Dynabeads M-270 Epoxy; 2.8 μ m bead size) were treated with

sodium phosphate buffer and incubated for 10 minutes with rotary mixing. The particles were washed with sodium phosphate buffer and resuspended in the same buffer. Anti-cTnI antibody was added, followed by the addition of ammonium sulfate (final: 1 mol/L). The reaction mixture was allowed to incubate for 24 hours with rotary mixing. After antibody immobilization, the magnetic particles were washed several times with PBS and once with ammonium bicarbonate.

3.2.3. Calibrant preparation

External calibrant solutions were prepared at two different ranges for the nanoparticle sets and microparticle sets, respectively. The magnetic particle sets were carried through the identical functionalization procedures to achieve matrix-matched calibration solutions, but were reconstituted with anti-cTnI antibody and ammonium bicarbonate (total volume 50 μ L) prior to digestion. Calibrants were not washed after adding antibody to ensure complete recovery. Anti-cTnI antibody (0.2 μ g/mL) was added at five different levels ranging from 1 μ g to 8 μ g to the functionalized magnetic microparticles (1 mg). Calibration solutions for the functionalized magnetic nanoparticle sets were prepared by adding anti-cTnI antibody (2 μ g/mL) at five different levels ranging from 10 μ g to 100 μ g.

3.2.4. Sample processing for ID-LC-MS/MS analysis

Calibrants and samples were digested with modified porcine trypsin without magnetic particle removal. The samples were denatured with 0.1 % RapigestTM SF in 50 mmol/L ammonium bicarbonate (100 μ L) and boiled for 2 minutes. The antibodies were reduced with a final concentration of 5 mmol/L dithiothreitol (DTT) at 60 °C for 45 minutes and alkylated with 15 mmol/L iodoacetamide (IAM) in the dark at room

temperature for 45 minutes. Trypsin was added to the samples (1:10 w/w trypsin-to-protein ratio) and all samples were incubated for 16 hours at 37 °C. The digests were acidified with a final concentration of 5 % (v/v) formic acid for 45 minutes at 37 °C and centrifuged at 4 °C to remove the Rapigest™ SF and the magnetic particles. The digests were dried using a vacuum centrifuge.

Dried peptides were reconstituted in 20 µL LC/MS grade H₂O / 0.1 % (v/v) formic acid containing labeled peptides corresponding to the constant region of anti-cTnI antibody. Isotopically labeled peptides (DLPSPIE[¹³C₅,¹⁵N]R and TDSFSC[CH₂CONH₂]NV[¹³C₅,¹⁵N]R) were prepared at constant concentrations for each magnetic particle support (1.9 µg/µL for nanoparticles and 0.14 µg/µL for microparticles). An additional 230 µL LC/MS grade H₂O / 0.1 % (v/v) formic acid was added to the nanoparticle sample set to dilute final protein concentrations similarly to the microparticle sample set (0.05 µg/µL to 0.5 µg/µL).

3.2.5. ID-LC-MS/MS analysis

After equilibration, 8 µL of sample was injected for each LC-MS/MS run. LC-MS/MS analysis (duplicate injections) was performed on an Agilent 1200 LC system coupled in-line with an Agilent 6490 triple quadrupole MS. For the peptide measurements, LC separation was performed at a flow rate of 200 µL/min on a Zorbax (Agilent) SB-C₁₈ reversed-phase analytical column (2.1 mm x 150 mm, 3.5 µm particles) at 45 °C using an increasing linear gradient of organic/aqueous solvent (ACN/H₂O containing 0.1 % (v/v) formic acid) starting at 5 % organic up to 70 % organic over 20 minutes, followed by a column wash and re-equilibration. The MS was operated in a positive-ion polarity. MRM transitions were predetermined using a

predicted amino acid sequence and a predictive MRM software tool (Skyline).⁵⁵ Potential tryptic peptides and MRM transitions were assembled for MRM screening to determine the most intensive fragmentation transitions for the IgG_{2b} isotype. Fragmentation transitions were optimized and monitored for each IgG_{2b} peptide. Source and fragmentation parameters were kept identical for analogous isotopically labeled and unlabeled peptides. Peak areas were integrated using MassHunter Qualitative Analysis B.06.00 software.

3.2.6. LC-MS/MS antibody sequence analysis for peptide selection

LC-MS/MS sequencing analysis was used to identify the antibody subclass (i.e. IgG₁, IgG_{2a}, IgG_{2b}) of monoclonal mouse anti-cTnI antibody 19C7. Antibody was digested with trypsin, as described in Section 3.2.4, and analyzed using a Thermo Dionex UltiMate 3000 LC system coupled to a Thermo Scientific hybrid LTQ linear ion trap-Orbitrap Elite MS/MS. The antibody digest (1.5 µg) was loaded onto a Zorbax (Agilent) SB-C₁₈ reversed-phase analytical column (2.1 mm x 150 mm, 3.5 µm particles) via autosampler. Peptide elution was achieved over a 55-minute linear gradient of organic/aqueous solvent (ACN/H₂O containing 0.1 % (v/v) formic acid) increasing from 5 % organic to 50 % organic over 55 mins, followed by a column wash and re-equilibration. Column temperature was maintained at 35 °C. MS data was collected in the Orbitrap mass analyzer using data dependent mode with one cycle of experiments consisting of one full-MS scan (400 *m/z* to 2,000 *m/z*, resolution = 30,000), followed by MS/MS data collection in the LTQ linear ion trap of the five most intense precursor peaks (Resolution = normal) with dynamic exclusion enabled. CID fragmentation was performed using a normalized collision energy of 35,

activation Q of 0.250, and activation time of 10 ms. Source conditions were as follows: heater temperature = 275 °C, sheath gas flow rate = 30 units, auxiliary gas flow rate = 5 units, spray voltage = 3500 V, capillary temperature = 350 °C, and S-lens RF level = 60 %.

MS data was interpreted using the Sequest HT algorithm (built into the Proteome Discoverer v1.3 software suite). Data was searched for peptides with variable modifications including cysteine carboxyamidomethylation (+57.021 Da) and methionine oxidation (+15.999 Da) using a mammalian UniProt protein database.

3.3. Results and discussion

3.3.1. ID-LC-MS/MS method development

The approach used for quantifying bound antibody on magnetic particles by ID-LC-MS/MS is depicted in Figure 3.2. After antibody immobilization, the

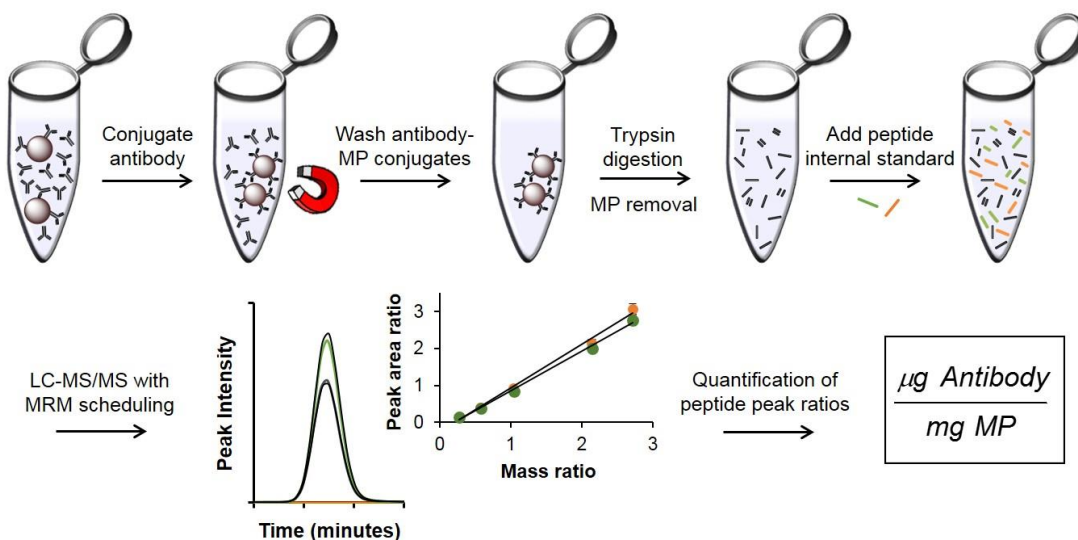


Figure 3.2 Schematic illustration of the ID-LC-MS/MS-based workflow to directly measure antibody bound to magnetic particles (MP).

antibody-magnetic particle conjugates were thoroughly washed to remove non-specifically adsorbed antibodies. The immobilized antibodies were digested with trypsin (*in situ* with the magnetic particles), spiked with internal standard, and directly analyzed by LC-MS/MS. Matrix-matched external calibrants consisting of antibody and internal standard were also prepared appropriately for quantitative analysis. ID-LC-MS/MS analysis was achieved through the use of isotopically labeled standards for protein quantification. Tryptic peptides from the constant region of the anti-cTnI antibody, part of the IgG_{2b} isotype subclass⁹⁰, were selected to act as the internal standard for quantification. Specific peptides were chosen by analyzing a tryptic digest of the antibody using an ion trap MS/MS. Figure 3.3 shows a total ion chromatogram of the digested sample, as well as, the extracted ion chromatograms of two tryptic antibody peptides and their corresponding MS/MS fragmentation patterns. Based off of this MS/MS data, these two tryptic peptides (DLPSPIER and TDSFSC[+57]NVR) and corresponding MRM transitions were assembled for initial MRM screening using a triple quadrupole MS/MS.⁵⁵ Initially, potential tryptic peptides were selected based on the following criteria: possess uniqueness to the constant region of IgG_{2b} isotype, possess high enough MS/MS signal intensity, contain 8-10 amino acid residues, and not contain amino acid residues susceptible to chemical modification, such as cysteine or methionine residues. However, during MRM screening, it was observed that the criteria had to allow tryptic peptides with amino acids susceptible to fixed chemical modifications so that more than one peptide could be used for antibody quantification. Two heavy isotope labeled synthetic peptides (DLPSPIER and TDSFSCNVR) were purchased to be used as internal

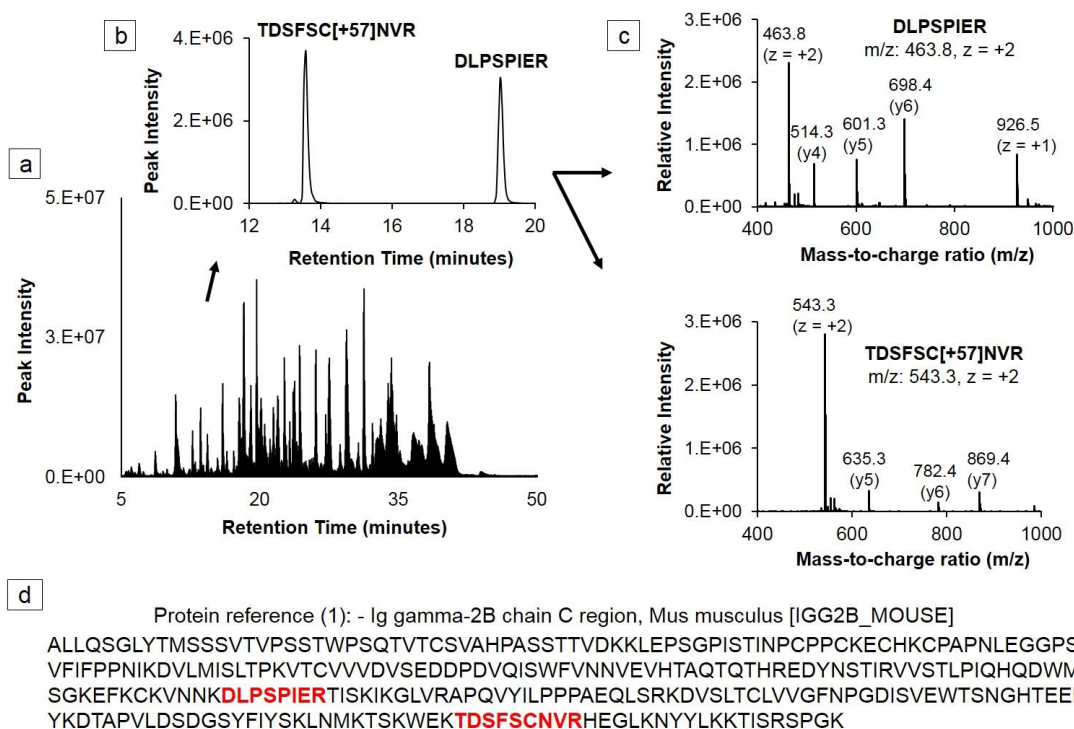


Figure 3.3 (a) Total ion chromatogram (TIC) of a tryptic digest of anti-cTnI antibody. Analysis of the digest was performed by LC-MS/MS (ion trap) and searched against a mammalian protein database using Sequest HT (Proteome Discover). (b) Two tryptic antibody peptides were selected based on signal intensity in the extracted ion chromatograms (subset) within the TIC trace. (c) MS/MS spectra of DLPSPIER and TDSFSC[+57]NVR (d) Amino acid sequence of the antibody constant region. The two target peptides used for antibody quantification are indicated in red font. The sequence was obtained from the National Center for Biotechnology Information protein database.

standards. TDSFSCNVR contained a cysteine residue that was alkylated with IAM by the manufacturer. In the procedure, antibodies were reduced with DTT and alkylated with IAM prior to digestion. IAM is a highly efficient alkylating agent that reacts with the free sulfhydryl groups of cysteine residues causing a fixed carboxyamidomethylation modification on cysteine.¹²⁹ To ensure complete alkylation of the TDSFSCNVR peptide, MRM transitions for both alkylated and non-alkylated versions of the peptide were monitored. MRM signals from non-alkylated (unlabeled) TDSFSCNVR were negligible in all sample sets (reaching a level of only 0.3 % of the maximum peak intensity); therefore, no correction for alkylation efficiency was

applied during data analysis. LC-MS/MS parameters for MRM analysis of the antibody peptides (unlabeled and labeled) were optimized and summarized in Table

3.1. Two suitable transition pairs were chosen for MRM analysis of each peptide.

Table 3.1 Optimized fragmentation parameters for MRM analysis of antibody peptides. The fragmentor voltage was set at 380 V. Labeled residues (indicated with an asterisk) contained ^{13}C and ^{15}N isotopes. The cysteine amino acid (AA) residues in the unlabeled and labeled TDSFSCNVR peptides were alkylated by the manufacturer, which increased the mass by 57 daltons.

Peptide AA sequence	Precursor Ion (m/z)	Product Ion (m/z)	Collision Energy (V)
DLPSPIER	[463.8] $^{2+}$	[514.2] $^{+}$	17
		[698.3] $^{+}$	7
DLPSPIE*R	[466.8] $^{2+}$	[520.2] $^{+}$	17
		[704.2] $^{+}$	7
TDSFSC[+57]NVR	[543.4] $^{2+}$	[635.3] $^{+}$	16
		[869.4] $^{+}$	14
TDSFSC[+57]NV*R	[546.4] $^{2+}$	[641.3] $^{+}$	16
		[875.4] $^{+}$	14
TDSFSCNVR	[514.7] $^{2+}$	[578.4] $^{+}$	16
		[812.4] $^{+}$	14

3.3.2. Antibody quantitation on magnetic particles

Antibodies immobilized onto magnetic particles by two different conjugation methods were analyzed using ID-LC-MS/MS with MRM detection. Figure 3.4 shows a representative MRM trace of the transitions monitored for the targeted peptides and corresponding isotopically labeled internal standard peptides. Target peptide peak areas were normalized to the peak area of the isotopically labeled peptide. Peak detection and integration were determined based on the following criteria: (1) similar retention times among the MRM peaks of the unlabeled and labeled peptides and (2) similar peak shape and peak intensity ratios among the MRM transitions between the unlabeled and labeled peptides. Ratios of the unlabeled and labeled MRM peak areas

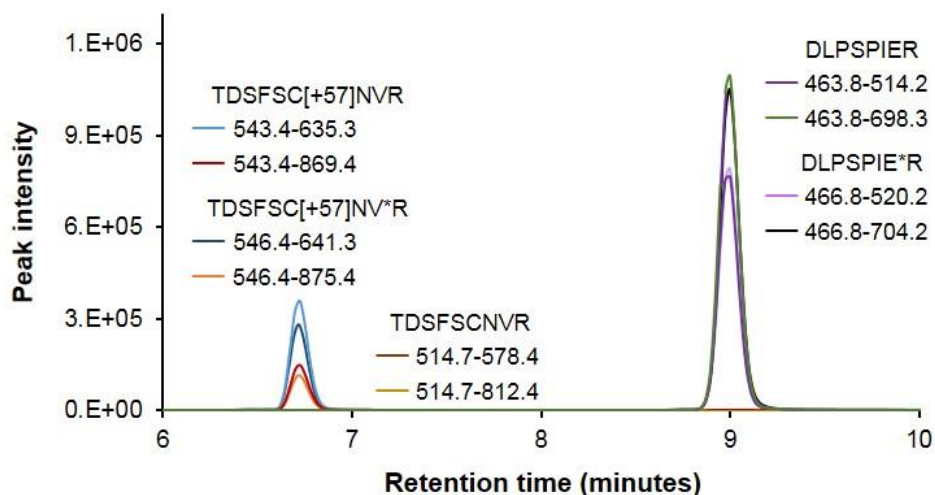


Figure 3.4 Representative extracted ion chromatogram for quantification of immobilized antibody using the glutaraldehyde coupling protocol with amine functionalized magnetic nanoparticles. Two transitions for the unlabeled and labeled targeted antibody peptide (TDSFSC[+57]NVR and DLPSPIER) were monitored, along with two transitions of the unlabeled TDSFSCNVR to monitor alkylation efficiency. Asterisk indicates the isotopically labeled amino acid.

were determined by integrating extracted ion chromatograms of each transition. As shown in Figure 3.5, calibration curves for each magnetic particle support were linear over the concentration range 0.05 $\mu\text{g}/\mu\text{L}$ to 0.5 $\mu\text{g}/\mu\text{L}$ with correlation coefficients (R^2) > 0.97 . Antibody concentrations were back-calculated against the linear equation and multiplied by the known amount of internal standard spiked into the sample prior to LC-MS/MS analysis. Antibody-magnetic particle conjugates were analyzed in triplicate to determine the consistency of antibody loading onto the magnetic particles via different conjugation techniques.

Among the four conjugated magnetic particles, the highest concentration of immobilized antibody was obtained by activating the nanoparticles with glutaraldehyde groups ($44 \mu\text{g}/\text{mg} \pm 1.4 \mu\text{g}/\text{mg}$), as shown in Figure 3.6. The epoxide coupling process of the nanoparticles produced the second highest concentration of

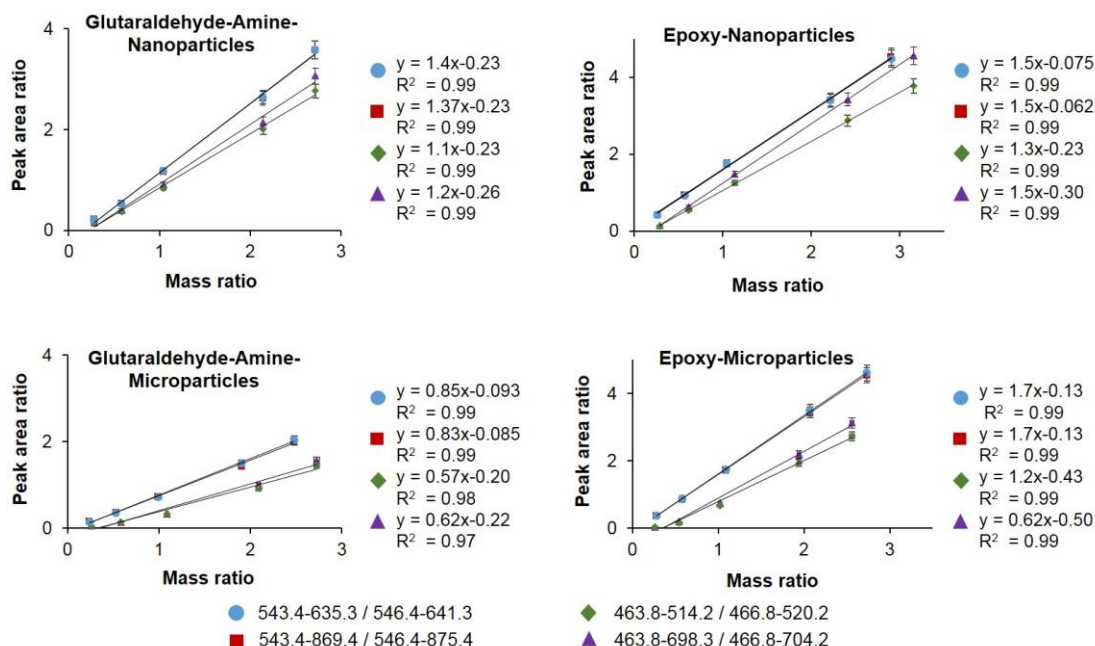


Figure 3.5 Calibration curves for each magnetic particle support are provided for monitored anti-cTnI antibody peptide transitions as a plot of unlabeled : labeled integrated peak area ratios versus unlabeled : labeled measured mass ratios. A regression equation of the best-fit line is provided for each plot along with a R^2 estimate of the correlation for fit to the line. The error bars represent standard deviation of the mean peak areas from duplicate injections.

immobilized antibody ($27 \mu\text{g}/\text{mg} \pm 5.3 \mu\text{g}/\text{mg}$). The lower amount of antibody bound to the epoxy-functionalized nanoparticles may be a result of partial epoxy ring opening during the silanization procedure and slower kinetics of the epoxy-amine reaction.¹³⁰

Overall microparticles produced a lower immobilization amount when used as the solid support due to the greater surface area of the nanoparticles. Unlike the nanoparticles, the epoxy-modified microparticles ($3.3 \mu\text{g}/\text{mg} \pm 0.49 \mu\text{g}/\text{mg}$) performed slightly better than the amine-modified microparticles activated with glutaraldehyde ($1.5 \mu\text{g}/\text{mg} \pm 0.20 \mu\text{g}/\text{mg}$). It is speculated that this is due to the additional conjugation step required to functionalize the amine-modified microparticles. According to the vendor's description of materials, the microparticles

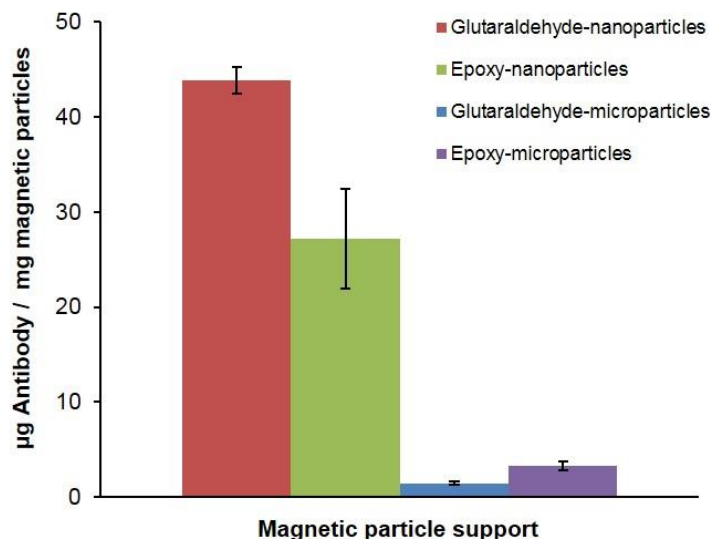


Figure 3.6 Bar graph summarizes the amount of immobilized anti-cTnI antibody per mg of nanoparticles and microparticles. Quantification was based on monitoring two transitions for two antibody peptides. The standard deviation error bars represent duplicate injections of all of the monitored transitions from triplicate sample preparations.

were coated with a layer of glycidyl ether (epoxy) functional groups. The amine-microparticles were then activated with amine groups using a short linker. In the case of the nanoparticles, silane reagents bearing either amine or epoxy functional groups were used to directly functionalize the nanoparticles via a one-step silanization reaction. Furthermore, the higher antibody binding per mg of nanoparticles in comparison with the microparticles was expected because the surface area/mass of nanoparticles was much higher than that of the microparticles.

Based on the data, the amine modified nanoparticles (85 nm) and microparticles (2.8 µm) activated with glutaraldehyde correlated well with the calculated surface area-to-mass ratios ($\approx 30:1$), while the epoxy case did not. Additionally, the magnetic nanoparticles had $< 10\%$ size variability, which was a slightly larger size variation compared to the commercial microparticles. This could

have compromised the reproducibility of the immobilization process. Antibody-particle conjugates were prepared in triplicate, but no significant differences were observed in bound antibody yields. On the basis of the results obtained, it was evident that particle size, composition and functionality effect antibody efficiency on a bulk mass scale.

3.3.3. Optimization of antibody-magnetic particle conjugates

Given that the highest amount of immobilized antibody was obtained by the glutaraldehyde-activated nanoparticles, this antibody-magnetic nanoparticle conjugate protocol was chosen for further optimization. As such, a quantitative ID-LC-MS/MS assay was developed to determine the amount of antibody required to efficiently saturate a given amount of nanoparticles. An increasing amount of anti-cTnI antibody (7.5, 18, 37.5, 75, 150, 225, 300, 375 μg) was incubated for 48 hours with a fixed amount of magnetic nanoparticles (0.25 mg) in a fixed volume (375 μL). Due to the high cost of antibody, the coupling protocol was cut by one fourth for optimization studies. The amount of antibody bound to the glutaraldehyde-activated magnetic nanoparticles was performed using the described ID-LC-MS/MS method. According to Figure 3.7, the amount of immobilized antibody increased up to 18.4 $\mu\text{g}/\text{mg} \pm 0.931$ $\mu\text{g}/\text{mg}$ for 0.25 mg nanoparticles using 150 μg of antibody. Therefore, 600 μg of antibody per mg of glutaraldehyde-activated magnetic nanoparticles (scaled up by one fourth) was used for the final conjugation protocol.

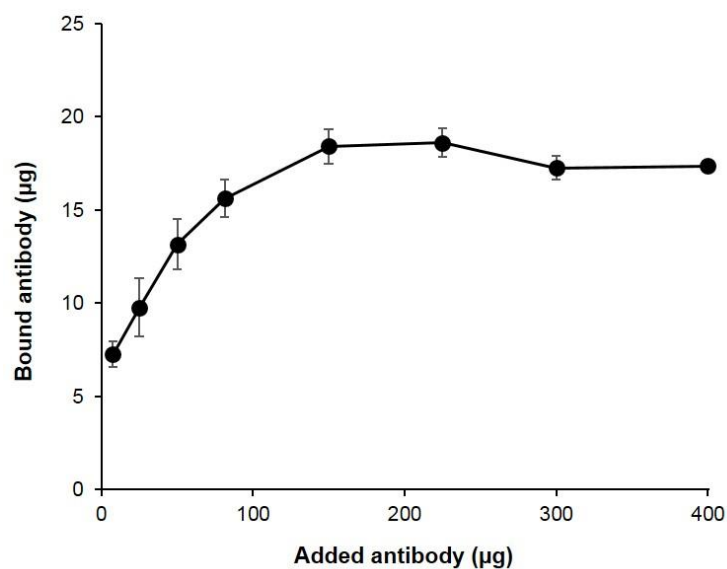


Figure 3.7 Glutaraldehyde-activated magnetic nanoparticles (0.25 mg) were incubated with an increasing amount of anti-cTnI antibody. Antibody binding capacity was determined using a ID-LC-MRM-MS/MS method specific for anti-cTnI antibody. The standard deviation error bars represent duplicate injections of all of the monitored transitions from each sample.

3.3.4. Advantages of the developed ID-LC-MS/MS method

Measuring antibodies immobilized to magnetic particles by ID-LC-MS/MS has several advantages in comparison with other semi-quantitative protein assay methods. For instance, protein assays with conventional optical detection methods, such as UV-visible spectrophotometry, cannot discriminate the antibody from interfering compounds that adsorb at the same wavelength. Many protein assays are prone to interferences from reagents used during the antibody-magnetic particle coupling process.¹³¹ Therefore, the choice of protein assay depends on many factors including tolerance to interfering compounds and reagent compatibility. In addition, most commercial antibodies are not provided with accurate extinction coefficients; therefore, antibody concentrations are estimated relative to the antibody standards.

Particularly for the epoxy coupling process, the immobilization supernatant and the wash supernatant consisted of different buffers, which would warrant a calibration curve series for each buffer using a protein assay. However, the developed method described uses LC-MS/MS detection, which can distinguish targeted peptides (both unlabeled and isotopically labeled corresponding to the antibody) from other components in the sample. The ID-LC-MS/MS methodology does not rely on the use of an extinction coefficient for absolute quantification, but instead directly measures targeted peptides based on molecular mass and fragmentation patterns. Therefore, this newly developed method can be applied as a universal approach to quantify the amount of antibody on magnetic particles in one measurement (per sample) that is independent of the coupling and washing processes, magnetic particle or antibody type.

Another notable advantage is that this LC-MS/MS method can be utilized to measure anti-cTnI antibody peptide concentrations simultaneously with cTnI peptide concentrations within the sample, which can help account for variations caused by the antibody-magnetic particle conjugates. Reproducibility of the enrichment step is highly dependent on the antibody-magnetic particle conjugates. As shown in Figure 3.8, monitoring anti-cTnI antibody peptides simultaneously with immuno-extracted cTnI during LC-MS/MS analysis can help provide quality assurance of the magnetic separation-based enrichment process.⁹¹ The amount of antibody observed in each sample should be consistent for reproducible magnetic-based enrichments. This method is sensitive enough to monitor antibody differences found between samples caused by inconsistent pipetting or micro-heterogeneity of the antibody-particle

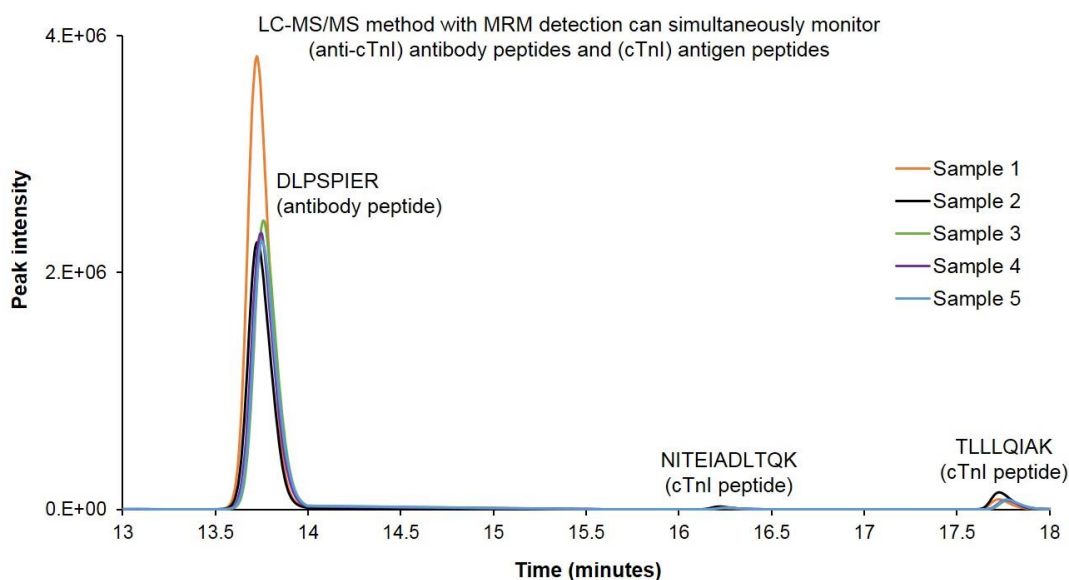


Figure 3.8 Representative total ion chromatograms of five cTnI samples enriched using magnetic nanoparticles conjugated with anti-cTnI antibody. MRM transitions for two cTnI peptides and one anti-cTnI antibody peptides are monitored. LC-MRM-MS/MS detection can be used to monitor antibody differences found between sample replicates, which may affect capture recoveries. A higher (relative) concentration of antibody (DLPSPIER) peptide was calculated in Sample 1 compared to the other samples, which resulted in a slightly higher cTnI recovery.

conjugates.^{90,91} Overall, this method can be used to evaluate antibody coupling processes with different magnetic particles and also help support enriched cTnI quantification by LC-MS/MS analysis, which will be discussed in Chapter 4.

3.4. Conclusion

Optimizing experimental design for antibody immobilization to magnetic particles is crucial for improving low abundant protein enrichment for subsequent LC-MS/MS detection. Here, an ID-LC-MS/MS method was developed to directly measure the amount of antibody covalently bound to magnetic particles in order to select the most efficient coupling procedure. The practical application of the ID-LC-MS/MS methodology was demonstrated to evaluate various antibody coupling

processes to magnetic particles of micrometer and nanometer dimensions. Antibody conjugation was achieved using glutaraldehyde or epoxy coupling processes with either nano- or microparticles. The results indicated that the nanoparticles conjugated significantly higher yields of antibody independent of the binding chemistry in comparison to the microparticles. The glutaraldehyde coupling process with the amine-functionalized silica coated magnetic nanoparticles was chosen for the cTnI capture procedure due to the high antibody coupling efficiency.

The primary advantages of this newly developed method are that (1) it can be used to measure bound antibody with various magnetic particle types and immobilization strategies, (2) it can be used in conjunction with cTnI LC-MS/MS analysis by simultaneously monitoring tryptic peptides from the anti-cTnI antibody to ensure batch-to-batch consistency of the magnetic separation, and (3) this method is transferrable to any LC-MS/MS-based assay using the same antibody isotype. In Chapter 4, this method will be used to monitor quality assurance of the enrichment step for cTnI quantification. The generic nature of this approach also suggests that it can be applied to any antibody as long as the subclass of the antibody can be determined and peptides from the antibody can be uniquely identified from the tryptic digest for subsequent LC-MS/MS analysis.

Chapter 4: Quantification of cTnI in human plasma by protein immunoaffinity capture and LC-MS/MS

This chapter will be reproduced in part with permission from: Schneek, N.A.; Phinney, K.W.; Lee, S.B.; and Lowenthal, M.S. “Quantification of cardiac troponin I in patient plasma by magnetic particle enrichment and targeted mass spectrometry.” *In preparation*.

4.1. Introduction

cTnI is a well-established diagnostic biomarker for heart muscle damage and is routinely analyzed by immunoassays in clinical laboratories to assess patient samples. However, the broad-scale use of immunoassays on various technology platforms from different vendors has resulted in considerable variability in cTnI measurements, which influences the interpretation and comparison of results.^{33,132} Therefore, it is critical to develop reference materials and reference measurement procedures to improve the accuracy and comparability of cTnI measurement results.

In this chapter, the development of a highly selective and sensitive ID-LC-MS/MS-based candidate reference measurement procedure is described to quantify cTnI in clinical samples from myocardial infarction patients. ID-LC-MS/MS has been extensively used as a reliable measurement method for standardization efforts. Unlike immunoassay detection methods, LC-MS/MS in MRM mode can directly detect defined m/z 's of surrogate cTnI peptides, generated by enzymatic digestion, with a high level of specificity and sensitivity.⁹⁴ Additionally, absolute quantification of cTnI by ID-LC-MS/MS can be achieved based on the peak area ratios of each surrogate peptide to its internal standard analog. An internal standard can account for sample complexity, sample processing, and instrument variations.¹³³

However, LC-MS/MS analysis of low abundant cTnI levels in patient samples is challenging due to the vast number of proteins found in plasma or serum, and the wide dynamic range of protein concentrations, which spans more than ten orders of magnitude.⁴⁹ Compared to some high-sensitivity cTnI immunoassays that have achieved limits of quantification in the low pg/mL range, current LC-MS/MS instruments can only directly detect proteins with concentrations at low µg/mL to the high ng/mL levels in complex matrices.^{28,75,134} To improve signal-to-noise (S/N) ratio, a protein immunoaffinity enrichment technique utilizing magnetic separation was developed to simultaneously enrich cTnI and reduce sample complexity. By including an immunoaffinity enrichment step prior to LC-MS/MS analysis, limits of quantification can be lowered to the low ng/mL range or below for reproducible measurement of cTnI.

Quantification of cTnI can be also improved by performing LC-MS/MS analysis in dynamic MRM mode. MRM data is typically collected by sequentially cycling through all of the MRM transitions, each with their own dwell time (a specified collection time to analyze a specific MRM transition), during the entire LC-MS/MS run.⁶⁴ Dynamic or triggered MRM analysis only monitors transitions of a specific peptide when eluted off the HPLC column at specific retention time windows, which optimizes dwell time and improves data quality.¹³⁵ Using the dynamic MRM approach, cycle and dwell time can be maximized for each peptide at its unique retention time.⁶⁴ Since transitions are only triggered at a known retention time corresponding to when they are eluted off the HPLC column, several MRM transitions for cTnI can be monitored without negatively impacting the S/N or

measurement precision of the individual peptides.^{64,136} Additionally, measurement of multiple tryptic peptides with different retention times can be easily achieved using dynamic MRM since no change in cycle or dwell times is needed.

Here, an immunoaffinity-based ID-LC-MS/MS assay was developed to measure surrogate tryptic peptides of cTnI in either serum or plasma. Key steps in the workflow, such as protein capture, digestion conditions, and LC-MS/MS instrument parameters, were optimized to enhance the enrichment of cTnI and subsequently improve LC-MS/MS detection. During method development, isotopically labeled cTnI peptides acted as the internal standard and were used to perform recovery studies. However, in the final workflow an isotopically labeled cTnI protein internal standard was used in order to avoid correcting for peptide recovery during cTnI quantification. The isotopically labeled cTnI protein internal standard corrected for protein losses throughout the enrichment process and compensated for digestion variability. Following method optimization, a proof-of-concept analysis was performed in which elevated levels of cTnI were quantified in five myocardial infarction patient plasma samples.

4.2. Experimental design

4.2.1. Materials

Standard Reference Material (SRM) 2921 – human cardiac troponin complex, a primary reference material in a buffered solution – which was extracted from human heart, was obtained from NIST. Monoclonal antibody against human cTnI (clone 19C7) was purchased from HyTest Ltd. (Turku, Finland). The synthetic, stable-isotope labeled peptides, NITEIADL*TQK, TLLLQIA*K and DLPSPIE*R

were purchased from AnaSpec, Inc. (California, USA). The isotopically labeled cTnI protein internal standard was expressed and labeled using cell-free *E. coli* lysate and purified by Promise Advanced Proteomics (Grenoble, France). cTnI-negative (undetectable cTnI by ELISA) and cTnI-positive patient plasma (heparinized) samples were provided through the Department of Laboratory Medicine at the University of Washington in Seattle, USA. All cTnI samples used were de-identified from clinical routine testing at the University of Washington and human subjects research determination forms can be found in Appendix A. A de-identified donor plasma pool with Na⁺ heparin (anti-coagulant), collected from 50 apparently healthy individuals, was also obtained through Golden West Biologicals, Inc. (California, USA). Goat serum, collected from a controlled donor herd, was purchased through Sigma Aldrich (Missouri, USA). Rapigest™ SF was purchased from Waters Corporation (Massachusetts, USA) and trypsin gold, MS grade, was purchased from Promega Corporation (Wisconsin, USA). High purity LC-MS grade water (H₂O)/formic acid and acetonitrile (ACN) /formic acid were purchased from Honeywell-Burdick and Jackson (Michigan, USA). Protein LoBind centrifuge tubes were purchased from Eppendorf (New York, USA). All other chemicals were purchased from Sigma-Aldrich (Missouri, USA).

4.2.2. Immobilization of anti-cTnI monoclonal antibody onto magnetic nanoparticles

Monoclonal anti-cTnI antibody was immobilized on the magnetic nanoparticles using the glutaraldehyde method, as described in Section 3.2.2. After conjugation, the supernatant was discarded and the antibody-nanoparticle conjugates were treated with ethanolamine in PBS (0.2 mmol/L, pH 7.4) for 1 hour to deactivate

unreacted aldehyde groups. Next, the antibody-nanoparticle conjugates were incubated in PBS containing 0.2 % (w/v) BSA/ 0.05 % (v/v) Tween 20 (1.5 mL) for 16 hours at room temperature to block any additional unreacted sites and limit non-specific binding. Finally, the antibody-nanoparticle conjugates were washed three times with PBS containing 0.1 % (w/v) BSA/ 0.05 % (v/v) Tween 20 and reconstituted in PBS (0.5 mL). The resultant nanoparticle sample contained 2 mg/mL nanoparticles and approximately 75 μ g of anti-cTnI antibody conjugated to the surface of 1 mg nanoparticles. Three batches of antibody-magnetic nanoparticle conjugates were prepared simultaneously and combined to form one lot of anti-cTnI antibody-nanoparticle conjugates for use in cTnI capture studies.

4.2.3. Calibrant and sample preparation for recoveries studies

For recovery studies, human cardiac troponin complex from NIST SRM 2921 stock was thawed to room temperature and prepared gravimetrically by diluting SRM 2921 in 0.05 % (w/v) BSA solution in ammonium bicarbonate. For the calibrants, anti-cTnI antibody conjugated nanoparticles were placed into centrifuge tubes, and the supernatant was removed by magnetic separation. SRM 2921 solution was added at discrete amounts (e.g. \approx 2.5, 6.0, 12, 18, 24, 30, 36 ng) and diluted up to 40 μ L with 0.05 % BSA in ammonium bicarbonate solution. For only these recovery studies, the calibrants did not undergo the enrichment or wash steps to ensure complete recovery.

Samples were prepared by spiking known amounts of SRM 2921 into either 0.2 % BSA/PBS (0.9 mL), goat serum (0.9 mL) or human donor plasma (0.9 mL). Samples were diluted 2-fold with PBS to reduce the viscosity of the plasma/serum

samples. To capture cTnI, 30 μ L of anti-cTnI antibody-magnetic nanoparticle conjugates were added to the samples, and incubated at room temperature with gentle rotary mixing. Following incubation, non-specific proteins were removed by washing the nanoparticles two times with tris buffer (20 mmol/L tris, 150 mmol/L sodium chloride) containing 0.05 % Tween 20 (1.8 mL) and once with ammonium bicarbonate (1.8 mL). The samples were resuspended in ammonium bicarbonate (40 μ L) for digestion.

4.2.4. Calibrant and sample preparation for patient plasma sample analysis using an isotopically labeled protein internal standard

Human cardiac troponin complex from NIST SRM 2921 stock was thawed to room temperature. SRM 2921 stocks were prepared gravimetrically by diluting SRM 2921 in 0.1 % BSA solution in PBS (BSA/PBS). Isotopically labeled cTnI internal standard was also prepared in 0.1 % BSA/PBS. Patient plasma samples were thawed and equilibrated to room temperature. Patient plasma samples were centrifuged for 10 minutes at 5000 g to sediment any precipitated material. Matrix-matched calibrants were prepared gravimetrically by mixing pooled cTnI-negative patient plasma (0.9 mL) with a range of concentrations of SRM 2921 and a constant concentration of isotopically labeled cTnI internal standard. Calibrants were diluted 2-fold in PBS (final volume 1.8 mL). Samples were prepared gravimetrically by mixing cTnI-positive patient plasma (0.9 mL) with the same constant concentration of isotopically labeled cTnI internal standard. Samples were diluted 2-fold with PBS (final volume: 1.8 mL). cTnI was then enriched from the patient plasma samples and calibrants, as described in Section 4.2.3.

4.2.5. Trypsin digestion

Captured proteins were digested *in situ* with the antibody conjugated nanoparticles. The samples and calibrants were denatured in 0.2 % (v/v) Rapigest™ SF surfactant in 50 mmol/L ammonium bicarbonate (40 µL) and boiled for 2 minutes. The released proteins were reduced with a final concentration of 10 mmol/L DTT at 60 °C with shaking for 45 minutes, and alkylated with 10 mmol/L IAM in the dark at room temperature for 45 minutes. Trypsin was added to the samples (1:2.5 w/w trypsin-to-protein ratio) and all samples were incubated for 16 hours at 37 °C. The digests were acidified with a final concentration of 5 % (v/v) formic acid for 45 minutes at 37 °C and centrifuged at 4 °C to remove the Rapigest™ SF and the magnetic particles. The digests were dried using a vacuum centrifuge.

For recovery studies, isotopically labeled peptides (TLLLQIA[¹³C₃, ¹⁵N]K, NITEIADL[¹³C₆]TQK, and DLPSPiE[¹³C₅, ¹⁵N]R) were prepared at constant concentrations at about a 1:1 ratio with the midpoint of the calibration curve and used as internal standards. Calibrants and samples were reconstituted with the isotopically labeled peptide internal standard solution (10 µL) prior to LC-MS/MS analysis.

For studies utilizing the isotopically labeled protein internal standard, calibrants and samples were reconstituted with isotopically labeled DLPSPiE[¹³C₅, ¹⁵N]R internal standard solution (10 µL). As described in Chapter 3, DLPSPiE[¹³C₅, ¹⁵N]R was a surrogate peptide for the anti-cTnI antibody and was used throughout the experiments to determine the relative amount of antibody in each sample using a one-point calibration.

4.2.6. LC-MS/MS analysis

LC-MS/MS (ion trap) sequencing analysis was used to determine unique cTnI peptides and CID fragmentation patterns. A tryptic digest of SRM 2921 was analyzed using a Thermo Dionex UltiMate 3000 LC system coupled to a high resolution Thermo Scientific hybrid LTQ linear ion trap-Orbitrap Elite MS/MS with the same method and parameters as described in Section 3.2.3.

LC-MS/MS (dynamic MRM) analysis was performed on an Agilent 1200 LC system coupled in-line with an Agilent 6490 triple quadrupole MS. For peptide measurements, 8 μ L of sample was injected via autosampler and the LC separation was performed at a flow rate of 200 μ L/min on a Zorbax (Agilent) SB-C₁₈ reversed-phase analytical column (2.1 mm x 150 mm, 3.5 μ m particles) at 35 °C using an increasing linear gradient of organic/aqueous solvent (ACN/H₂O containing 0.1 % (v/v) formic acid) starting at 5 % organic and increasing up to 70 % (v/v) organic over 30 minutes, followed by a column wash and re-equilibration. The MS was operated in a positive-ion polarity. The following MS settings were used: fragmentor 380 V, cell accelerator 4 V, electron multiplier 800 V, capillary voltage 3500 V. Dynamic MRM scan type was used with a delta retention time of 1 minute for (unlabeled and labeled) NITEIADLTQK, TLLLQIAK, DLPSPIER peptides and a delta retention time of 3 minutes for (unlabeled and labeled) AYATEPHAK peptide. Collision energies were optimized experimentally for each peptide transition by MRM monitoring and noting maximum signal intensity. Two fragmentation transitions were monitored for three cTnI peptides (NITEIADLTQK, TLLLQIAK, AYATEPHAK)

and one antibody peptide (DLPSPIER) for both the isotopically labeled and unlabeled peptides in the final method.

Peak areas were integrated using MassHunter Qualitative Analysis B.06.00 software. The concentration of cTnI was determined by generating calibration curves using SRM 2921 as the calibrant and plotting peak area ratios of unlabeled to labeled cTnI peptide versus known mass ratios of unlabeled to labeled cTnI peptide. Peptide concentrations were interpolated against the linear equation and multiplied by the known concentration of internal standard. The average concentration of all peptides detected using multiple transitions was used to determine cTnI concentration since peptide abundance is used as a surrogate for protein abundance.

4.3. Results and discussion

4.3.1. Development of the LC-MS/MS-based assay

To determine surrogate peptides that could represent cTnI, SRM 2921 – human cardiac troponin complex (cTnI, cTnT, cTnC) – was digested and analyzed using LC-MS/MS (ion trap). Accordingly, the subsequent MS/MS data was analyzed against an *in silico* protein sequence database using Sequest HT to identify peptide sequences. Figure 4.1 shows a total ion chromatogram of the protein digest and an extracted ion chromatogram of a surrogate cTnI peptide (TLLLQIAK), along with the peptide sequence and its MS/MS fragmentation pattern. A total of 23 peptides were identified, which provided a combined sequence coverage of 68 % of cTnI, as depicted in Figure 4.2.

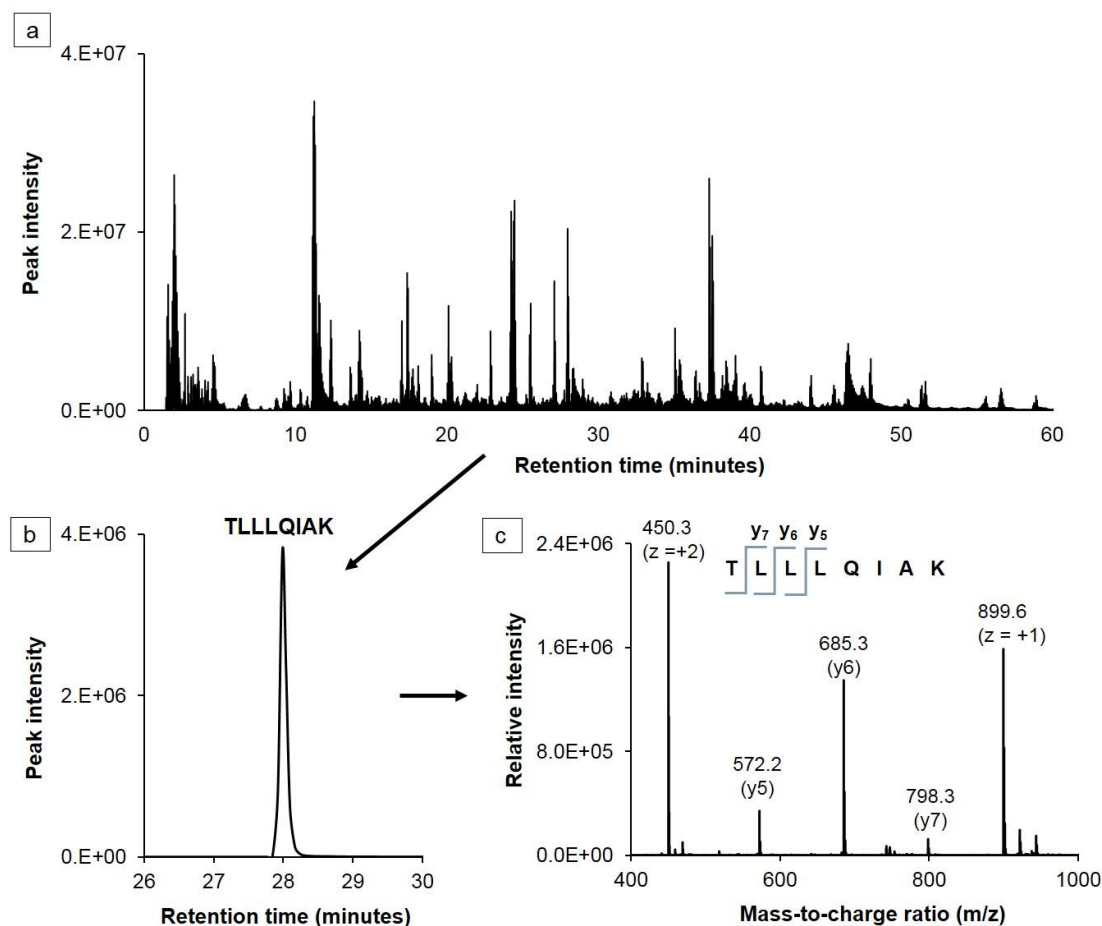


Figure 4.1 (a) Total ion chromatogram (TIC) of a tryptic digest of human cardiac troponin complex from SRM 2921. (b) Representative extracted ion chromatogram of tryptic cTnI peptide, TLLLQIAK. (c) and MS/MS spectra of TLLLQIAK.

A targeted LC-MS/MS with MRM analysis, using the triple quadrupole MS, was performed on the protein (SRM 2921) digest to screen for the most intense MRM signals from a panel of tryptic cTnI peptides. As demonstrated in Figure 4.3, twenty transitions corresponding to a total of eight cTnI peptides and two modified cTnI peptides were selected for LC-MS/MS evaluation. Of the 10 total peptides, CQPLELAGLGFAELQDLCR, NIDALSGM(oxidized)R, and ISADAM(oxidized)M(oxidized)QALLGAR peptides were not ambiguously detected during MRM screening and not selected to be used in the LC-MS/MS-based assay.

Protein reference: - Troponin I, cardiac muscle, Homo sapiens [TNNI3_HUMAN]

MADGSSDAAREPRPAPAPIRRRSSNYRAYATEPHAKKSKISASRKLQLKTL
LQIAKQELEREAEERRGEKGRALSTRCQPLELAGLGFAELQDLCRQLHARVD
KVDEERYDIEAKVTKNITEIADLTQKIFDLRGKFKRPTLRRVRSADAMMQALL
GARAKESLDLRAHLKQVKKEDTEKENREVGDWKNIDALSGMEGRKKKFES

Figure 4.2 Amino acid sequence of human cTnI. Peptides in blue were identified from a digest of SRM 2921 (human cardiac troponin complex) during sequence coverage analysis by LC-MS/MS (ion trap). Tryptic peptides underlined were selected for subsequent MRM screening and assay development.

TLLLQIAK and NITEIADLTQK peptides were selected to be used for quantification of cTnI during method development and optimization. Both peptides were unique to cTnI, did not possess known post-translational modifications, and were reproducibly detected in samples of trypsin digested SRM 2921. Additionally, the peptides and their respective MRM transitions produced the highest S/N ratios, which allowed for improved sensitivity of the LC-MS/MS method. The MRM transition ions chosen to analyze the cTnI peptides by LC-MS/MS are listed in Table 4.1. Additionally, DLPSPIER, a peptide from the anti-cTnI antibody, was monitored and used as a qualitative control to assess the antibody-magnetic particle enrichment, as described in Chapter 3. The sensitivity of the method was further enhanced by optimizing instrument parameters, such as collision energies and source parameters.

Virtually all LC-MS/MS-based quantitation work is performed exclusively at the peptide level.¹³⁷ Since digestion conditions can significantly influence peptide formation yields, it was imperative to optimize the trypsin digestion protocol. In order to enhance sample recovery by limiting clean-up steps, Rapigest™ SF (surfactant) was chosen to act as the denaturant since its degradation products could easily be removed by acidification and centrifugation.¹³⁸ After denaturation, proteins were

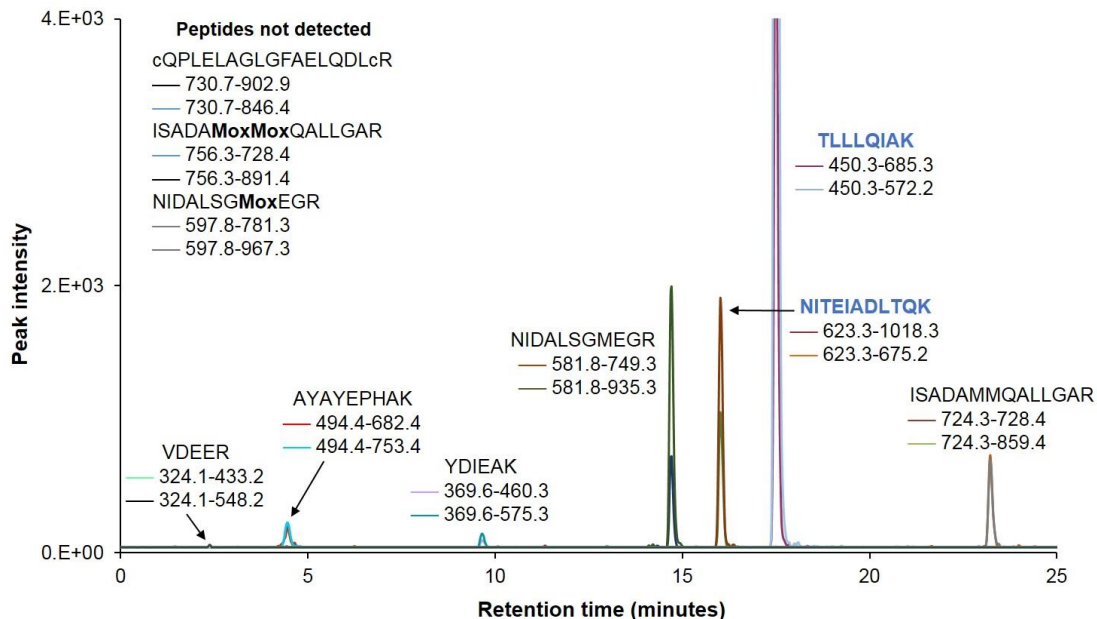


Figure 4.3 Extracted ion chromatogram of tryptic cTnI peptides screened for MRM analysis and assay development. Two transitions per cTnI peptide were analyzed. The blue highlighted tryptic peptides NITEIADLTQK and TLLLQIAK produced the highest signal response in electrospray LC-MS/MS (triple quadrupole). These peptides are referred to as “surrogate peptides,” and were used to build a MRM-based assay for cTnI. Isotopically labeled versions of these peptides were synthesized to act as internal standards for LC-MS/MS quantification.

reduced with DTT and alkylated with IAM under three different conditions (*blue*: 10 mM DTT, 10 mM IAM; *red*: 5 mM DTT, 15 mM IAM; and *green*: 0.5 mM DTT, 2 mM IAM, 1.5 mM DTT); followed by the addition of trypsin at enzyme-to-protein ratios of 1:2.5, 1:5, 1:10, 1:20, and 1:50. Promega trypsin gold, MS grade was used to avoid increasing chemical background from autolysis of the enzyme.¹³⁹ As depicted in Figure 4.4, digestion conditions were optimal when proteins were reduced with 10 mM DTT and alkylated with 10 mM IAM. Highest peak area ratios were obtained for the NITEIADLTQK and TLLLQIAK peptides using a 1:2.5 trypsin-to-protein ratio.

Table 4.1 Optimized MS parameters and two peptides (unlabeled and labeled) with two transitions each were selected to represent cTnI and a single peptide (unlabeled and labeled) with two transitions was used to represent the capture antibody (IgG_{2b}).

Peptide AA sequence	Precursor Ion (<i>m/z</i>)	Product Ion (<i>m/z</i>)	Collision Energy (V)	Retention Time (minutes)
NITEIADLTQK	[623.3] ²⁺	[1018.3] ⁺	10	16.2
		[675.2] ⁺	11	
NITEIADL*TQK	[626.3] ²⁺	[1024.5] ⁺	10	
		[681.4] ⁺	11	
TLLLQIAK	[450.3] ²⁺	[685.3] ⁺	7	17.8
		[572.2] ⁺	8	
TLLLQIA*K	[452.3] ²⁺	[689.3] ⁺	7	
		[576.2] ⁺	8	
DLPSPIER (IgG)	[463.8] ²⁺	[698.3] ⁺	7	13.7
		[514.2] ⁺	17	
DLPSPIE*R (IgG)	[466.8] ²⁺	[704.2] ⁺	7	
		[520.2] ⁺	17	

The digestion parameters were further optimized with antibody-magnetic nanoparticle conjugates present in the sample. Captured proteins from the enrichment step were released from the magnetic nanoparticles via denaturation to decrease the risk of potential protein loss that may occur if an elution step was instead used. Eluting the captured proteins prior to digestion would have entailed an additional tube transfer and drying step. After the trypsin digestion, Rapigest™ SF degradation products and the magnetic nanoparticles were removed simultaneously by centrifugation and magnetic separation. Traditional protein digestion methods for LC-MS/MS analysis typically use an enzyme-to-protein ratio between 1:10 and 1:100; however, excess trypsin was required to produce higher peptide formation yields in the presence of the antibody-magnetic nanoparticle conjugates.¹³⁸

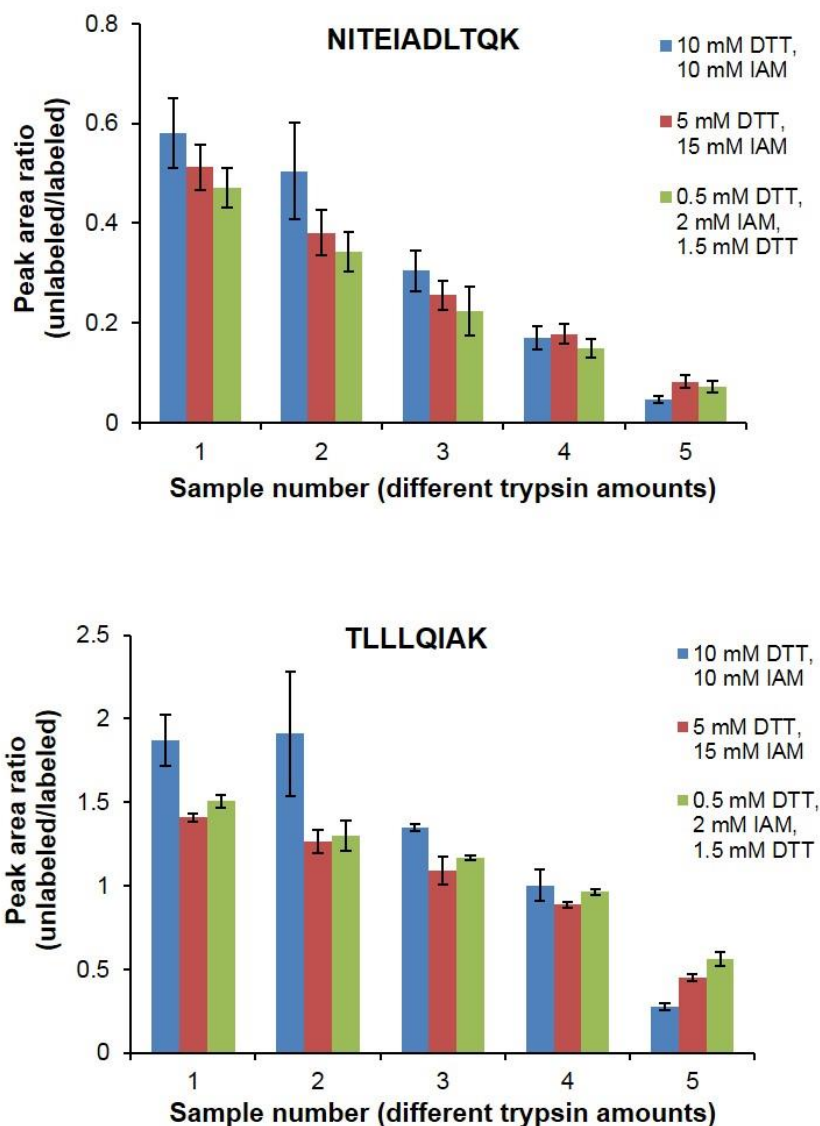


Figure 4.4 Effect of digestion condition on peptide formation yield. Bar graphs represent the peak area ratio of the unlabeled peptide to the spiked-in labeled peptide. Reduction and alkylation conditions were varied: 10 mM DTT, 10 mM IAM (blue line), 5 mM DTT, 15 mM IAM (red line), and 0.5 mM DTT, 2 mM IAM, 1.5 mM DTT (green line). For each of the reduction and alkylation conditions, the trypsin-to-protein ratios were varied (1) 1:2.5, (2) 1:5, (3) 1:10, (4) 1:20, (5) 1:50. Data and error bars represent the mean and standard deviation for two transitions per peptide and duplicate sample preparations.

Following optimization of the protein digestion, the limits of detection and quantification of the LC-MS/MS system were determined by digesting SRM 2921 at various concentrations with a constant amount of antibody-magnetic nanoparticle

conjugates. Representative extracted ion chromatograms of digested SRM 2921 samples with final concentrations of 0.0203 ng/ μ L and 0.0403 ng/ μ L are presented in Figure 4.5.

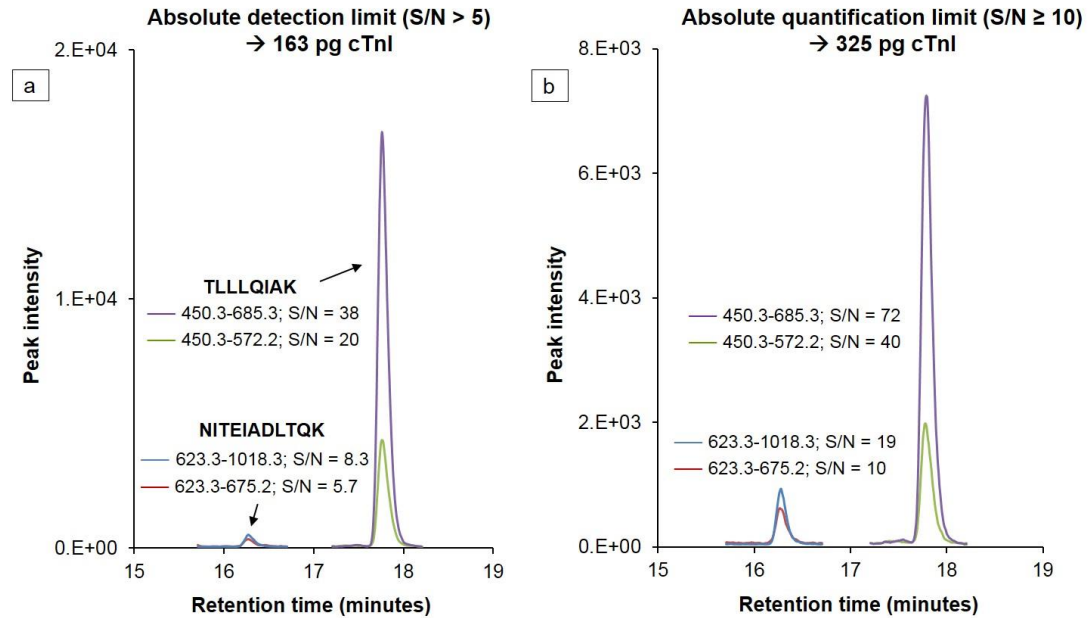


Figure 4.5 Representative MRM chromatograms of cTnI (from SRM 2921 digest), monitoring two transitions of the unlabeled cTnI peptides (NITEIADLTQK and TLLLQIAK) at the (a) absolute limits of detection at 163 pg and (b) absolute limits of quantification at 325 pg cTnI. S/N ratios are shown for each transition.

By injecting almost all of the sample (i.e., 8 μ L injection volume of 10 μ L sample volume) into the LC-MS/MS system, the absolute limit of detection was calculated to be 163 pg cTnI ($S/N \geq 3$ for each MRM transition), and the limit of quantification was estimated to be 325 pg cTnI ($S/N \geq 10$ for each MRM transition). Therefore, with reasonable enrichment, the LC-MS/MS-based assay allowed for the detection of cTnI (1-10 ng/mL) from \approx 1 mL of plasma from a patient who experienced myocardial infarction. However, the current sensitivity of the LC-MS/MS would not be able to detect cTnI levels in healthy individuals (\approx 1-10 pg/mL)

even if full recovery (100%) of cTnI from plasma was achieved during magnetic particle-based immunoaffinity enrichment.

4.3.2. Recovery efficiency of the magnetic particle-based protein immunoaffinity enrichment

Sensitivity of the LC-MS/MS-based assay is also dependent on the enrichment step; therefore, recovery of cTnI was optimized. An increasing amount of antibody-nanoparticle conjugates (20 μ L, 30 μ L, 40 μ L, 50 μ L) were incubated in buffer (0.2 % BSA in PBS, 1.8 mL) with a fixed amount of cTnI (SRM 2921, 35 ng) for 8 hours. Percent recovery of cTnI was determined by LC-MS/MS analysis using external calibration curves with SRM 2921 as the calibrant and isotopically labeled peptide internal standards (NITEIADL*TQK and TLLLIQA*K). As depicted in Figure 4.6, cTnI recovery saturated at 92.5 % with the addition of 30 μ L of antibody-nanoparticle

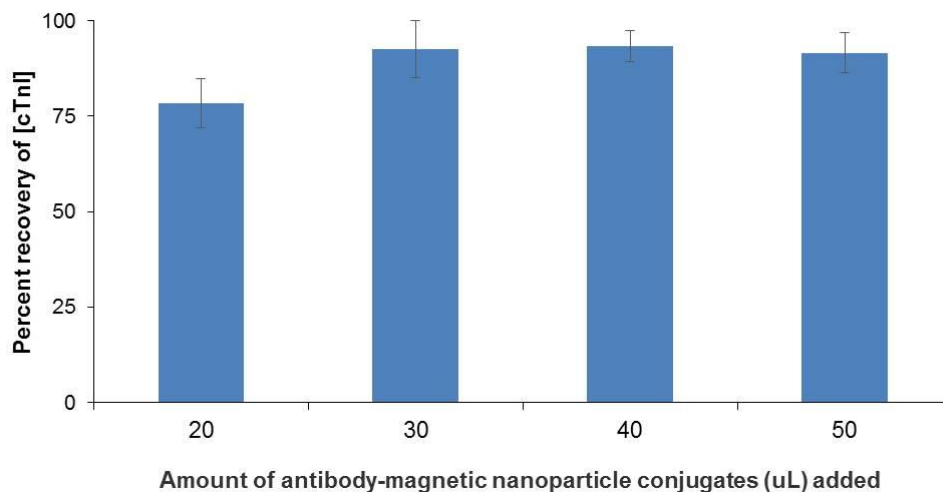


Figure 4.6 Percent recovery of cTnI was tested using different volumes of antibody-nanoparticle conjugates during immunoaffinity enrichment. Quantification was determined by analyzing two transitions for two cTnI peptides. The standard deviation error bars represent all of the monitored transitions from duplicate sample preparations.

conjugates ($\approx 4.5 \mu\text{g}$ antibody). Protein low-retention microtubes were used for all cTnI studies; however, losses due to protein/peptide adsorption to the microtubes or during trypsin digestion may account for the unrecovered cTnI.

Recovery of cTnI was also evaluated by varying the incubation time of the immunoaffinity enrichment process utilizing goat serum as a proof-of-concept medium. Goat serum acted as a cTnI-negative control matrix for initial method optimization studies because the reagent was cheap and easily accessible. cTnI was not expected to be present in the goat serum, however any trace of native cTnI would be distinguishable from the spiked cTnI from SRM 2921 due to the variation in amino acid sequence. Each targeted human cTnI peptide (TLLLQIAK and NITEIADLTQK) varied from the goat cTnI peptides (TLMLQIAK and NITEIADLNQK) by one amino acid, which would change the overall mass of the goat cTnI peptides, allowing the peptides to pass through MRM analysis undetected.

Constant amounts of cTnI (35 ng) and anti-cTnI antibody-nanoparticle conjugates were spiked into goat serum (0.9 mL; followed by 2x dilution, final 1.8 mL). The samples were incubated for 1, 2, 4, 8, 12, 16, 20, and 24 hours at room temperature with rotary mixing. The samples were then washed using a magnetic separator, digested, and reconstituted with isotopically labeled peptide internal standards prior to LC-MS/MS analysis. In addition, a negative control sample set was tested, which involved adding nanoparticles immobilized with antibody not specific to cTnI.

The highest percent recovery (68 %) of cTnI was achieved after a 20-hour incubation period as shown in Figure 4.7. Percent recovery of cTnI was determined by averaging the recoveries of each individual peptide using different transitions,

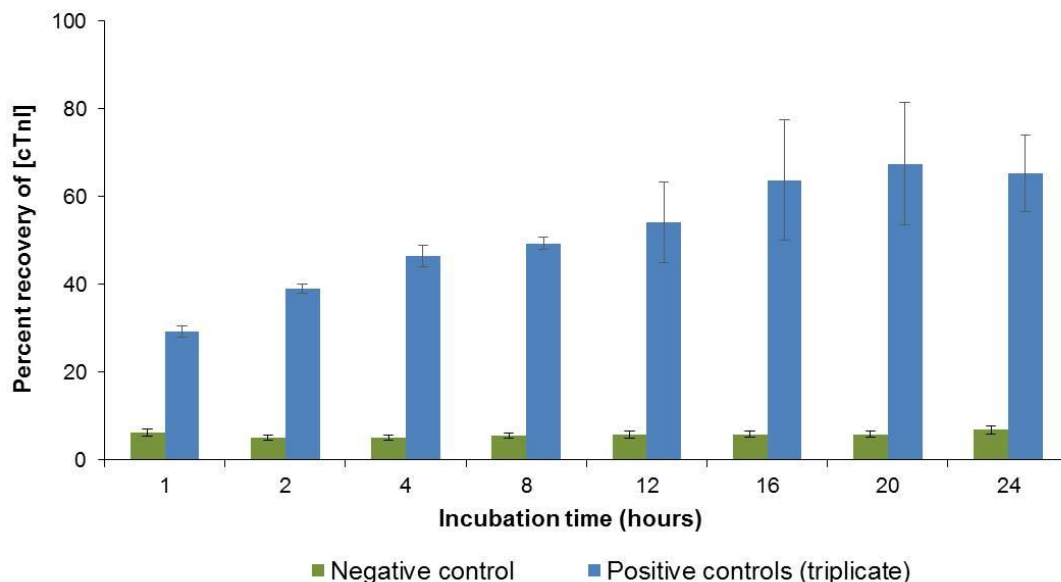


Figure 4.7 Percent recovery of cTnI (at the protein level) from diluted goat serum following a range of incubation time periods. Quantification was determined by analyzing two transitions for each cTnI peptides; followed by averaging the four transitions (total) for overall cTnI recovery. For the positive control samples, the standard deviation error bars represent all of the monitored transitions from triplicate sample preparations. For the negative control samples, the standard deviation error bars represent all of the monitored transitions from a single sample preparation.

which correlated to the overall percent recovery of cTnI. Large standard deviations were observed at the 12, 16, 20, and 24-hour incubation time points, which were due to the high variability between peptide measurements associated with stability and digestion differences. cTnI recovery can also be depicted for each individual peptide, as shown in Figure 4.8. Deviations of percent recovery between the NITEIADLTQK

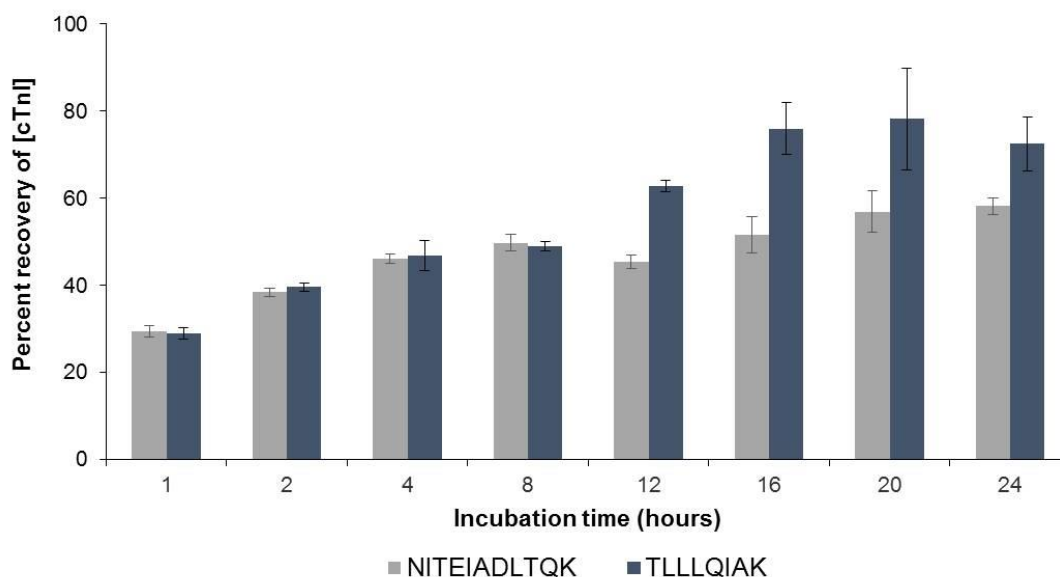


Figure 4.8 Percent recovery of cTnI (at the peptide level) from diluted goat serum following a range of incubation time periods. Quantification was determined by analyzing two transitions for each cTnI peptide. The standard deviation error bars represent the monitored transitions per peptide from triplicate sample preparations.

and TLLLQIAK peptides occurred after the 8-hour incubation time point. Unlike TLLLQIAK, NITEIADLTQK is located outside of the stable region (30-110 amino acid range) of cTnI and therefore may be degraded or modified in serum after 8 hours. Lower recovery of NITEIADLTQK, which contains an N-linked glycosylation motif, may also result from glycosylation modification; however, no reference to glycosylation of this peptide has been documented in the literature.¹⁴⁰ Ideally, recoveries from the two peptides should agree for accurate and precise quantification results. In order to achieve the highest recovery while maintaining comparable results among the peptides, an 8-hour incubation period was used for future cTnI enrichment studies. As a result, a 50 % recovery of cTnI was expected from serum samples.

Recovery and repeatability of the assay were evaluated by analyzing three replicates of cTnI (from SRM 2921) spiked at three levels (5, 10, 15 ng) in goat

serum on three different days. These levels represent the medium to high range of cTnI levels in ≈ 1 mL from plasma or serum of patients who have experienced myocardial infarction.^{23,141} Calibration curves were obtained by plotting the peak area ratios of cTnI peptide (from SRM 2921) to peptide internal standard versus known concentration ratios of SRM 2921 to each peptide internal standard. The calculated intra- and inter-day percent recovery and precision (percent coefficient of variation, % CV) of the assay are shown in Table 4.2.

Table 4.2 Intra- and interday repeatability statistics for cTnI in diluted goat serum.

Day	Statistics	cTnI spiked into 2x diluted serum		
		5 ng	10 ng	15 ng
1 (N = 3)	Mean recovery	61	52 (N=2)	51
	CV (%)	7.5	1.0	5.3
2 (N = 3)	Mean recovery	57	49	53
	CV (%)	5.7	3.8	7.0
3 (N = 3)	Mean recovery	59	56	53
	CV (%)	8.8	11	7.9
Overall (n = 9)	Mean recovery	59	52 (n=8)	52
	CV (%)	7.6	9.5	6.8

After demonstrating the repeatability of the method, recovery of spiked samples of cTnI near pathological levels from human donor plasma was evaluated for proof-of-principle. SRM 2921 (5, 10, and 15 ng) was spiked into normal human plasma (≈ 0.9 mL) and diluted 2-fold with PBS. cTnI was then quantified by immunoaffinity capture and ID-LC-MS/MS analysis. As shown in Figure 4.9, approximately 28 % of cTnI was recovered from plasma after an 8-hour incubation

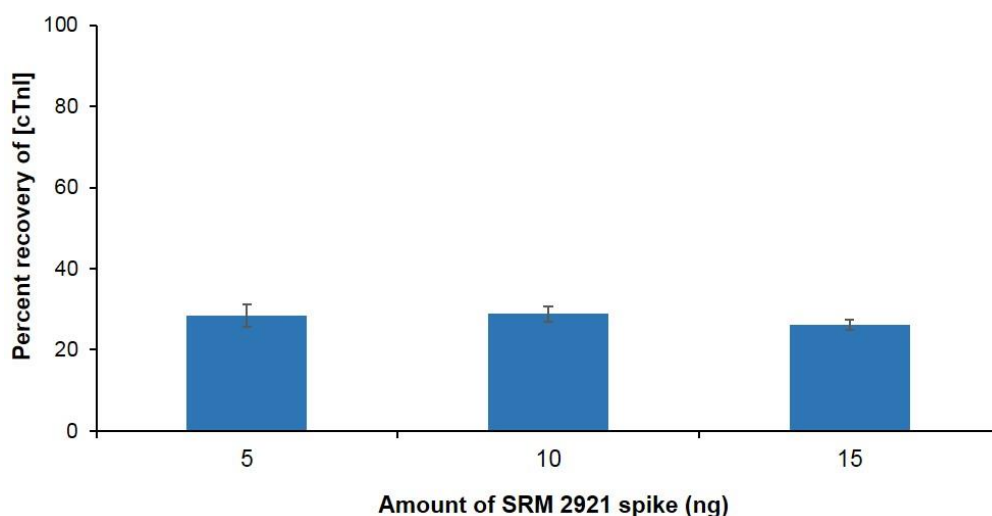


Figure 4.9 Percent recovery of cTnI (at the protein level) from normal plasma at three different amounts. Quantification was determined by analyzing two transitions of two cTnI peptides. The standard deviation error bars represent all of the monitored transitions from triplicate sample preparations.

period. The lower recovery in human matrix when compared to the goat serum matrix was attributed to the increased sample complexity. The goat serum was sterile-filtered by the vendor, which reduced the complexity of the matrix and allowed for improved recovery efficiency. Moreover, previous studies published in the literature show that significant protein losses can occur during sample preparation, especially when trying to enrich low abundant proteins from highly complex matrices like human plasma.^{81,142} Although a relatively low percent recovery of SRM 2921 from normal human plasma was achieved, this workflow provided enough enrichment to analyze cTnI at pathological levels.

During the recovery studies, the isotopically labeled cTnI peptide internal standard was added in the final step of the sample preparation workflow (i.e. after immunocapture and digestion) prior to LC-MS/MS analysis. For the internal standard to be most effective, it should be present during all stages of the sample preparation,

especially since it was clear from the recovery studies that large protein losses occurred throughout the workflow.⁷⁰ Therefore, a full-length isotopically labeled protein internal standard, instead of a labeled peptide internal standard, was utilized in the ID-LC-MS/MS-based assay to improve cTnI measurement quality. Provided that the isotopically labeled protein behaves exactly like cTnI, the internal standard can correct for protein losses during sample enrichment and compensate for variable digestion yields.^{84,143}

The commercial isotopically labeled cTnI protein was first digested and analyzed by LC-MS/MS (ion trap) to verify that lysine (K- $^{13}\text{C}_6$, $^{15}\text{N}_2$) and arginine (R- $^{13}\text{C}_6$, $^{15}\text{N}_4$) residues were labeled and that the peptide sequence matched to human cTnI. Figure 4.10 shows the extracted ion chromatograms of labeled TLLLQIAK*

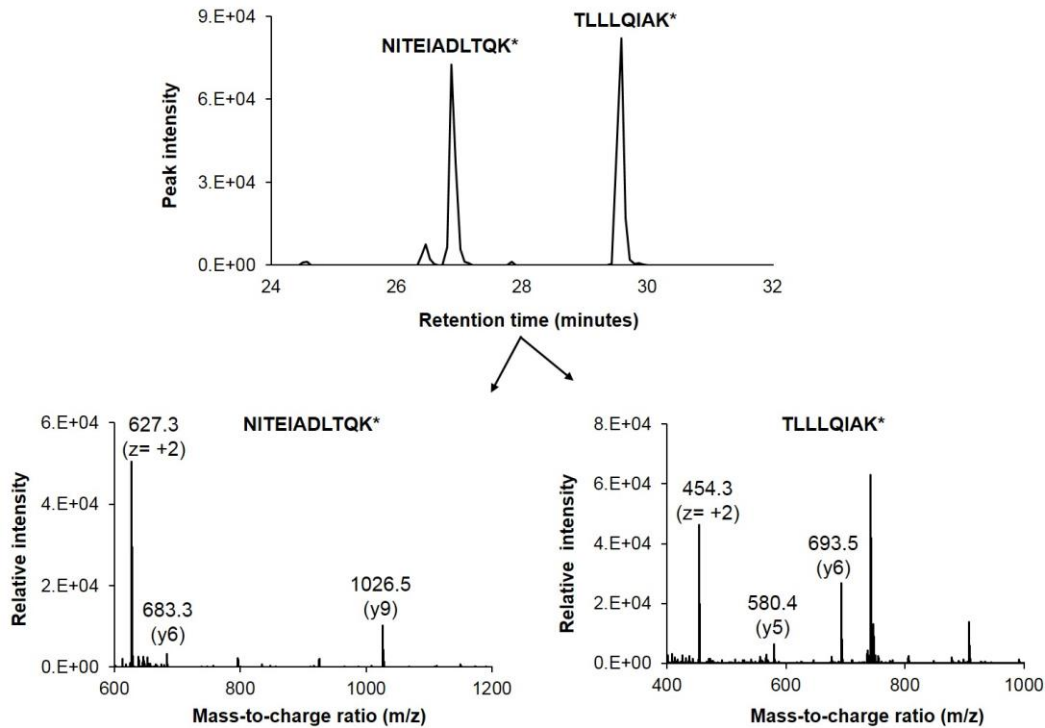


Figure 4.10 Extracted ion chromatograms of TLLLQIAK* and NITEIADLTQK* from a digest of isotopically labeled cTnI protein internal standard. Asterisk indicates the isotopically labeled amino acid. MS/MS spectra of both cTnI peptides are also shown.

and NITEIADLTQK*. Compared to the synthetic isotopically labeled cTnI peptides (NITEIADL*TQK where L* represents L-¹³C₆ and TLLLQIA*K where A* represents A-¹³C₃, ¹⁵N) that were used as the internal standard for recovery studies, the isotopically labeled cTnI was labeled at lysine or arginine amino acids, which changed the mass of the labeled peptides used for quantification. Therefore, MRM transitions were adjusted to monitor tryptic peptides derived from the isotopically labeled cTnI protein, as shown in Table 4.3. Similarly, the digested cTnI protein internal standard was analyzed via MRM analysis using the LC-MS/MS (triple quadrupole) to check isotope incorporation level on the labeled amino acid residues. Labeled and unlabeled cTnI peptides with their specific MRM transition were targeted during LC-MS/MS analysis, and peak areas from the unlabeled peptides

Table 4.3 MRM transitions of NITEIADLTQK* and TLLLQIAK* from the isotopically labeled cTnI protein internal standard. Asterisk indicates the isotopically labeled amino acid.

Peptide AA sequence	Precursor Ion (<i>m/z</i>)	Product Ion (<i>m/z</i>)	Collision Energy (V)
NITEIADLTQK*	[627.3] ²⁺	[1026.5] ⁺	10
		[683.3] ⁺	11
TLLLQIAK*	[454.3] ²⁺	[693.5] ⁺	7
		[580.4] ⁺	8

were compared to the labeled peptides. Figure 4.11 shows a representative chromatogram of cTnI tryptic peptides from the digested isotopically labeled cTnI protein sample. The protein standard was 99.7 % isotopically labeled, and no correction was applied during data analysis to account for the negligible 0.3 % unlabeled form. This data was in agreement with data provided from the vendor.

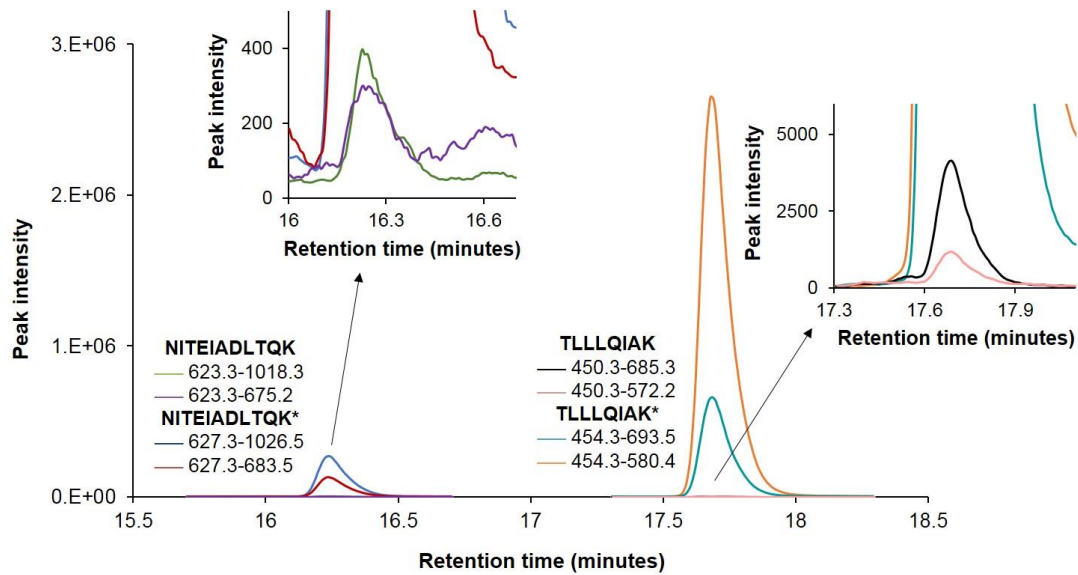


Figure 4.11 Representative MRM chromatograms of digested isotopically labeled cTnI protein internal standard to determine isotope incorporation level. Unlabeled and labeled MRM transitions for NITEIADLTQK and TLLLQIAK were monitored. Zoomed insets of the unlabeled peptides are shown.

For proof-of-concept, five replicates of SRM 2921 and isotopically labeled cTnI were spiked into normal human plasma, enriched and digested for LC-MS/MS measurement. Matrix-matched calibrants were also prepared by spiking normal plasma with a range of concentrations of SRM 2921 and a defined concentration of isotopically labeled cTnI. ID-LC-MS/MS analysis revealed that > 90 % (CV = 5.0 %) of cTnI had been recovered throughout all of the sample processing steps, indicating the isotopically labeled cTnI internal standard acted similarly to SRM 2921 throughout the analytical workflow and corrected for most biases linked to protein losses during enrichment and digestion. Therefore, the isotopically labeled protein was selected as an internal standard for quantification of endogenous cTnI in patient plasma samples.

4.3.3. cTnI quantification in patient plasma samples

The developed method was applied to the analysis of cTnI in (de-identified) myocardial patient plasma samples obtained from the University of Washington. Human subjects research determination forms can be found in Appendix A. cTnI-positive patient samples needed to be obtained from a clinical medicine laboratory since elevated concentrations of cTnI are highest approximately 18 ± 24 hours after the onset of a myocardial infarction. Additionally, only 0.5 mL to 2 mL of leftover plasma from each consented patient was provided; therefore, individual patient samples had to be pooled for replicate sample preparations.

To determine repeatability of the assay, five replicates were prepared from a pooled myocardial infarction patient plasma sample lot. Isotopically labeled cTnI internal standard (≈ 6.66 ng) was spiked into the cTnI-positive pooled patient sample prior to sample processing. For cTnI quantification, an external calibration was employed by spiking SRM 2921 ($\approx 1.22, 2.42, 5.96, 11.9, 18.2$ ng) and the isotopically labeled cTnI internal standard (≈ 6.66 ng) into negative-cTnI patient plasma samples (≈ 0.9 mL) to generate five matrix-matched calibrants. Figure 4.12 shows a representative MRM chromatogram of cTnI peptides derived from a pooled patient plasma sample. The linearity of the external calibration curves for all of the monitored transitions was demonstrated to be ≥ 0.992 , as shown in Figure 4.13.

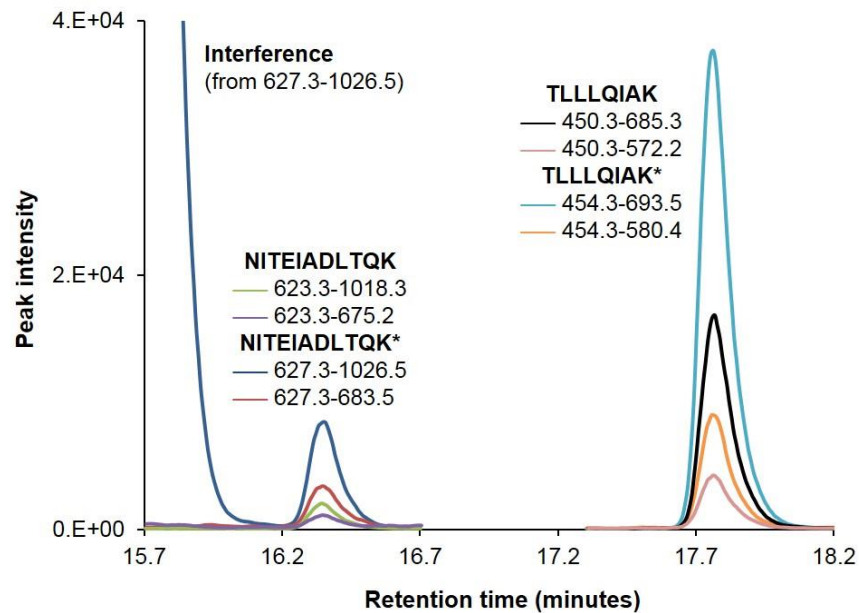


Figure 4.12 MRM chromatogram of cTnI enriched from a pooled cTnI-positive patient plasma sample.

The average concentration of endogenous cTnI in plasma was determined to be 2.65 ng/mL and the CV was 25.0 % ($n = 5$), as shown in Table 4.4. Despite comparability in the measurement of cTnI by transitions of the same peptide, there was considerable discrepancy between the peptides, which increased measurement variability and impeded the overall quantification of cTnI in plasma. The acceptable range of intra-assay CV is typically below < 20% for quantification of low abundant proteins in plasma.^{43,144}

As speculated in Section 4.3.2, the lower measurement values for NITEIADLTQK were likely due to enhanced degradation of the calibrant compared to the endogenous form since this peptide is located outside the stable region of cTnI. Overall, high variability between peptide measurements could compromise the

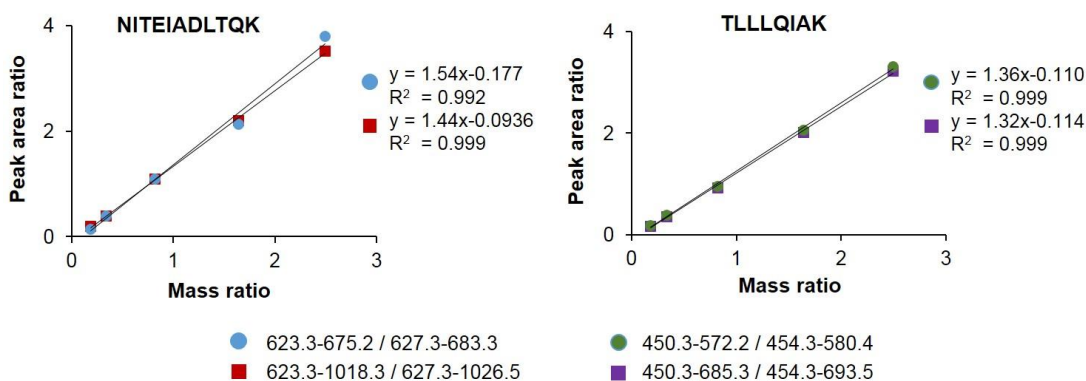


Figure 4.13 Calibration curves are provided for monitored cTnI peptide transitions as a plot of unlabeled : labeled integrated peak area ratios versus unlabeled : labeled measured mass ratios. A regression equation of the best-fit line is provided for each plot along with a R^2 estimate of the correlation for fit to the line.

applicability of the ID-LC-MS/MS-based assay for robust and accurate measurements of a new secondary (matrixed-matched) reference material. To improve the precision and accuracy of the quantification results, additional cTnI peptides from different regions of the protein were added to the LC-MS/MS method.

The measurement of a higher number of tryptic peptides has the potential to increase the precision and provide higher confidence in the accuracy of cTnI quantification. Revisiting Figure 4.3, NIDALSGMEGR and AYATEPHAK peptides also produced relatively high MRM signals compared to other cTnI tryptic peptides screened by MRM analysis. The tryptic peptide ISADAMMQALLGAR was avoided, mainly due to the presence of the serine residue, which has been known to undergo phosphorylation.^{84,145}

In comparison to isotopically labeled peptides, one benefit of using a full-length isotopically labeled protein as the internal standard is the flexibility to add or change the surrogate peptides used to quantify cTnI during LC-MS/MS analysis.¹⁴² The analysis of additional tryptic peptides can also provide information on the

Table 4.4 cTnI levels in five replicate sample preparations from a pooled myocardial infarction patient plasma sample lot.

Replicate #	NITEIADLTQK 623.3-1018.3	NITEIADLTQK 623.3-675.2	TLLLQIAK 450.3-685.3	TLLLQIAK 450.3-572.2	Mean (protein) ng/mL	Std. dev.	%CV
Replicate 1	1.77	1.91	3.02	2.96	2.41	0.667	27.6
Replicate 2	1.87	2.01	3.22	3.15	2.56	0.721	28.1
Replicate 3	2.00	2.21	3.47	3.38	2.77	0.771	27.9
Replicate 4	2.06	2.17	3.38	3.35	2.74	0.723	26.4
Replicate 5	1.93	2.37	3.40	3.42	2.78	0.752	27.0
Mean (peptide) ng/mL	1.92	2.14	3.30	3.25	2.65		
Std. dev.	0.113	0.179	0.180	0.197		0.663	
%CV	5.87	8.39	5.46	6.05			25.0

stability or heterogeneity of cTnI.¹³⁶ To this end, the LC-MS/MS method was expanded to monitor NIDALSGMEGR and AYATEPHAK as additional surrogate cTnI peptides in order to increase the precision of the measurement. The labeled versions of these two peptides for each MRM transition were also added for ID-LC-MS/MS analysis and were determined using the MRM prediction tool, Skyline.⁵⁵ On another note, the AYATEPHAK peptide had a wider MRM peak width and a slightly less stable retention time compared to other cTnI peptides; therefore, the dynamic MRM window for that particular peptide was extended to ± 3 minutes, and AYATEPHAK did not co-elute or interfere with other monitored peptides. Dynamic MRM monitors individual peptides at specific retention times only; therefore, if the MRM window is too narrow, the AYATEPHAK may not be completely detected during elution, which would negatively affect quantification.

A proof-of-principle experiment was performed to determine the effect of two additional tryptic peptides on the average cTnI measurement. To assess recovery of

the additional peptides, known constant amounts (12.5 ng) of SRM 2921 and isotopically labeled cTnI internal standard were spiked into normal human plasma ($n = 5$). A matrixed-matched calibration was also generated by spiking SRM 2921 ($\approx 1.34, 2.61, 12.5, 25.6, 37.8$ ng) and isotopically labeled protein internal standard (≈ 12.5 ng) into normal human plasma (≈ 0.9 mL). Samples and calibrants were then enriched using magnetic particle-based immunoaffinity enrichment, digested with trypsin and prepared for LC-MS/MS analysis. Figure 4.14 shows a representative MRM chromatogram from one of the five replicates.

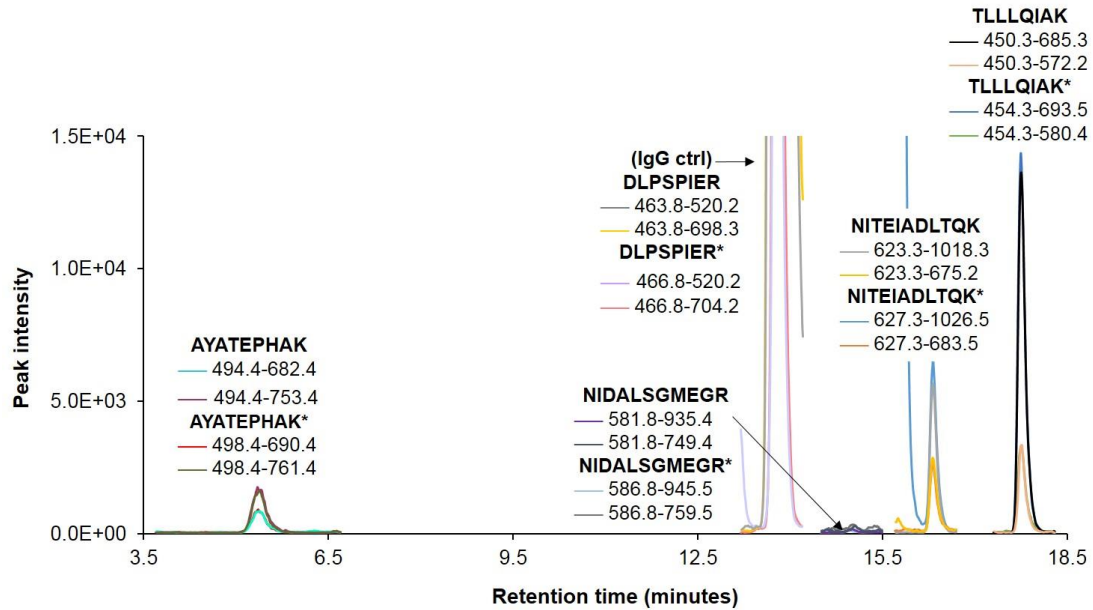


Figure 4.14 MRM chromatogram of cTnI recovered from normal plasma samples (spiked with SRM 2921). Two transitions from each (unlabeled and labeled) cTnI peptide, AYATEPHAK, NIDALSGMEGR, NITEIADLTQK and TLLLQIAK were monitored. Two transitions for (unlabeled and labeled) DLPSPiER, representative of the antibody, were also monitored.

It is important to note that neither the unlabeled nor labeled NIDALSGMEGR peptide was detected in any of the samples, which supports the hypothesis that SRM 2921 in plasma matrix is degrading or modifying near the C-terminus of the cTnI protein. Conversely, AYATEPHAK, which is located near and within the stable

region of cTnI, was reproducibly detected in the digested samples, enabling it to be used for cTnI quantification. Overall recovery of cTnI was > 90% with CV \leq 6.31 % for the five replicate samples. To this end, Table 4.5 shows the updated MRM transition list for the three cTnI tryptic peptides used for quantification and one antibody tryptic peptide used as a qualitative control to assess the antibody-magnetic particle enrichment.

After confirming sufficient peptide recovery and measurement precision, the magnetic nanoparticle-based immunoaffinity approach coupled with targeted LC-

Table 4.5 Updated MRM transitions of cTnI surrogate peptides used for quantification, and MRM transitions for the antibody peptide (for identification and relative quantification).

Peptide AA sequence	Precursor ion (<i>m/z</i>)	Product ion (<i>m/z</i>)	Collision energy (V)	Retention time (minutes)
NITEIADLTQK	[623.3] ²⁺	[1018.3] ⁺	10	16.2 \pm 1
		[675.2] ⁺	11	
NITEIADLTQK*	[627.3] ²⁺	[1026.5] ⁺	10	
		[683.4] ⁺	11	
TLLLQIAK	[450.3] ²⁺	[685.3] ⁺	7	17.8 \pm 1
		[572.2] ⁺	8	
TLLLQIAK*	[454.3] ²⁺	[693.5] ⁺	7	
		[580.4] ⁺	8	
AYATEPHAK	[494.4] ²⁺	[753.4] ⁺	9	5.2 \pm 3
		[682.4] ⁺	9	
AYATEPHAK*	[498.4] ²⁺	[761.4] ⁺	9	
		[690.4] ⁺	9	
DLPSPiER (IgG)	[463.8] ²⁺	[698.3] ⁺	7	13.7 \pm 1
		[514.2] ⁺	17	
DLPSPiE*R (IgG)	[466.8] ²⁺	[704.2] ⁺	7	
		[520.2] ⁺	17	

MS/MS was applied to quantify cTnI concentrations in five individual cTnI-positive patient plasma samples. Calibration curves were generated by spiking known

amounts of SRM 2921 ($\approx 1.78, 2.48, 6.04, 12.1, 18.4, 24.5$ ng) and isotopically labeled protein internal standard (≈ 12.1 ng) into cTnI-negative patient plasma (≈ 0.9 mL). Individual myocardial infarction patient plasma samples (≈ 0.9 mL) were spiked with defined amounts (≈ 12.1 ng) of isotopically labeled protein internal standard. cTnI was captured from the samples and calibrants by magnetic nanoparticle-based immunoaffinity enrichment, washed, and digested with trypsin. Isotopically labeled DLPSPIE*R, a surrogate peptide from the constant region of the anti-cTnI antibody, was prepared at 0.0466 ng/ μ L and used to reconstitute the digests (10 μ L final volume) prior to LC-MS/MS analysis.

Figure 4.15 shows a representative MRM chromatogram of the tryptic peptides used to quantify cTnI concentration in an individual myocardial infarction

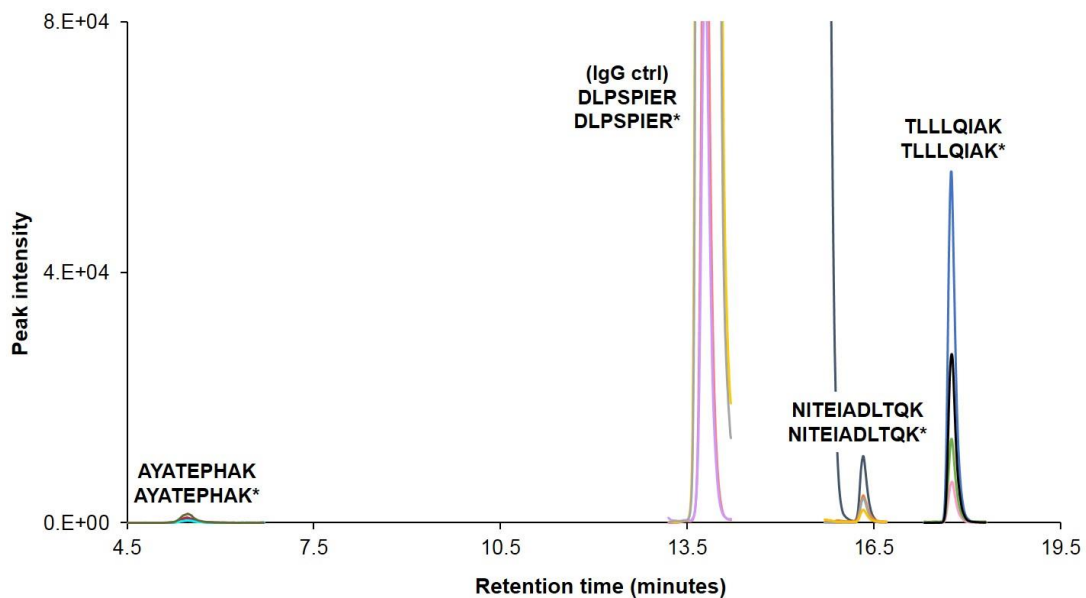


Figure 4.15 Representative MRM chromatogram of cTnI enriched from an individual cTnI-positive patient plasma sample.

patient plasma sample. As shown in Figure 4.16, the method was linear between 1.98 ng/mL and 27.2 ng/mL with $R^2 \geq 0.994$ for all monitored transitions. Using a matrix-matched calibration, peptide concentrations from a total of six transitions were calculated and averaged to determine the overall cTnI concentration for each individual patient plasma sample. Overall cTnI concentrations ranged between 4.83 ng/mL and 11.3 ng/mL with CV's $\leq 14.3\%$ for the five patient samples, as demonstrated in Table 4.6.

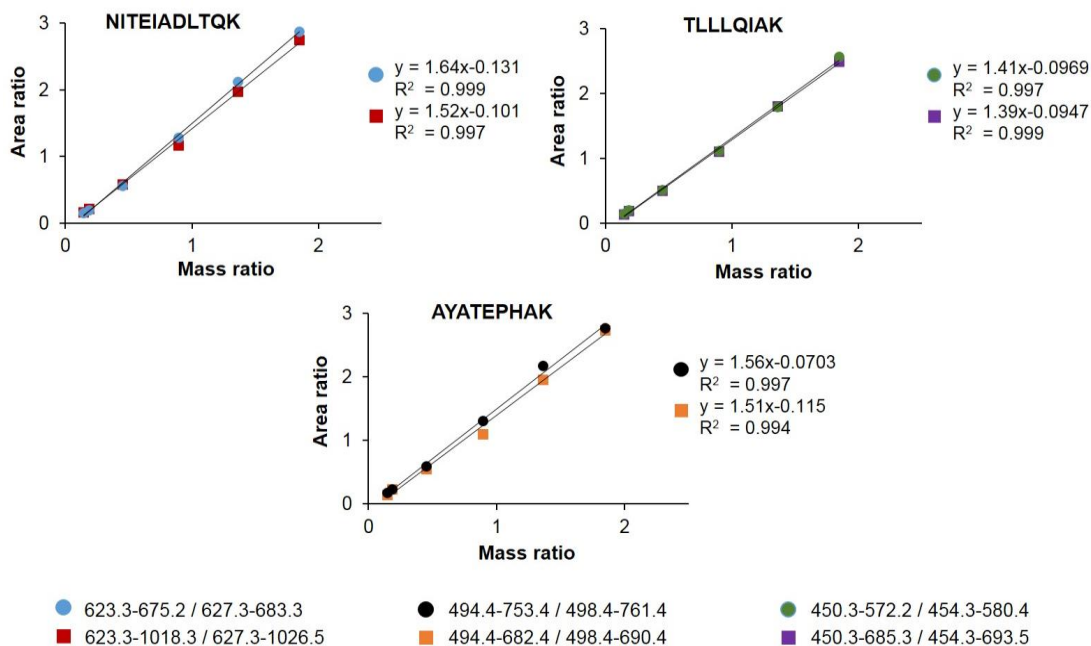


Figure 4.16 Calibration curves are provided for monitored cTnI peptide transitions as a plot of unlabeled : labeled integrated peak area ratios versus unlabeled : labeled measured mass ratios. A regression equation of the best-fit line is provided for each plot along with a R^2 estimate of the correlation for fit to the line.

Quantifying three cTnI tryptic peptides simultaneously and independently provided confidence in the accuracy of the ID-LC-MS/MS measurement results.¹³⁸ Based on the data, it was important to choose surrogate peptides within or near the stable region of cTnI for bottom-up ID-LC-MS/MS analysis. Results indicated that

cTnI in both SRM 2921 and recombinant isotopically labeled protein degrades near the C-terminus of cTnI once spiked into plasma. Therefore, surrogate peptides should be avoided near this region.

Table 4.6 cTnI levels in five individual myocardial infarction patient plasma samples.

cTnI peptide	Patient Sample 1	Patient Sample 2	Patient Sample 3	Patient Sample 4	Patient Sample 5
NITEIADLTQK (1)	4.78	10.44	6.59	5.10	4.13
NITEIADLTQK (2)	5.17	10.44	6.51	5.22	3.86
TLLLQIAK (1)	6.23	13.20	8.08	6.35	5.43
TLLLQIAK (2)	6.31	12.83	8.21	6.39	5.49
AYATEPHAK (1)	5.74	11.0	7.84	5.37	5.19
AYATEPHAK (2)	5.32	9.72	7.06	5.55	5.03
Mean (ng/mL)	5.59	11.3	7.38	5.66	4.86
Std. dev.	0.610	1.41	0.759	0.567	0.695
%CV	10.9	12.5	10.3	10.0	14.3

4.4. Conclusion

An immunoaffinity enrichment strategy based on magnetic particle-based separation was utilized to selectively isolate cTnI from clinical patient samples, such as plasma. Following immunocapture, cTnI was digested with trypsin to release surrogate tryptic peptides for LC-MS/MS analysis. The success of the enrichment approach was measured by experimentally determining percent recovery of cTnI (SRM 2921) from different matrices using ID-LC-MS/MS analysis with isotopically labeled peptide internal standards. Significant protein losses were expected during enrichment because cTnI is in low abundance, even in plasma samples from myocardial infarction patients. Following method development, an isotopically labeled protein internal standard

was utilized to account for protein losses and digestion variability, and enabled accurate protein quantification.

Overall, the ID-LC-MS/MS assay coupled with immunoaffinity enrichment was able to quantify low abundant cTnI in human plasma in the low ng/mL range with excellent CV's using three surrogate cTnI peptides. This work demonstrates significant improvements in magnetic particle-based immunoaffinity enrichment techniques and LC-MS/MS detection limits for the analysis of cTnI in patient samples. Furthermore, this method has the potential to act as a candidate reference measurement procedure for value assignment of cTnI in serum-based reference materials.

Chapter 5: cTnI analysis by peptide immunoaffinity enrichment and LC-MS/MS analysis

5.1. Introduction

As an alternative to protein immunoaffinity enrichment as described in Chapter 4, another enrichment strategy for cTnI involves using anti-peptide antibodies coupled to magnetic particles to capture and isolate cTnI at the peptide level rather than at the protein level by first performing a proteolytic digestion on the sample. Peptide enrichment by anti-peptide antibodies (also termed SISCAPA) coupled with MRM analysis has been reported to achieve limits of detection of ≈ 1 ng/mL for proteins using as little as 10 μ L of plasma.^{67,96,140,146} Anti-peptide antibodies can be generated against specific peptides from the target protein.^{52,92} The drawback is that a unique antibody has to be generated for each peptide of interest, which is relatively expensive (ranging upwards of \$2000 per anti-peptide antibody) and requires a long lead time (3-4 months).^{86,147} Although the production of anti-peptide antibodies is a lengthy and expensive process, the combination of peptide immunoaffinity enrichment with LC-MS/MS analysis is advantageous for cTnI quantification for two reasons. First, interferences caused by autoantibodies or antireagent antibodies are avoided because these proteins are enzymatically digested early in the sample preparation workflow. Second, the assay has the ability to readily multiplex with other targets, such as peptides derived from cTnT and cTnC, which would allow quantification of the entire cardiac troponin complex in a single reference measurement procedure.^{28,89} Using this approach, anti-peptide antibodies (coupled to magnetic particles) can be used to capture surrogate cTnI peptides from

digested plasma and serum samples.^{76,86,148} The captured cTnI peptides can be then released from the antibody-magnetic particles and analyzed via LC-MS/MS.

This work aims to improve upon previously published SISCAPA-LC-MS/MS work by capturing two surrogate peptides from cTnI in plasma. In 2009, Kuhn et al.¹⁴⁰ reported a LC-MS/MS-based method coupled with peptide immunoaffinity enrichment to quantify cTnI in plasma using a single peptide (NITEIADLTQK). In this chapter, anti-peptide antibodies were raised against NITEIADLTQK and TLLLQIAK for cTnI peptide capture studies. In general, developing a peptide and protein immunoaffinity enrichment method coupled with LC-MS/MS analysis can ultimately be used to postulate the true values of cTnI in plasma and serum. A higher confidence in the certified value of cTnI in a serum-based reference material can be achieved if both enrichment methods are used to analyze identical clinical samples and a small % CV is calculated between the two methods.

In this chapter, preliminary cTnI peptide recovery studies demonstrating proof-of-principle are presented. Additionally, some existing and foreseen challenges are discussed regarding the development of a peptide immunoaffinity enrichment method for cTnI. Key steps in the workflow include target peptide selection, anti-peptide antibody reagent production, and optimization of the digestion, peptide capture, and peptide release.

5.2. Experimental design

5.2.1. Materials

Rabbit anti-peptide polyclonal antibodies specific for cTnI surrogate peptides NITEIADLTQK and TLLLQIAK were produced by Pacific Immunology (California, USA). Briefly, the selected peptides were synthesized with an N-terminal cysteine, conjugated to KLH, and the KLH/adjuvant formulations were then injected into two rabbits (per peptide) following a 13-week antibody production protocol. Antisera were tested by ELISA and reactive bleeds (against the two peptides) were selected for purification via affinity chromatography. Purified polyclonal antibodies were stored at -20 °C in PBS, pH 7.4 containing 0.02 % (w/v) sodium azide.

SRM 2921 – Human cardiac troponin complex was obtained from NIST. The synthetic isotopically labeled peptides, NITEIADL*TQK and TLLLQIA*K were purchased from AnaSpec, Inc. (California, USA). A donor plasma pool, collected from 50 apparent healthy individuals, was obtained through Golden West Biologicals, Inc. (California, USA). Rapigest™ SF was purchased from Waters Corporation (Massachusetts, USA) and trypsin gold, MS grade, was purchased from Promega Corporation (Wisconsin, USA). High purity LC-MS grade water (H₂O)/formic acid and acetonitrile (ACN) /formic acid were purchased from Honeywell-Burdick and Jackson (Michigan, USA). Protein LoBind centrifuge tubes were purchased from Eppendorf (New York, USA). All other chemicals were purchased from Sigma-Aldrich (Missouri, USA).

5.2.2. Immobilization of anti-peptide polyclonal antibodies onto magnetic nanoparticles

Polyclonal anti-NITEIADLTQK and anti-TLLLQIAK antibodies were immobilized on the magnetic nanoparticles using the glutaraldehyde method, as described in Section 4.2.2. After conjugation, blocking, and wash steps, the antibody-nanoparticle conjugates were reconstituted in ammonium bicarbonate (0.25 mL). The resultant nanoparticle sample contained 4 mg/mL nanoparticles. A single batch of antibody-magnetic nanoparticle conjugates were prepared for each peptide, and then combined to form one lot of antibody-nanoparticle conjugates for use in cTnI peptide capture studies.

5.2.3. Calibrant and sample preparation for recovery studies

Human cardiac troponin complex (cTnI, cTnT, cTnC) from NIST SRM 2921 stock was thawed to room temperature and prepared gravimetrically by diluting SRM 2921 in 0.1 % BSA solution in ammonium bicarbonate. SRM 2921 solution was added at discrete amounts (e.g., \approx 1.3, 2.5, 5.0, 10, 20 ng) and diluted up to 40 μ L with 0.1 % (w/v) BSA in ammonium bicarbonate (pH 7.8) solution. Known amounts of SRM 2921 (5, 10, 15 ng) were added to centrifuge tubes and diluted up to 40 μ L with 0.1 % (w/v) BSA in ammonium bicarbonate solution. All samples were prepared in duplicate.

The samples and calibrants were denatured in 0.2 % (v/v) Rapigest™ SF in 50 mmol/L ammonium bicarbonate (40 μ L) and boiled for 2 minutes. The proteins were reduced with a final concentration of 10 mmol/L DTT at 60 °C with shaking for 45 minutes, and alkylated with 10 mmol/L IAM in the dark at room temperature for 45

minutes. Trypsin was added to the samples (1:2.5 w/w trypsin-to-protein ratio) and all samples were incubated for 16 hours at 37 °C. The digests were acidified with a final concentration of 5 % (v/v) formic acid for 45 minutes at 37 °C and centrifuged at 4 °C to remove the Rapigest™ SF. The digests were transferred to fresh centrifuge tubes and then dried using a vacuum centrifuge. Calibrants were reconstituted with 30 µL antibody-magnetic nanoparticles and diluted up to 40 µL with ammonium bicarbonate. To ensure complete recovery, the calibrants did not undergo the following enrichment or wash steps.

To capture NITEIADLTQK and TLLLQIAK peptides, samples were reconstituted in 0.9 mL PBS, pH 7.4, and then 30 µL of antibody-magnetic nanoparticle conjugates were added. Samples were incubated at room temperature with gentle rotary mixing for 8 hours. Following incubation, non-specific peptides were removed from the samples by washing the nanoparticles two times with tris buffer (20 mmol/L tris, 150 mmol/L sodium chloride) containing 0.05 % (v/v) Tween 20 (0.9 mL) and once with ammonium bicarbonate (0.9 mL). The samples were resuspended in ammonium bicarbonate (40 µL) for a second digestion.

Captured peptides and anti-peptide antibodies were released from the magnetic nanoparticles by denaturation. The samples and calibrants were denatured in 0.2 % (v/v) Rapigest™ SF in 50 mmol/L ammonium bicarbonate (40 µL) and boiled for 2 minutes. Trypsin was added to the samples (1:10 w/w trypsin-to-protein ratio) and all samples were incubated for 2 hours at 37 °C. The digests were acidified with a final concentration of 5 % (v/v) formic acid for 45 minutes at 37 °C and centrifuged at 4 °C to remove the Rapigest™ SF and the magnetic nanoparticles. The

digests were transferred to fresh autosampler vials and then dried using a vacuum centrifuge.

Isotopically labeled peptides (TLLLQIA[¹³C₃,¹⁵N]K and NITEIADL[¹³C₆]TQK, were prepared at constant concentrations for use as internal standards. Calibrants and samples were reconstituted with the isotopically labeled peptide internal standard solution (10 µL) prior to LC-MS/MS analysis.

5.2.4. LC-MS/MS analysis

LC-MS/MS (dynamic MRM) analysis was performed on an Agilent 1200 LC system coupled in-line with an Agilent 6490 triple quadrupole MS as described in Section 4.2.6. Two fragmentation transitions were monitored by dynamic MRM for two cTnI peptides (NITEIADLTQK and TLLLQIAK) for both the isotopically labeled and unlabeled peptides, as shown in Table 5.1. Delta retention time windows were set to 1 minute for each MRM transition. Data analysis was performed as described in Section 4.2.6.

Table 5.1 Optimized MS parameters and monitored transitions for cTnI identification and quantification. Two transitions (unlabeled and labeled) were monitored for each peptide.

Peptide AA sequence	Precursor Ion (<i>m/z</i>)	Product Ion (<i>m/z</i>)	Collision Energy (V)	Retention Time (minutes)
NITEIADLTQK	[623.3] ²⁺	[1018.3] ⁺	10	16.2
		[675.2] ⁺	11	
		[1024.5] ⁺	10	
NITEIADL*TQK	[626.3] ²⁺	[681.4] ⁺	11	
TLLLQIAK	[450.3] ²⁺	[685.3] ⁺	7	17.8
		[572.2] ⁺	8	
		[689.3] ⁺	7	
TLLLQIA*K	[452.3] ²⁺	[576.2] ⁺	8	

5.3. Results and discussion

5.3.1. Polyclonal anti-peptide antibodies

NITEIADLTQK and TLLLQIAK peptide sequences were used to generate anti-peptides antibodies for cTnI peptide immunoaffinity enrichment. These peptides were selected based on their detectability and high LC-MS/MS signal responses after trypsin digestion of cTnI (from SRM 2921), as described in Section 4.3.1.

Polyclonal antibody production yields (provided from the vendor) were highly variable. The anti-TLLLQIAK antibody only yielded ≈ 1 mg after immunization and purification using two rabbits, whereas the anti-NITEIADLTQK antibody yields were ≈ 24 mg. TLLLQIAK was predicted to be less immunogenic than NITEIADLTQK due to its hydrophobic nature and short peptide length. Therefore, an additional four rabbits were immunized by the vendor to generate higher anti-TLLLQIAK antibody yields. Antisera was titrated and measured by ELISA in all four rabbits, and the two rabbits producing the highest titers proceeded with the 13-week protocol. The second immunization project produced ≈ 1.75 mg of anti-TLLLQIAK antibody. Because the anti-TLLLQIAK antibody was limited in supply, few preliminary studies could be performed.

5.3.2. Magnetic particle-based peptide immunoaffinity recovery

Percent recovery studies were performed to initially evaluate the peptide immunoaffinity enrichment workflow and demonstrate proof-of-principle. cTnI (from SRM 2921) was spiked at three different levels (5, 10, 15 ng) into an ammonium bicarbonate solution containing 0.1 % BSA. Samples were digested with trypsin, and enriched with anti-peptide (NITEIADLTQK and TLLLQIAK) antibodies conjugated

to magnetic nanoparticles; followed by a second digestion to release the peptides and antibodies from the magnetic nanoparticles. Isotopically labeled peptide internal standards were spiked into the samples prior to LC-MS/MS analysis. Figure 5.1 shows a representative MRM chromatogram of cTnI peptides simultaneously captured from a buffered solution using peptide immunoaffinity enrichment.

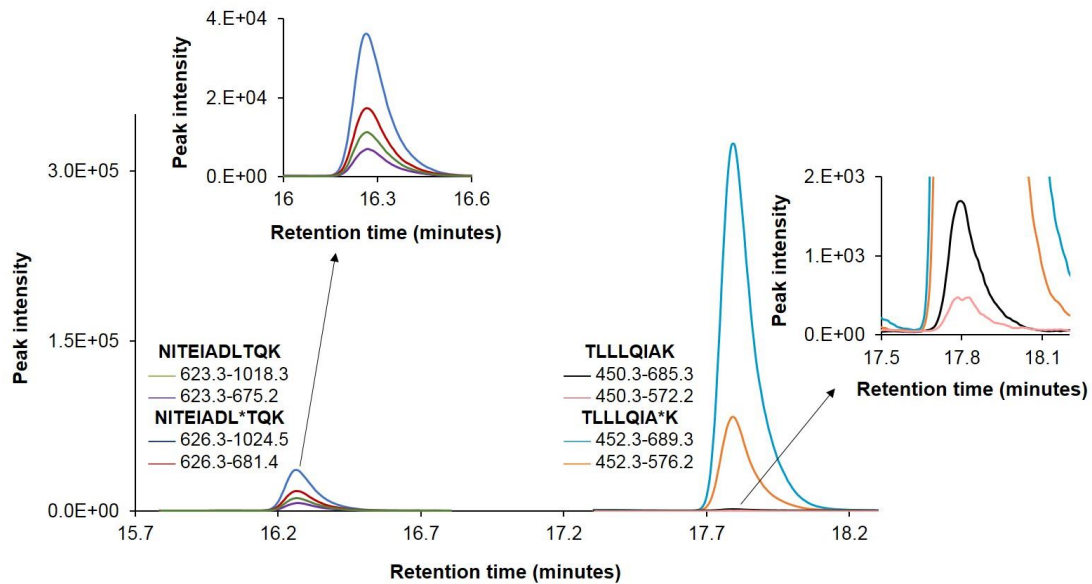


Figure 5.1 MRM chromatogram of cTnI enriched from buffer using magnetic nanoparticle-based peptide immunoaffinity capture.

Percent recovery of cTnI was determined by LC-MS/MS analysis using external calibration curves with SRM 2921 as the calibrant and isotopically labeled peptide internal standards (NITEIADL*TQK and TLLLQIA*K). The linearity of the external calibration curves for all of the monitored transitions was demonstrated to be ≥ 0.994 , as shown in Figure 5.2.

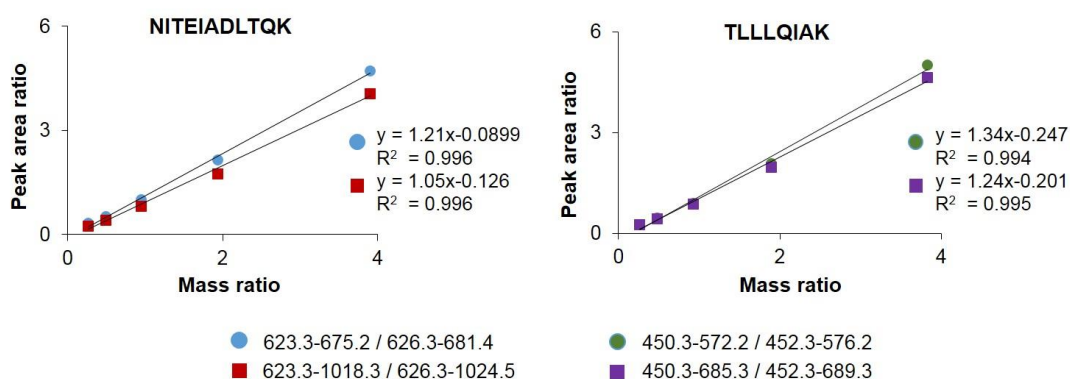


Figure 5.2 Calibration curves are provided for monitored cTnI peptide transitions as a plot of unlabeled : labeled integrated peak area ratios versus unlabeled : labeled measured mass ratios. A regression equation of the best-fit line is provided for each plot along with a R^2 estimate of the correlation for fit to the line.

As shown in Figure 5.3, percent recoveries of NITEIADLTQK from buffer ranged from 27 % to 38 % with CV's ≤ 7.0 %, indicating that the assay needed to be further optimized to improve antibody capture and digestion efficiency. Furthermore, recoveries for TLLLQIAK were lower and only ranged between 6.1 % and 17 % with CV's ≤ 7.6 %. It appeared that TLLLQIAK elicited a weaker antibody response than the NITEIADLTQK peptide, as evidenced by the lower recoveries.

Peptide recoveries were also examined by spiking constant amounts of SRM 2921 (35 ng) into buffer (0.1 % BSA in ammonium bicarbonate, 30 μ L) and normal human plasma (30 μ L). An isotopically labeled peptide internal standard was added after sample processing and used to estimate percent recoveries for each peptide via a one-point calibration curve. Figure 5.4 shows MRM chromatograms of cTnI peptides captured from buffer and plasma. As predicted, a higher relative percent recovery of each cTnI peptide was achieved when peptide immunoaffinity enrichment was performed in buffer rather than plasma. For example, approximately 15 % of

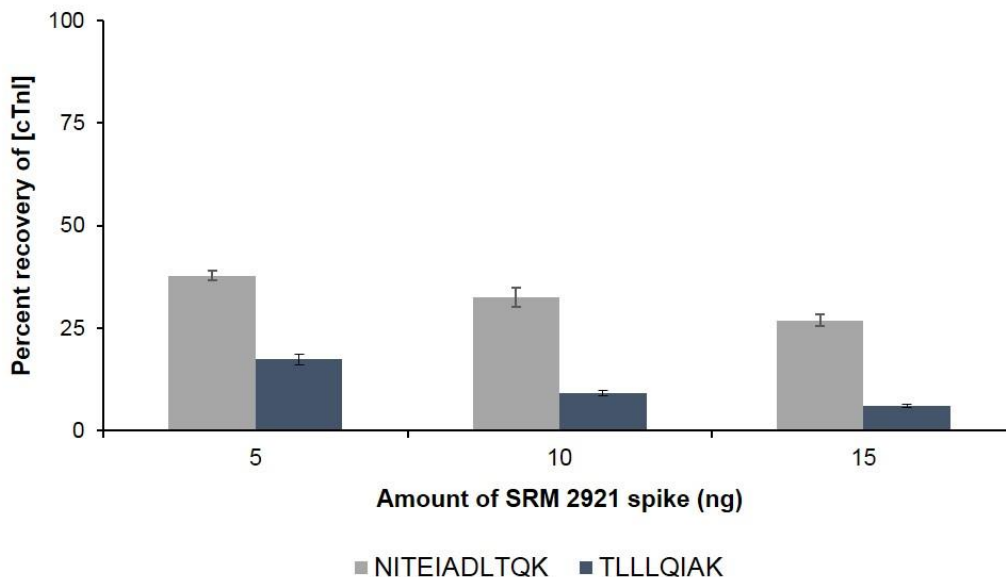


Figure 5.3 Percent recovery of cTnI (at the peptide level) spiked into buffer at three different amounts. Quantification was determined by analyzing two transitions for two cTnI peptides. The standard deviation error bars represent the monitored transitions per peptide from duplicate sample preparations.

NITEIADLTQK was recovered from the buffer matrix compared to the $\approx 5\%$ recovery from plasma. Relative percent recoveries of TLLLQIAK were estimated to be $< 1\%$ in both matrices, suggesting that the peptide has poor antigenicity to the polyclonal anti-TLLLQIAK antibody and that the workflow needed further optimization.

Overall percent recoveries varied between NITEIADLTQK and TLLLQIAK during the preliminary studies, which was determined by adding an isotopically labeled peptide internal standard in the final step of the sample preparation (i.e. after digestion, immunocapture and peptide release) prior to LC-MS/MS analysis. Ideally, the isotopically labeled peptide internal standard can be added as early as the immunoaffinity capture step. By spiking the isotopically labeled peptide internal standard at different steps in the workflow following digestion (i.e. immunoaffinity

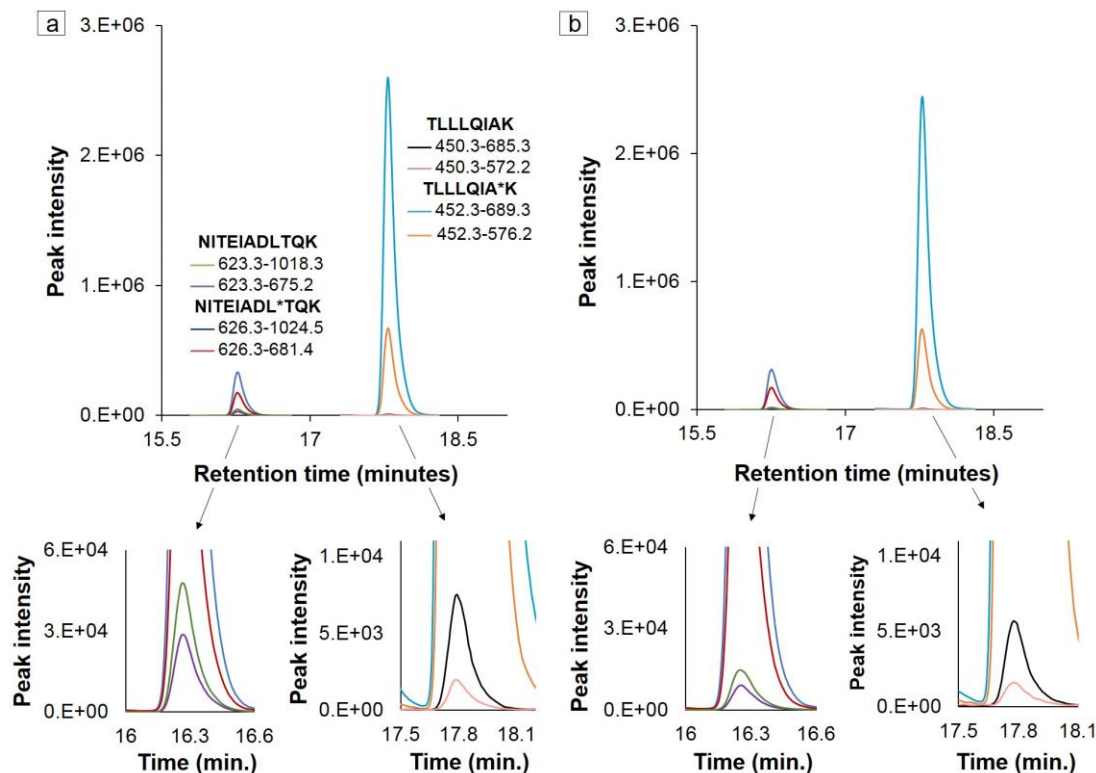


Figure 5.4 Representative MRM chromatograms of spiked cTnI enriched from (a) buffer and (b) normal plasma using magnetic nanoparticle-based peptide immunoaffinity capture and LC-MS/MS analysis.

capture and peptide release steps), peptide recoveries can be evaluated to provide insight into which steps need additional optimization. An example of this is shown in Appendix B. After method development, an isotopically labeled protein internal standard can be incorporated into the workflow to account for the digestion step, a well-known source of variability. The protein internal standard can correct for most biases linked to peptide losses during digestion, enrichment, and release, as demonstrated in sections 4.3.2 and 4.3.3.

5.3.3. Potential considerations for improvement of cTnI recovery via peptide immunoaffinity enrichment in further studies

In order to quantify cTnI at the low or sub ng/mL range using peptide immunoaffinity enrichment, large volumes of human plasma (i.e. ≈ 1 mL) may need

to be digested. During preliminary studies, reduction (with DTT) and alkylation (with IAM) of 30 μ L plasma made the sample cloudy, suggesting that some of the denatured proteins formed aggregates. Overnight digestion with trypsin, however, made the solution less opaque.¹⁴⁹ Insolubility of protein aggregates can hinder trypsin digestion and cause protein/peptide losses.¹⁵⁰ Therefore, the current trypsin digestion protocol needs to be optimized and scalable to 1 mL of plasma. Razavi et al.¹⁵¹ have reported an “addition only” method to efficiently and reproducibly digest 1 mL of plasma using urea as the denaturant and tris-(2-carboxethyl)phosphine (TCEP) as the reducing agent prior to peptide immunoaffinity enrichment. This protocol may be a better approach to digest large volumes of plasma for cTnI peptide immunoaffinity studies.

A second digestion step was performed to release cTnI peptides from the antibody-magnetic nanoparticle conjugates. During preliminary studies, bound peptides were initially released from the antibody via elution using 5 % acetic acid. However, acid elution demonstrated inconsistent removal of peptides between replicate samples. Therefore, a quick on-particle digestion was performed to release the cTnI peptides and antibodies from the magnetic nanoparticles. However, the antibodies cannot be reused if the sample is digested to release the captured peptides. Zhao et al.¹⁵² demonstrated that polyclonal antibodies (conjugated to magnetic beads) can be recycled after stripping off bound peptide analytes via acid washing using 5 % acetic acid with 3% acetonitrile in water. In the multiplexed assay tested by Zhao et al., antibodies were regenerated after each acid wash and reused for least 10 peptide capture cycles with consistent analytical performance. Extending the use of the

polyclonal antibodies via acid washing would enable more studies for assay development and application, while reducing overall assay cost.^{94,152} It would also extend the productive life of limited resources, such as the anti-TLLLQIAK antibody.

5.4. Conclusion

Peptide immunoaffinity enrichment coupled with LC-MS/MS analysis has the potential for high sensitivity LC-MS/MS analysis and allows for a highly multiplexed quantitative assay. Preliminary studies using polyclonal anti-peptide antibodies to capture NITEIADLTQK and TLLLQIAK peptides were described for enrichment of cTnI. These peptides were selected to be surrogate peptides for cTnI, which would allow a comparison between the two enrichment (peptide and protein) methods.

Evaluation and method development of the peptide immunoaffinity enrichment workflow was restricted due to the limited resource of anti-TLLLQIAK antibody. Polyclonal antibody production can be highly variable, with the anti-TLLLQIAK antibody only yielding \approx 1-2 mg of antibody due to its poor immunogenicity. Other cTnI peptides may prove to be better surrogate peptides for cTnI peptide capture. For instance, AYATEPHAK has a higher predicted immunogenicity for polyclonal antibody production, and it possesses high LC-MS/MS ionization efficiency.

Furthermore, a trypsin digestion protocol for large plasma/serum volumes also needs to be further optimized to improve digestion efficiencies prior to immunocapture. Various elution methods should also be evaluated to recover the bound cTnI peptides from the magnetic nanoparticles in order to improve the overall

recovery of cTnI. The ideal eluent would be able to retain the polyclonal antibodies on the magnetic nanoparticles for regeneration and reuse in additional immunoaffinity capture studies. However, this work demonstrates two proof-of-concept studies and the potential for peptide immunoaffinity capture as another enrichment strategy for cTnI prior to LC-MS/MS analysis.

Chapter 6: Summary and outlook

Measurement of cTnI in patient samples by immunoassays is already a useful clinical tool for detecting cardiac damage; however, the clinical community also recognizes that these immunoassays need improvement with respect to specificity and standardization. As such, the ultimate goal of this work was to develop a robust and traceable reference measurement procedure to certify concentration values of cTnI in a serum-based reference material, which can then be used by different immunoassay manufacturers to evaluate and harmonize the performance of their products. ID-LC-MS/MS is considered the gold standard for protein quantification. However, unlike immunoassay, the sensitivity and relatively small dynamic range of LC-MS/MS has been insufficient to measure concentrations of cTnI in serum. Therefore, the specific aim of this dissertation was to develop novel magnetic particle-based immunoaffinity enrichment strategies to isolate and enrich cTnI from serum and plasma for improved LC-MS/MS detection.

6.1. Summary

In this dissertation, silica coated magnetic nanoparticles with an average size of 85 nm were synthesized and used as solid supports for immunoaffinity enrichment. The spherical magnetic nanoparticles exhibited good monodispersity, maintained high paramagnetic properties and dispersed well in aqueous buffered solution, which were important characteristics to be of practical use for immunoaffinity enrichment applications. Furthermore, various immobilization strategies were investigated to bind anti-cTnI antibody to the magnetic nanoparticles. The immobilization of antibody

onto magnetic particles was a critical step in the enrichment process and directly influenced the performance of the targeted separation. As such, an ID-LC-MS/MS method was developed to accurately quantify the amount of antibody bound to magnetic particles. Using this method, two antibody immobilization strategies (glutaraldehyde versus epoxide reaction) and two different magnetic particle sizes (synthesized nanoparticles versus commercial microparticles) were evaluated. This study demonstrated that nanoparticles more efficiently bound antibody compared to microparticles due to the larger surface area-to-mass ratio. Higher antibody loading was thought to result in higher protein capture efficiency.

The optimized antibody-magnetic nanoparticle conjugates were then utilized to capture cTnI from various biological matrices and analyzed by ID-LC-MS/MS. Comprehensive optimization studies were undertaken to improve the overall recovery of cTnI during enrichment and subsequent sample processing. During method validation, the LC-MS/MS-based assay coupled with protein immunoaffinity enrichment demonstrated the necessary precision, robustness, and sensitivity to accurately quantify cTnI in serum or plasma. Furthermore, results demonstrated that surrogate peptides should be chosen near the central region (amino acid residues 30-110) of cTnI, which is more stable and more resistant to proteolysis or post-translational modification. In the final LC-MS/MS-based assay, the concentration of cTnI in plasma was quantified using an external standard curve with SRM 2921 as the mass calibrant and an isotopically labeled cTnI internal standard. The internal standard was used to account for instrument variations, as well as protein losses and digestion inefficiencies during sample processing.

Later work involved application of the optimized protein immunoaffinity enrichment technique and ID-LC-MS/MS method for absolute quantification of cTnI from plasma of myocardial infarction patient samples. The method was capable of measuring cTnI from an individual patient plasma samples at a concentration of ≈ 4 ng/mL with good precision ($CV < 15\%$). Therefore, it was concluded that this method can be used to postulate true clinical concentration values of cTnI in diseased serum or plasma, and in the future, may be utilized to quantify cTnI in a serum-based reference material.

Finally, due to the growing application of peptide immunoaffinity enrichment for low abundant protein quantification (via LC-MS/MS detection) reported in the literature, a study was undertaken to explore the potential of using magnetic nanoparticles coupled with anti-peptide antibodies to capture surrogate cTnI peptides, rather than the cTnI protein, for improved LC-MS/MS detection. Anti-peptide antibodies raised against NITEIADLTQK and TLLLQIAK were used for capture studies. However, in all of the studies, extremely low recoveries of TLLLQIAK after peptide immunoaffinity enrichment were observed. Therefore, further method development is required. To ensure accurate and reliable measurement, more than one surrogate peptide for cTnI should be used for quantification. Overall, the data revealed several challenges posed by peptide immunoaffinity enrichment with regard to peptide affinity and limited resources of antibody reagents. However, this proof-of-principle work demonstrated the potential for this enrichment approach.

6.2. Outlook and future work

This work demonstrates progress towards the development of a candidate reference measurement procedure for cTnI using immunoaffinity enrichment coupled with ID-LC-MS/MS analysis. Due to the limited sensitivity of the LC-MS/MS, a magnetic nanoparticle-based immunoaffinity enrichment strategy was needed to capture and isolate cTnI, while reducing the complexity and dynamic range of the sample. Further attempts will be made to improve the sensitivity and sample throughput of the reference measurement procedure.

Ideally, the objective is to reproducibly quantify cTnI levels in myocardial infarction patients (1-10 ng/mL) and healthy donors (1-10 pg/mL) by ID-LC-MS/MS. Further, an automated workflow would permit higher sample throughput, reduce analyst-to-analyst variation, and improve method reproducibility. Future work will focus on implementing the magnetic nanoparticle-based immunoaffinity enrichment and digestion protocols onto a liquid handling automation platform. A robotic platform will be beneficial for meeting testing demands during value assignment of cTnI in a secondary reference material.

Moreover, data published in the literature and in this dissertation demonstrate the potential of using anti-peptide antibodies to capture cTnI peptides for ID-LC-MS/MS analysis. However, in order to efficiently enrich cTnI at the peptide level, additional efforts are needed to improve overall peptide recovery. In this respect, various polyclonal anti-peptides antibodies, digestion approaches, and elution methods can be explored. A panel of anti-peptide antibodies specific to multiple cTnI

peptides should be tested to increase the success rate of antibody production, and to develop a more specific and robust assay.

Overall, this work highlights significant improvements in magnetic particle-based protein immunoaffinity enrichment techniques and LC-MS/MS detection for the analysis of cTnI in clinical patient samples. However, cTnI may be released and available in many forms, such as multiple complexes (e.g., cTnI-cTnC, cTnI-cTnC-cTnT) or in free form. Expanding the LC-MS/MS method to monitor peptides from cTnT and cTnC will shed light on which cTnI form is captured using anti-cTnI antibody. Further studies will include characterizing the heterogeneity of cTnI captured in patient samples using intact protein LC-MS/MS analysis.

With magnetic-nanoparticle immunoaffinity enrichment playing a significant role in the ID-LC-MS/MS analysis of cTnI, the methods described herein offer promise for the development of a reference measurement procedure to support the implementation of a reference measurement system for cTnI. It is critical that intra- and inter-standardization of cTnI quantification is achieved for improved patient treatment and management. Lastly, few reference measurement procedures and matrix-based reference materials are available for low abundant clinical protein biomarkers. The enrichment protocols and LC-MS/MS methods discussed will also provide the necessary tools to develop reference measurement procedures for other clinically relevant protein biomarkers.

Appendix A: Human subject determination forms from the University of Maryland, College Park, and the National Institute of Standards and Technology (NIST)



1204 Marie Mount Hall
College Park, MD 20742-5125
TEL 301.405.4212
FAX 301.314.1475
irb@umd.edu
www.umresearch.umd.edu/IRB

DATE: February 22, 2016

TO: Sang Bok Lee
FROM: University of Maryland College Park (UMCP) IRB

PROJECT TITLE: [867554-1] Development of Measurement Techniques for Cardiac Troponins in Human Serum

SUBMISSION TYPE: New Project

ACTION: DETERMINATION OF NOT HUMAN SUBJECT RESEARCH
DECISION DATE: February 22, 2016

Thank you for your submission of New Project materials for this project. The University of Maryland College Park (UMCP) IRB has determined this project does not meet the definition of human subject research under the purview of the IRB according to federal regulations.

We will retain a copy of this correspondence within our records.

If you have any questions, please contact the IRB Office at 301-405-4212 or irb@umd.edu. Please include your project title and reference number in all correspondence with this committee.

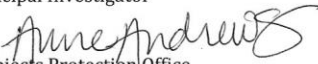
This letter has been electronically signed in accordance with all applicable regulations, and a copy is retained within University of Maryland College Park (UMCP) IRB's records.



UNITED STATES DEPARTMENT OF COMMERCE
National Institute of Standards and Technology
Gaithersburg, Maryland 20899

8 March 2016

MEMORANDUM FOR Eric Kilpatrick
Principal Investigator

From: Anne Andrews, PhD 
Director, Human Subjects Protection Office

Subject: Determination for MML Project # MML-019 Amendment 1 entitled, "Quality control materials in analysis of standard reference materials"

The above referenced proposed amendment was submitted to the Human Subjects Protection Office (HSPO) on 2 March 2016. The original determination was completed on 3 September 2015 and was determined to be *not research*.

I have reviewed your proposed project and determined that it has to changed to research, but is *not human subjects research* as defined in Department of Commerce Regulations, 15 CFR 27, also known as the Common Rule (45 CFR 46, Subpart A), for the Protection of Human Subjects. The additional study aims which will validate new or existing methods and develop novel measurement procedures meets the definition of research under the Common Rule. The project continues to use coded samples from the University of Washington that are leftover tissue from samples collected for clinical purposes. The code will never be provided to the NIST researchers and the researchers will not attempt to identify individual patients. In addition, this amendment adds Nicole Schneck as a researcher.

This determination was based on reviewing the following documents:

1. NIST Determination Form, dated 2 March 2016
2. Email from Karen E. Moe, PhD, Director, Human Subjects Division, Assistant Vice Provost for Research, University of Washington, August 11, 2015
3. Material Transfer Agreement Between NIST and University of Washington
4. Email from Andrew N. Hoofnagle, MD, PhD, Associate Professor, Lab Medicine, University of Washington, February 5, 2016.

This determination is valid only for this project. You are responsible for conducting this project as outlined in the above documents.

This project may proceed with no further requirement for review by the HSPO, but may require other required agreements, grant, contract and/or OU approvals. In the event that there is a change to the above-described project that may affect its determination status, send a description of the change to the HSPO. The HSPO will re-evaluate the project, if necessary.

You are responsible for keeping other NIST offices, (e.g., purchasing, technology transfer, etc.), and external collaborators informed about this determination or any approved changes to the project.

When your project is completed, notify your Supervisor, the OU Director and the HSPO.

Cc: Mike Tarlov
Mike Fasolka
Laurie Locascio

NIST

Appendix B: Estimation of recovery efficiency of peptide immunoaffinity enrichment using Protein A/G beads

A known amount of SRM 2921 was spiked into buffer (50 mmol/L ammonium bicarbonate containing 0.1 % (w/v) BSA) and digested using the protocol described in Section 5.2.3 except that trypsin was added at a 1:40 w/w trypsin-to-protein ratio. After digestion, the sample was dried and a known amount of isotopically labeled peptide (NITEIADL*TQK and TLLLQIA*K) internal standard was spiked into the sample. The sample was analyzed by LC-MS/MS analysis to determine the amount of unlabeled peptide in the sample relative to the spiked internal standard.

In another sample, a known amount of SRM 2921 was spiked into buffer (50 mmol/L ammonium bicarbonate containing 0.1% BSA) and digested using a similar protocol as described in Section 5.2.3, except that trypsin was added at a 1:40 w/w trypsin-to-protein ratio. Equal amounts ($\approx 7 \mu\text{g}$) of affinity-purified anti-NITEIADLTQK antibody and anti-TLLLQIAK antibody (Pocono Rabbit Farm & Laboratory Inc., Pennsylvania, USA, in PBS containing 0.02 % (w/v) sodium azide and 1 % (w/v) BSA), free in solution, were added to the sample digest and diluted up to 500 μL with PBS. The sample was incubated for 2 hours, followed by the addition of Protein A/G magnetic beads (25 μL , Pierce™, ThermoFisher Scientific, Massachusetts, USA, product number 88802, 10 mg/mL reported concentration). The sample was incubated for another 2 hours to subsequently capture the antibodies on the magnetic beads. Following incubation, non-specific peptides were removed by washing the magnetic beads two times with tris buffer (20 mmol/L tris, 150 mmol/L

sodium chloride) containing 0.05 % (v/v) Tween 20 (0.5 mL) and once with water (0.5 mL). Captured peptides were eluted two times with 30 μ L 5 % acetic acid. The eluents were transferred to an autosampler tube and dried using a vacuum centrifuge. Isotopically labeled peptide (NITEIADL*TQK and TLLLQIA*K) internal standard was used to reconstitute the sample prior to LC-MS/MS analysis. LC-MS/MS conditions and analysis are described in Section 5.2.4; however basic MRM analysis was used instead of dynamic MRM. Dwell time for each transition was set to 100 milliseconds. Relative ratio of unlabeled to labeled peptide following the enrichment process was compared to the unlabeled to labeled peptide ratio after the digestion step (via one-point calibration curve).

First, relative recovery (average of 2 transitions for each peptide) from the digestion step was approximately 50 % and 83 % for NITEIADLTQK and TLLLQIAK, respectively. Peptide recovery from the protein digest (without enrichment) was below theoretical, indicating that the digestion step could be further optimized. Furthermore, recovery from the entire peptide immunoaffinity workflow was demonstrated to be much lower. A recovery of 27 % for NITEIADLTQK was achieved and less than 1 % was achieved for TLLLQIAK, which deemed the anti-TLLLQIAK polyclonal antibody to be non-working. Figure B-1 shows the MRM chromatograms from both samples. The experiment was able to identify peptide losses at two different steps in the sample preparation workflow for future optimization studies.

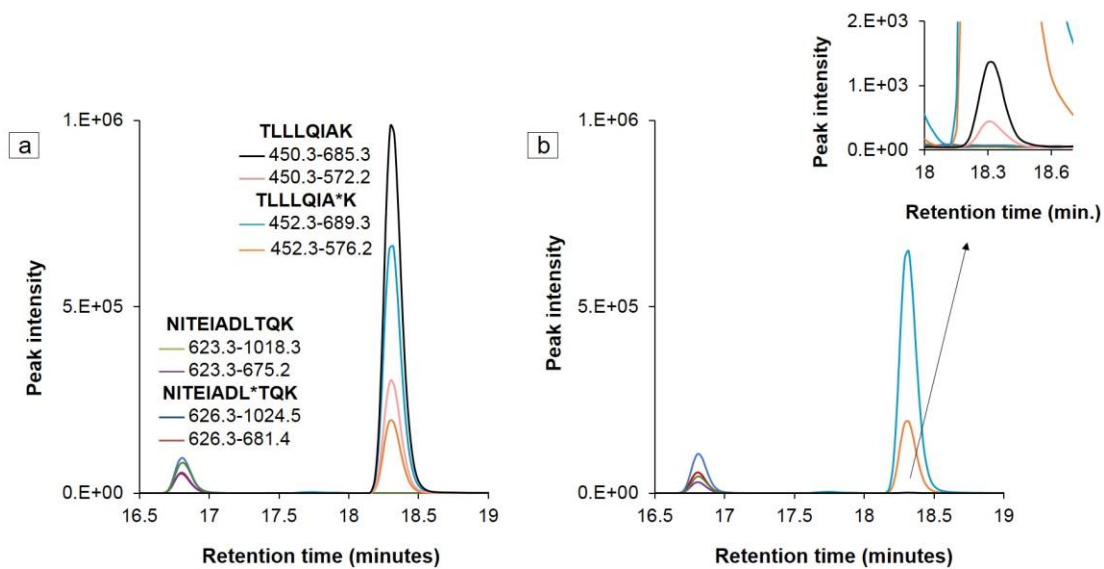


Figure B- 1 Representative MRM chromatograms of cTnI after (a) trypsin digestion only and (b) after digestion, peptide immunoaffinity enrichment, and peptide elution. Zoomed inset shows unlabeled peptides of TLLLQIAK, which cannot be clearly seen in chromatogram b.

References

- 1 Christenson, E. & Christenson, R. H. The role of cardiac biomarkers in the diagnosis and management of patients presenting with suspected acute coronary syndrome. *Ann. Lab. Med.* **33**, 309-318, doi:10.3343/alm.2013.33.5.309 (2013).
- 2 Thygesen, K. *et al.* Third Universal Definition of Myocardial Infarction. *Circulation* **126**, 2020-+, doi:10.1161/CIR.0b013e31826e1058 (2012).
- 3 Thygesen, K. *et al.* Universal definition of myocardial infarction. *Eur. Heart J.* **28**, 2525-2538 (2007).
- 4 Anderson, N. L. & Anderson, N. G. The human plasma proteome - history, character, and diagnostic prospects. *Molecular & Cellular Proteomics* **1**, 845-867, doi:10.1074/mcp.R200007-MCP200 (2002).
- 5 Wu, A. H. B. in *Cardiovascular biomarkers: pathophysiology and disease management* (ed D. A. Morrow) Ch. Chapter 2, 27-40 (Humana Press, 2006).
- 6 Christenson, R. H., Bunk, D. M., Schimmel, H., Tate, J. R. & T, I. W. G. S. POINT - Put Simply, Standardization of Cardiac Troponin I Is Complicated. *Clinical Chemistry* **58**, 165-168, doi:10.1373/clinchem.2011.166140 (2012).
- 7 Panteghini, M. Assay-related issues in the measurement of cardiac troponins. *Clinica Chimica Acta* **402**, 88-93, doi:10.1016/j.cca.2008.12.037 (2009).
- 8 Panteghini, M. Role and importance of biochemical markers in clinical cardiology. *Eur. Heart J.* **25**, 1187-1196, doi:10.1016/j.ehj.2004.04.026 (2004).
- 9 Schneck, N. A., Lowenthal, M., Phinney, K. & Lee, S. B. Current trends in magnetic particle enrichment for mass spectrometry-based analysis of cardiovascular protein biomarkers. *Nanomedicine* **10**, 433-446, doi:10.2217/nnm.14.188 (2015).
- 10 Ryan, T. J. *et al.* 1999 Update: ACC/AHA guidelines for the management of patients with acute myocardial infarction - A report of the American College of Cardiology/American Heart Association Task Force on Practice Guidelines (Committee on Management of Acute Myocardial Infarction). *J. Am. Coll. Cardiol.* **34**, 890-909, doi:10.1016/s0735-1097(99)00351-4 (1999).
- 11 Liquori, M. E., Christenson, R. H., Collinson, P. O. & deFilippi, C. R. Cardiac biomarkers in heart failure. *Clinical Biochemistry* **47**, 327-337, doi:10.1016/j.clinbiochem.2014.01.032 (2014).
- 12 Babuin, L. & Jaffe, A. S. Troponin: the biomarker of choice for the detection of cardiac injury. *Canadian Medical Association Journal* **173**, 1191-1202, doi:10.1503/cmaj/051291 (2005).
- 13 Chapelle, J. P. Cardiac troponin I and troponin T: Recent players in the field of myocardial markers. *Clinical Chemistry and Laboratory Medicine* **37**, 11-20, doi:10.1515/cclm.1999.002 (1999).
- 14 Gomes, A. V., Potter, J. D. & Szczesna-Cordary, D. The role of troponins in muscle contraction. *IUBMB Life* **54**, 323-333, doi:10.1080/15216540290114676 (2002).

- 15 Mair, J. Cardiac troponin I and troponin T: Are enzymes still relevant as cardiac markers? *Clinica Chimica Acta* **257**, 99-115, doi:10.1016/s0009-8981(96)06436-4 (1997).
- 16 Buiten, M. S. *et al.* Serum Cardiac Troponin-I is Superior to Troponin-T as a Marker for Left Ventricular Dysfunction in Clinically Stable Patients with End-Stage Renal Disease. *Plos One* **10**, 13, doi:10.1371/journal.pone.0134245 (2015).
- 17 Hetland, O. & Dickstein, K. Cardiac troponins I and T in patients with suspected acute coronary syndrome: a comparative study in a routine setting. *Clinical Chemistry* **44**, 1430-1436 (1998).
- 18 Aldous, S. J. Cardiac biomarkers in acute myocardial infarction. *International Journal of Cardiology* **164**, 282-294, doi:10.1016/j.ijcard.2012.01.081 (2013).
- 19 Katrukha, A., Bereznikova, A., Filatov, V. & Esakova, T. Biochemical factors influencing measurement of cardiac troponin I in serum. *Clinical Chemistry and Laboratory Medicine* **37**, 1091-1095, doi:10.1515/cclm.1999.159 (1999).
- 20 Katrukha, A. G. *et al.* Troponin I is released in bloodstream of patients with acute myocardial infarction not in free form but as complex. *Clinical Chemistry* **43**, 1379-1385 (1997).
- 21 Giuliani, I. *et al.* Determination of cardiac troponin I forms in the blood of patients with acute myocardial infarction and patients receiving crystalloid or cold blood cardioplegia. *Clinical Chemistry* **45**, 213-222 (1999).
- 22 Freda, B. J., Tang, W. H. W., Van Lente, F., Peacock, W. F. & Francis, G. S. Cardiac troponins in renal insufficiency - Review and clinical implications. *J. Am. Coll. Cardiol.* **40**, 2065-2071, doi:10.1016/s0735-1097(02)02608-6 (2002).
- 23 Agewall, S., Giannitsis, E., Jernberg, T. & Katus, H. Troponin elevation in coronary vs. non-coronary disease. *Eur. Heart J.* **32**, 404-411B, doi:10.1093/eurheartj/ehq456 (2011).
- 24 Katrukha, A. G. *et al.* Degradation of cardiac troponin I: implication for reliable immunodetection. *Clinical Chemistry* **44**, 2433-2440 (1998).
- 25 Wu, A. H. B. & Christenson, R. H. Analytical and assay issues for use of cardiac troponin testing for risk stratification in primary care. *Clinical Biochemistry* **46**, 969-978, doi:10.1016/j.clinbiochem.2013.04.013 (2013).
- 26 Bunk, D. M., Dalluge, J. J. & Welch, M. J. Heterogeneity in human cardiac troponin I standards. *Analytical Biochemistry* **284**, 191-200, doi:10.1006/abio.2000.4710 (2000).
- 27 Apple, F. S., Collinson, P. O. & Applicati, I. T. F. C. Analytical Characteristics of High-Sensitivity Cardiac Troponin Assays. *Clinical Chemistry* **58**, 54-61, doi:10.1373/clinchem.2011.165795 (2012).
- 28 Whiteaker, J. R. & Paulovich, A. G. Peptide immunoaffinity enrichment coupled with mass spectrometry for peptide and protein quantification. *Clinics in Laboratory Medicine* **31**, 385-396, doi:10.1016/j.cll.2011.07.004 (2011).
- 29 Moser, A. C. & Hage, D. S. Immunoaffinity chromatography: an introduction to applications and recent developments. *Bioanalysis* **2**, 769-790, doi:10.4155/bio.10.31 (2010).

- 30 Venge, P., James, S., Jansson, L. & Lindahl, B. Clinical Performance of Two Highly Sensitive Cardiac Troponin I Assays. *Clinical Chemistry* **55**, 109-116, doi:10.1373/clinchem.2008.106500 (2009).
- 31 Apple, F. S., Smith, S. W., Pearce, L. A., Ler, R. & Murakami, M. M. Use of the centaur TnI-Ultra assay for detection of myocardial infarction and adverse events in patients presenting with symptoms suggestive of acute coronary syndrome. *Clinical Chemistry* **54**, 723-728, doi:10.1373/clinchem.2007.097162 (2008).
- 32 Panteghini, M. *et al.* Evaluation of imprecision for cardiac troponin assays at low-range concentrations. *Clinical Chemistry* **50**, 327-332, doi:10.1373/clinchem.2003.026815 (2004).
- 33 Bunk, D. M. & Welch, M. J. Characterization of a new certified reference material for human Cardiac Troponin I. *Clinical Chemistry* **52**, 212-219, doi:10.1373/clinchem.2005.051359 (2006).
- 34 Eriksson, S. *et al.* Negative interference in cardiac troponin I immunoassays from a frequently occurring serum and plasma component. *Clinical Chemistry* **49**, 1095-1104, doi:10.1373/49.7.1095 (2003).
- 35 Eriksson, S., Junikka, M. & Pettersson, K. An interfering component in cardiac troponin I immunoassays - Its nature and inhibiting effect on the binding of antibodies against different epitopes. *Clinical Biochemistry* **37**, 472-480, doi:10.1016/j.clinbiochem.2004.01.007 (2004).
- 36 Eriksson, S. *et al.* Comparison of cardiac troponin I immunoassays variably affected by circulating autoantibodies. *Clinical Chemistry* **51**, 848-855, doi:10.1373/clinchem.2004.040089 (2005).
- 37 Eriksson, S., Halenius, H., Pulkki, K., Hellman, J. & Pettersson, K. Negative interference in cardiac troponin I immunoassays by circulating troponin autoantibodies. *Clinical Chemistry* **51**, 839-847, doi:10.1373/clinchem.2004.040063 (2005).
- 38 Panteghini, M. *et al.* Standardization of troponin I measurements: an update. *Clinical Chemistry and Laboratory Medicine* **46**, 1501-1506, doi:10.1515/cclm.2008.291 (2008).
- 39 Bunk, D. M. Reference materials and reference measurement procedures: an overview from a national metrology institute. *The Clinical biochemist. Reviews / Australian Association of Clinical Biochemists* **28**, 131-137 (2007).
- 40 Panteghini, M. Standardization of cardiac troponin I measurements: The way forward? *Clinical Chemistry* **51**, 1594-1597, doi:10.1373/clinchem.2005.054551 (2005).
- 41 Christenson, R. H. *et al.* Toward standardization of cardiac troponin I measurements part II: Assessing commutability of candidate reference materials and harmonization of cardiac troponin I assays. *Clinical Chemistry* **52**, 1685-1692, doi:10.1373/068437 (2006).
- 42 Noble, J. E. *et al.* Development of a candidate secondary reference procedure (immunoassay based measurement procedure of higher metrological order) for cardiac troponin I: I. antibody characterization and preliminary validation. *Clinical Chemistry and Laboratory Medicine* **48**, 1603-1610, doi:10.1515/cclm.2010.316 (2010).

- 43 Vitzthum, F. *et al.* Metrological sharp shooting for plasma proteins and peptides: The need for reference materials for accurate measurements in clinical proteomics and in vitro diagnostics to generate reliable results. *Proteomics Clinical Applications* **1**, 1016-1035, doi:10.1002/prca.200700223 (2007).
- 44 Christenson, R. H. *et al.* Standardization of cardiac troponin I assays: Round robin of ten candidate reference materials. *Clinical Chemistry* **47**, 431-437 (2001).
- 45 Tate, J. R. *et al.* The harmonization of cardiac troponin I measurement is independent of sample time collection but is dependent on the source of calibrator. *Clinica Chimica Acta* **324**, 13-23, doi:10.1016/s0009-8981(02)00214-0 (2002).
- 46 Cobbaert, C. M., Weykamp, C. W., Michielsen, E., Baadenhuijsen, H. & van Dieijen-Visser, M. P. Time-Dependent Instability of Cardiac Troponins in Human Plasma Spiked with NIST Reference Material 2921. *Clinical Chemistry* **54**, 2078-2079, doi:10.1373/clinchem.2008.104182 (2008).
- 47 Pan, S. *et al.* Mass Spectrometry Based Targeted Protein Quantification: Methods and Applications. *Journal of Proteome Research* **8**, 787-797, doi:10.1021/pr800538n (2009).
- 48 Nedelkov, D. Mass spectrometry-based immunoassays for the next phase of clinical applications. *Expert Review of Proteomics* **3**, 631-640, doi:10.1586/14789450.3.6.631 (2006).
- 49 Gerszten, R. E., Asnani, A. & Carr, S. A. Status and prospects for discovery and verification of new biomarkers of cardiovascular disease by proteomics. *Circulation Research* **109**, 463-474, doi:10.1161/circresaha.110.225003 (2011).
- 50 Addona, T. A. *et al.* Multi-site assessment of the precision and reproducibility of multiple reaction monitoring-based measurements of proteins in plasma. *Nature Biotechnology* **27**, 633-U685, doi:10.1038/nbt.1546 (2009).
- 51 Picotti, P. & Aebersold, R. Selected reaction monitoring-based proteomics: workflows, potential, pitfalls and future directions. *Nature Methods* **9**, 555-566, doi:10.1038/nmeth.2015 (2012).
- 52 Boja, E. S. & Rodriguez, H. Mass spectrometry-based targeted quantitative proteomics: Achieving sensitive and reproducible detection of proteins. *Proteomics* **12**, 1093-1110, doi:10.1002/pmic.201100387 (2012).
- 53 Lange, V., Picotti, P., Domon, B. & Aebersold, R. Selected reaction monitoring for quantitative proteomics: a tutorial. *Molecular Systems Biology* **4**, 1-14, doi:10.1038/msb.2008.61 (2008).
- 54 Calvo, E., Camafeita, E., Fernandez-Gutierrez, B. & Lopez, J. A. Applying selected reaction monitoring to targeted proteomics. *Expert Review of Proteomics* **8**, 165-173, doi:10.1586/epr.11.11 (2011).
- 55 MacLean, B. *et al.* Skyline: an open source document editor for creating and analyzing targeted proteomics experiments. *Bioinformatics* **26**, 966-968, doi:10.1093/bioinformatics/btq054 (2010).
- 56 Hu, Q. Z. *et al.* The Orbitrap: a new mass spectrometer. *J. Mass Spectrom.* **40**, 430-443, doi:10.1002/jms.856 (2005).

- 57 Domon, B. & Aebersold, R. Review - Mass spectrometry and protein analysis. *Science* **312**, 212-217, doi:10.1126/science.1124619 (2006).
- 58 Han, X. M., Aslanian, A. & Yates, J. R. Mass spectrometry for proteomics. *Curr. Opin. Chem. Biol.* **12**, 483-490, doi:10.1016/j.cbpa.2008.07.024 (2008).
- 59 Yates, J. R., Ruse, C. I. & Nakorchevsky, A. in *Annual Review of Biomedical Engineering* Vol. 11 *Annual Review of Biomedical Engineering* 49-79 (Annual Reviews, 2009).
- 60 Cottrell, J. S. Protein identification using MS/MS data. *Journal of Proteomics* **74**, 1842-1851, doi:10.1016/j.jprot.2011.05.014 (2011).
- 61 Nesvizhskii, A. I. in *Mass Spectrometry Data Analysis in Proteomics Methods in Molecular Biology* (ed Rune Matthiesen) 87-119 (Humana Press, 2007).
- 62 Eng, J. K., McCormack, A. L. & Yates, J. R. An approach to correlate tandem mass spectral data of peptides with amino acid sequences in a protein database. *J. Am. Soc. Mass Spectrom.* **5**, 976-989, doi:10.1016/1044-0305(94)80016-2 (1994).
- 63 Nesvizhskii, A. I., Vitek, O. & Aebersold, R. Analysis and validation of proteomic data generated by tandem mass spectrometry. *Nature Methods* **4**, 787-797, doi:10.1038/nmeth1088 (2007).
- 64 Colangelo, C. M., Chung, L. S., Bruce, C. & Cheung, K. H. Review of software tools for design and analysis of large scale MRM proteomic datasets. *Methods* **61**, 287-298, doi:10.1016/j.ymeth.2013.05.004 (2013).
- 65 Kitteringham, N. R., Jenkins, R. E., Lane, C. S., Elliott, V. L. & Park, B. K. Multiple reaction monitoring for quantitative biomarker analysis in proteomics and metabolomics. *Journal of Chromatography B-Analytical Technologies in the Biomedical and Life Sciences* **877**, 1229-1239, doi:10.1016/j.jchromb.2008.11.013 (2009).
- 66 Bronstrup, M. Absolute quantification strategies in proteomics based on mass spectrometry. *Expert Review of Proteomics* **1**, 503-512, doi:10.1586/14789450.1.4.503 (2004).
- 67 Rauh, M. LC-MS/MS for protein and peptide quantification in clinical chemistry. *Journal of Chromatography B-Analytical Technologies in the Biomedical and Life Sciences* **883**, 59-67, doi:10.1016/j.jchromb.2011.09.030 (2012).
- 68 Takeda, S., Yamashita, A., Maeda, K. & Maeda, Y. Structure of the core domain of human cardiac troponin in the Ca²⁺-saturated form. *Nature* **424**, 35-41, doi:10.1038/nature01780 (2003).
- 69 Meng, Z. J. & Veenstra, T. D. Targeted mass spectrometry approaches for protein biomarker verification. *Journal of Proteomics* **74**, 2650-2659, doi:10.1016/j.jprot.2011.04.011 (2011).
- 70 Kilpatrick, E. L. & Bunk, D. M. Reference measurement procedure development for C-reactive protein in human serum. *Analytical Chemistry* **81**, 8610-8616, doi:10.1021/ac901597h (2009).
- 71 Lowenthal, M. S., Liang, Y. X., Phinney, K. W. & Stein, S. E. Quantitative Bottom-Up Proteomics Depends on Digestion Conditions. *Analytical Chemistry* **86**, 551-558, doi:10.1021/ac4027274 (2014).

- 72 Gianazza, E., Tremoli, E. & Banfi, C. The selected reaction monitoring/multiple reaction monitoring-based mass spectrometry approach for the accurate quantitation of proteins: clinical applications in the cardiovascular diseases. *Expert Review of Proteomics* **11**, 771-788, doi:10.1586/14789450.2014.947966 (2014).
- 73 Pieper, R. *et al.* Multi-component immunoaffinity subtraction chromatography: an innovative step towards a comprehensive survey of the human plasma proteome. *Proteomics* **3**, 422-432, doi:10.1002/pmic.200390057 (2003).
- 74 Hortin, G. L., Sviridov, D. & Anderson, N. L. High-abundance polypeptides of the human plasma proteome comprising the top 4 logs of polypeptide abundance. *Clinical Chemistry* **54**, 1608-1616, doi:10.1373/clinchem.2008.108175 (2008).
- 75 Boja, E. *et al.* Evolution of Clinical Proteomics and its Role in Medicine. *Journal of Proteome Research* **10**, 66-84, doi:10.1021/pr100532g (2011).
- 76 Shi, T. J. *et al.* Advancing the sensitivity of selected reaction monitoring-based targeted quantitative proteomics. *Proteomics* **12**, 1074-1092, doi:10.1002/pmic.201100436 (2012).
- 77 Tu, C. J. *et al.* Depletion of Abundant Plasma Proteins and Limitations of Plasma Proteomics. *Journal of Proteome Research* **9**, 4982-4991, doi:10.1021/pr100646w (2010).
- 78 Pernemalm, M., Lewensohn, R. & Lehtio, J. Affinity prefractionation for MS-based plasma proteomics. *Proteomics* **9**, 1420-1427, doi:10.1002/pmic.200800377 (2009).
- 79 Fortin, T. *et al.* Clinical Quantitation of Prostate-specific Antigen Biomarker in the Low Nanogram/Milliliter Range by Conventional Bore Liquid Chromatography-Tandem Mass Spectrometry (Multiple Reaction Monitoring) Coupling and Correlation with ELISA Tests. *Molecular & Cellular Proteomics* **8**, 1006-1015, doi:10.1074/mcp.M800238-MCP200 (2009).
- 80 Keshishian, H., Addona, T., Burgess, M., Kuhn, E. & Carr, S. A. Quantitative, multiplexed assays for low abundance proteins in plasma by targeted mass spectrometry and stable isotope dilution. *Molecular & Cellular Proteomics* **6**, 2212-2229, doi:10.1074/mcp.M700354-MCP200 (2007).
- 81 Keshishian, H. *et al.* Quantification of cardiovascular biomarkers in patient plasma by targeted mass spectrometry and stable isotope dilution. *Molecular & Cellular Proteomics* **8**, 2339-2349, doi:10.1074/mcp.M900140-MCP200 (2009).
- 82 Gundry, R. L., Fu, Q., Jelinek, C. A., Van Eyk, J. E. & Cotter, R. J. Investigation of an albumin-enriched fraction of human serum and its albuminome. *Proteomics Clinical Applications* **1**, 73-88, doi:10.1002/prca.200600276 (2007).
- 83 Lowenthal, M. S. *et al.* Analysis of albumin-associated peptides and proteins from ovarian cancer patients. *Clinical Chemistry* **51**, 1933-1945, doi:10.1373/clinchem.2005.052944 (2005).
- 84 Huillet, C. *et al.* Accurate Quantification of Cardiovascular Biomarkers in Serum Using Protein Standard Absolute Quantification (PSAQ (TM)) and

- Selected Reaction Monitoring. *Molecular & Cellular Proteomics* **11**, 12, doi:10.1074/mcp.M111.008235 (2012).
- 85 Addona, T. A. *et al.* A pipeline that integrates the discovery and verification of plasma protein biomarkers reveals candidate markers for cardiovascular disease. *Nature Biotechnology* **29**, 635-643, doi:10.1038/nbt.1899 (2011).
- 86 Shen, J. X., Liu, G. W. & Zhao, Y. Strategies for improving sensitivity and selectivity for the quantitation of biotherapeutics in biological matrix using LC-MS/MS. *Expert Review of Proteomics* **12**, 125-131, doi:10.1586/14789450.2015.1024225 (2015).
- 87 Dunham, W. H., Mullin, M. & Gingras, A. C. Affinity-purification coupled to mass spectrometry: Basic principles and strategies. *Proteomics* **12**, 1576-1590, doi:10.1002/pmic.201100523 (2012).
- 88 Hage, D. S. IMMUNOASSAYS. *Analytical Chemistry* **67**, R455-R462 (1995).
- 89 Becker, J. & Hoofnagle, A. N. Replacing immunoassays with tryptic digestion-peptide immunoaffinity enrichment and LC-MS/MS. *Bioanalysis* **4**, 281-290, doi:10.4155/bio.11.319 (2012).
- 90 Lowenthal, M. S., Gasca-Aragon, H., Schiel, J. E., Dodder, N. G. & Bunk, D. M. A quantitative LC-MS/MS method for comparative analysis of capture-antibody affinity toward protein antigens. *Journal of Chromatography B-Analytical Technologies in the Biomedical and Life Sciences* **879**, 2726-2732, doi:10.1016/j.jchromb.2011.07.037 (2011).
- 91 Rogstad, S. M., Sorkina, T., Sorkin, A. & Wu, C. C. Improved precision of proteomic measurements in immunoprecipitation based purifications using relative quantitation. *Analytical Chemistry* **85**, 4301-4306, doi:10.1021/ac4002222 (2013).
- 92 Anderson, N. L. *et al.* Mass spectrometric quantitation of peptides and proteins using stable isotope standards and capture by anti-peptide antibodies (SISCAPA). *Journal of Proteome Research* **3**, 235-244, doi:10.1021/pr034086h (2004).
- 93 Ackermann, B. L. & Berna, M. J. Coupling immunoaffinity techniques with MS for quantitative analysis of low-abundance protein biomarkers. *Expert Review of Proteomics* **4**, 175-186, doi:10.1586/14789450.4.2.175 (2007).
- 94 Anderson, N. L. *et al.* SISCAPA peptide enrichment on magnetic beads using an in-line bead trap device. *Molecular & Cellular Proteomics* **8**, 995-1005, doi:10.1074/mcp.M800446-MCP200 (2009).
- 95 Peter, J. F. & Otto, A. M. Magnetic particles as powerful purification tool for high sensitive mass spectrometric screening procedures. *Proteomics* **10**, 628-633, doi:10.1002/pmic.200800535 (2010).
- 96 Whiteaker, J. R. *et al.* Antibody-based enrichment of peptides for mass-spectrometry-based quantification on magnetic beads of serum biomarkers. *Analytical Biochemistry* **362**, 44-54, doi:10.1016/j.ab.2006.12.023 (2007).
- 97 Safarik, I. & Safarikova, M. Magnetic techniques for the isolation and purification of proteins and peptides. *Biomagnetic research and technology* **2**, 7, doi:10.1186/1477-044x-2-7 (2004).

- 98 Safarik, I. & Safarikova, M. Use of magnetic techniques for the isolation of cells. *Journal of Chromatography B* **722**, 33-53, doi:10.1016/s0378-4347(98)00338-7 (1999).
- 99 Mani, V., Chikkaveeraiah, B. V. & Rusling, J. F. Magnetic particles in ultrasensitive biomarker protein measurements for cancer detection and monitoring. *Expert opinion on medical diagnostics* **5**, 381-391, doi:10.1517/17530059.2011.607161 (2011).
- 100 Horak, D., Babic, M., Mackova, H. & Benes, M. J. Preparation and properties of magnetic nano- and microsized particles for biological and environmental separations. *J. Sep. Sci.* **30**, 1751-1772, doi:10.1002/jssc.200700088 (2007).
- 101 Hasany, S. F., Abdurahman, N. H., Sunarti, A. R. & Jose, R. Magnetic iron oxide nanoparticles: chemical synthesis and applications review. *Current Nanoscience* **9**, 561-575 (2013).
- 102 Hyeon, T. Chemical synthesis of magnetic nanoparticles. *Chemical Communications*, 927-934, doi:10.1039/b207789b (2003).
- 103 Cheng, C. M., Xu, F. J. & Gu, H. C. Facile synthesis and morphology evolution of magnetic iron oxide nanoparticles in different polyol processes. *New J. Chem.* **35**, 1072-1079, doi:10.1039/c0nj00986e (2011).
- 104 Bai, X. *et al.* Synthesis of superparamagnetic nanotubes as MRI contrast agents and for cell labeling. *Nanomedicine* **3**, 163-174, doi:10.2217/17435889.3.2.163 (2008).
- 105 Cai, W. & Wan, J. Q. Facile synthesis of superparamagnetic magnetite nanoparticles in liquid polyols. *J. Colloid Interface Sci.* **305**, 366-370, doi:10.1016/j.jcis.2006.10.023 (2007).
- 106 Zhang, W., Shen, F. L. & Hong, R. Y. Solvothermal synthesis of magnetic Fe₃O₄ microparticles via self-assembly of Fe₃O₄ nanoparticles. *Particuology* **9**, 179-186, doi:10.1016/j.partic.2010.07.025 (2011).
- 107 Cha, J., Lee, J. S., Yoon, S. J., Kim, Y. K. & Lee, J. K. Solid-state phase transformation mechanism for formation of magnetic multi-granule nanoclusters. *Rsc Advances* **3**, 3631-3637, doi:10.1039/c3ra21639j (2013).
- 108 Joseyphus, R. J., Shinoda, K., Kodama, D. & Jeyadevan, B. Size controlled Fe nanoparticles through polyol process and their magnetic properties. *Mater. Chem. Phys.* **123**, 487-493, doi:10.1016/j.matchemphys.2010.05.001 (2010).
- 109 Park, J., Joo, J., Kwon, S. G., Jang, Y. & Hyeon, T. Synthesis of monodisperse spherical nanocrystals. *Angewandte Chemie-International Edition* **46**, 4630-4660, doi:10.1002/anie.200603148 (2007).
- 110 Cao, S. W., Zhu, Y. J. & Chang, J. Fe₃O₄ polyhedral nanoparticles with a high magnetization synthesized in mixed solvent ethylene glycol-water system. *New J. Chem.* **32**, 1526-1530, doi:10.1039/b719436f (2008).
- 111 Shen, L. H. *et al.* One-step synthesis of monodisperse, water-soluble ultra-small Fe₃O₄ nanoparticles for potential bio-application. *Nanoscale* **5**, 2133-2141, doi:10.1039/c2nr33840h (2013).
- 112 Lu, A. H., Salabas, E. L. & Schuth, F. Magnetic nanoparticles: Synthesis, protection, functionalization, and application. *Angewandte Chemie-International Edition* **46**, 1222-1244, doi:10.1002/anie.200602866 (2007).

- 113 Gupta, A. K. & Gupta, M. Synthesis and surface engineering of iron oxide nanoparticles for biomedical applications. *Biomaterials* **26**, 3995-4021, doi:10.1016/j.biomaterials.2004.10.012 (2005).
- 114 Stöber, W., Fink, A. & Bohn, E. Controlled growth of monodisperse silica spheres in the micron size range. *J. Colloid Interface Sci.* **26**, 62-69, doi:http://dx.doi.org/10.1016/0021-9797(68)90272-5 (1968).
- 115 Kralj, S., Makovec, D., Čampelj, S. & Drofenik, M. Producing ultra-thin silica coatings on iron-oxide nanoparticles to improve their surface reactivity. *Journal of Magnetism and Magnetic Materials* **322**, 1847-1853, doi:10.1016/j.jmmm.2009.12.038 (2010).
- 116 Bumb, A. *et al.* Synthesis and characterization of ultra-small superparamagnetic iron oxide nanoparticles thinly coated with silica. *Nanotechnology* **19**, 6, doi:10.1088/0957-4484/19/33/335601 (2008).
- 117 Čampelj, S., Makovec, D. & Drofenik, M. Functionalization of magnetic nanoparticles with 3-aminopropyl silane. *Journal of Magnetism and Magnetic Materials* **321**, 1346-1350, doi:http://dx.doi.org/10.1016/j.jmmm.2009.02.036 (2009).
- 118 Deng, Y., Qi, D., Deng, C., Zhang, X. & Zhao, D. Superparamagnetic high-magnetization microspheres with an Fe₃O₄@SiO₂ core and perpendicularly aligned mesoporous SiO₂ shell for removal of microcystins. *Journal of the American Chemical Society* **130**, 28-29, doi:10.1021/ja0777584 (2008).
- 119 He, T., Chen, D. R. & Jiao, X. L. Controlled synthesis of Co₃O₄ nanoparticles through oriented aggregation. *Chem. Mat.* **16**, 737-743, doi:10.1021/cm0303033 (2004).
- 120 Pena-Pereira, F., Duarte, R. & Duarte, A. C. Immobilization strategies and analytical applications for metallic and metal-oxide nanomaterials on surfaces. *Trac-Trends Anal. Chem.* **40**, 90-105, doi:10.1016/j.trac.2012.07.015 (2012).
- 121 Bruce, I. J. & Sen, T. Surface modification of magnetic nanoparticles with alkoxysilanes and their application in magnetic bioseparations. *Langmuir* **21**, 7029-7035, doi:10.1021/la050553t (2005).
- 122 Zhang, Q., Huang, R. F. & Guo, L. H. One-step and high-density protein immobilization on epoxysilane-modified silica nanoparticles. *Chin. Sci. Bull.* **54**, 2620-2626, doi:10.1007/s11434-009-0210-7 (2009).
- 123 Li, Y., Zhang, X. M. & Deng, C. H. Functionalized magnetic nanoparticles for sample preparation in proteomics and peptidomics analysis. *Chemical Society Reviews* **42**, 8517-8539, doi:10.1039/c3cs60156k (2013).
- 124 Koh, I. *et al.* Magnetic iron oxide nanoparticles for biorecognition: Evaluation of surface coverage and activity. *Journal of Physical Chemistry B* **110**, 1553-1558, doi:10.1021/jp0556310 (2006).
- 125 Balthasar, S. *et al.* Preparation and characterisation of antibody modified gelatin nanoparticles as drug carrier system for uptake in lymphocytes. *Biomaterials* **26**, 2723-2732, doi:10.1016/j.biomaterials.2004.07.047 (2005).
- 126 Dinauer, N. *et al.* Selective targeting of antibody-conjugated nanoparticles to leukemic cells and primary T-lymphocytes. *Biomaterials* **26**, 5898-5906, doi:10.1016/j.biomaterials.2005.02.038 (2005).

- 127 Puertas, S. *et al.* Taking advantage of unspecific interactions to produce highly active magnetic nanoparticle - antibody conjugates. *Acs Nano* **5**, 4521-4528, doi:10.1021/nn200019s (2011).
- 128 McCarthy, S. A., Davies, G. L. & Gun'ko, Y. K. Preparation of multifunctional nanoparticles and their assemblies. *Nat. Protoc.* **7**, 1677-1693, doi:10.1038/nprot.2012.082 (2012).
- 129 Gundry, R. L. *et al.* in *Current Protocols in Molecular Biology* Ch. Unit 10.25, (John Wiley & Sons, Inc., 2009).
- 130 Li, D., Teoh, W. Y., Gooding, J. J., Selomulya, C. & Amal, R. Functionalization strategies for protease immobilization on magnetic nanoparticles. *Adv. Funct. Mater.* **20**, 1767-1777, doi:10.1002/adfm.201000188 (2010).
- 131 Noble, J. E. & Bailey, M. J. A. in *Guide to Protein Purification, Second Edition* Vol. 463 *Methods in Enzymology* (eds R. R. Burgess & M. P. Deutscher) 73-95 (Elsevier Academic Press Inc, 2009).
- 132 Leinenbach, A. *et al.* Mass Spectrometry-Based Candidate Reference Measurement Procedure for Quantification of Amyloid-beta in Cerebrospinal Fluid. *Clinical Chemistry* **60**, 987-994, doi:10.1373/clinchem.2013.220392 (2014).
- 133 Brun, V., Masselon, C., Garin, J. & Dupuis, A. Isotope dilution strategies for absolute quantitative proteomics. *Journal of Proteomics* **72**, 740-749, doi:10.1016/j.jprot.2009.03.007 (2009).
- 134 Zhao, C. *et al.* Epitope mapping and targeted quantitation of the cardiac biomarker troponin by SID-MRM mass spectrometry. *Proteomics* **14**, 1311-1321, doi:10.1002/pmic.201300150 (2014).
- 135 Stone, P., Glauner, T., Kuhlmann, F., Schlaback, T.; Miller, K. New dynamic MRM mode improves data quality and triple quad quantification in complex analyses. *Agilent publication* (2009).
- 136 Beasley-Green, A., Burris, N. M., Bunk, D. M. & Phinney, K. W. Multiplexed LC-MS/MS Assay for Urine Albumin. *Journal of Proteome Research* **13**, 3930-3939, doi:10.1021/pr500204c (2014).
- 137 Brownridge, P. & Beynon, R. J. The importance of the digest: Proteolysis and absolute quantification in proteomics. *Methods* **54**, 351-360, doi:10.1016/j.ymeth.2011.05.005 (2011).
- 138 Norrgran, J. *et al.* Optimization of digestion parameters for protein quantification. *Analytical Biochemistry* **393**, 48-55, doi:10.1016/j.ab.2009.05.050 (2009).
- 139 Berna, M. J., Zhen, Y. J., Watson, D. E., Hale, J. E. & Ackermann, B. L. Strategic use of immunoprecipitation and LC/MS/MS for trace-level protein quantification: myosin light chain 1, a biomarker of cardiac necrosis. *Analytical Chemistry* **79**, 4199-4205, doi:10.1021/ac070051f (2007).
- 140 Kuhn, E. *et al.* Developing multiplexed assays for troponin I and interleukin-33 in plasma by peptide immunoaffinity enrichment and targeted mass spectrometry. *Clinical Chemistry* **55**, 1108-1117, doi:10.1373/clinchem.2009.123935 (2009).

- 141 Twerenbold, R., Jaffe, A., Reichlin, T., Reiter, M. & Mueller, C. High-sensitive troponin T measurements: what do we gain and what are the challenges? *Eur. Heart J.* **33**, 579-586, doi:10.1093/eurheartj/ehr492 (2012).
- 142 Heudi, O. *et al.* Towards absolute quantification of therapeutic monoclonal antibody in serum by LC-MS/MS using isotope-labeled antibody standard and protein cleavage isotope dilution mass spectrometry. *Analytical Chemistry* **80**, 4200-4207, doi:10.1021/ac800205s (2008).
- 143 Picard, G. *et al.* PSAQ (TM) standards for accurate MS-based quantification of proteins: from the concept to biomedical applications. *J. Mass Spectrom.* **47**, 1353-1363, doi:10.1002/jms.3106 (2012).
- 144 Carr, S. A. & Anderson, L. Protein Quantitation through Targeted Mass Spectrometry: The Way Out of Biomarker Purgatory? *Clinical Chemistry* **54**, 1749-1752, doi:10.1373/clinchem.2008.114686 (2008).
- 145 Buscemi, N., Foster, D. B., Neverova, I. & Van Eyk, J. E. p21-activated kinase increases the calcium sensitivity of rat triton-skinned cardiac muscle fiber bundles via a mechanism potentially involving novel phosphorylation of troponin I. *Circulation Research* **91**, 509-516, doi:10.1161/01.res.0000035246.27856.53 (2002).
- 146 Kuhn, E. *et al.* Interlaboratory evaluation of automated, multiplexed peptide immunoaffinity enrichment coupled to multiple reaction monitoring mass spectrometry for quantifying proteins in plasma. *Molecular & Cellular Proteomics* **11**, 14-26, doi:10.1074/mcp.M111.013854 (2012).
- 147 Shi, T. J. *et al.* Targeted quantification of low ng/ml level proteins in human serum without immunoaffinity depletion. *Journal of Proteome Research* **12**, 3353-3361, doi:10.1021/pr400178v (2013).
- 148 Hoofnagle, A. N. & Wener, M. H. The fundamental flaws of immunoassays and potential solutions using tandem mass spectrometry. *Journal of Immunological Methods* **347**, 3-11, doi:10.1016/j.jim.2009.06.003 (2009).
- 149 Hoofnagle, A. N., Becker, J. O., Wener, M. H. & Heinecke, J. W. Quantification of Thyroglobulin, a Low-Abundance Serum Protein, by Immunoaffinity Peptide Enrichment and Tandem Mass Spectrometry. *Clinical Chemistry* **54**, 1796-1804, doi:10.1373/clinchem.2008.109652 (2008).
- 150 Park, Z. Y. & Russell, D. H. Thermal denaturation: A useful technique in peptide mass mapping. *Analytical Chemistry* **72**, 2667-2670, doi:10.1021/ac991444k (2000).
- 151 Razavi, M. *et al.* High-Throughput SISCAPA Quantitation of Peptides from Human Plasma Digests by Ultrafast, Liquid Chromatography-Free Mass Spectrometry. *Journal of Proteome Research* **11**, 5642-5649, doi:10.1021/pr300652v (2012).
- 152 Zhao, L., Whiteaker, J. R., Voytovich, U. J., Ivey, R. G. & Paulovich, A. G. Antibody-coupled magnetic beads can be reused in immuno-MRM assays to reduce cost and extend antibody supply. *Journal of Proteome Research* **14**, 4425-4431, doi:10.1021/acs.jproteome.5b00290 (2015).